Supporting Information

Highly Efficient Luminescence from Boron *β*-Dialdiminates and Their π-Conjugated Polymers in Both Solutions and Solids: Significant Impact of Substituent Position on Luminescence Behavior

Shunichiro Ito,[1] Miyako Hashizume,[1] Hideo Taka,[2] Hiroshi Kita,[2] Kazuo Tanaka[1] and Yoshiki Chujo[1]*

[1]Department of Polymer Chemistry, Graduate School of Engineering, Kyoto University, Katsura, Nishikyo-ku, Kyoto 615-8510, Japan
[2]Konica Minolta, Inc., 2970 Ishikawa-machi, Hachiojishi, Tokyo 192-8505, Japan

E-mail: tanaka@poly.synchem.kyoto-u.ac.jp

Table of Contents

Measurements

NMR Spectroscopy

^{1}H (400 MHz), $^{13}C\{^{1}H\}$ (101 MHz) and $^{11}B\{^{1}H\}$ (128 MHz) NMR spectra were recorded on a JEOL JNM-AL400 spectrometer. Heteronuclear multiple quantum coupling (HMQC, ^{1}H–^{13}C) and heteronuclear multiple bond coupling (HMBC, ^{1}H–^{13}C) spectra were recorded on a JEOL JNM-ECZ600R spectrometer. In ^{1}H and $^{13}C\{^{1}H\}$ spectra, tetramethylsilane (TMS) was used as an internal standard in $CDCl_3$. In other solvents (CD_2Cl_2 and DMSO-d_6), the residual solvent peaks were used as an internal standard. $^{11}B\{^{1}H\}$ NMR spectra were referenced externally to $BF_3{\cdot}OEt_2$ (sealed capillary). The following abbreviations are used: s, singlet; d, doublet; t, triplet; m, multiplet; br, broad; dd, double doublet; tt, triplet of triplets.

Mass Spectrometry and Elemental Analysis

High-resolution mass (HRMS) spectrometry was conducted at the Technical Support Office (Department of Synthetic Chemistry and Biological Chemistry, Graduate School of Engineering, Kyoto University). HRMS spectra were obtained on a Thermo Fisher Scientific EXACTIVE Plus spectrometer for electrospray ionization (ESI) and for atmospheric-pressure chemical ionization (APCI) and a Burker Daltonics Ultraflex III for matrix-assisted laser desorption ionization time-of-flight mass spectrometry (MALDI-TOF MS).

Elemental analysis was conducted at the Microanalytical Center of Kyoto University using one of the following micro corders: MT-5 (Yanaco Co., Ltd.), MT-6 (Yanaco Co., Ltd.), JM10 (J-Science Lab Co., Ltd.), and JM11 (J-Science Lab Co., Ltd.) for C, H, and N analysis.

Silica Gel Chromatography

Analytical thin-layer chromatography was performed with SiO_2 60 Merck F_{254} plates. Column chromatography was performed with Wakogel C-300 SiO_2 (Wako).

Size-Exclusion Chromatography

Number-average molecular weight (M_n) and molecular weight distribution ($Đ = M_w/M_n$) values of all polymers were estimated by size exclusion chromatography (SEC) with a TOSOH 8020 series (a dual pump system (DP-8020), a column oven (CO-8020), and a degasser (SD-8020)) equipped with three consecutive polystyrene gel columns (TSKgel: G4000H, G3000H and G2000H) and a refractive-index (RI-8020) and an ultraviolet detector (UV-8020) at 40 °C. The system was operated at a flow rate of 1.0 mL/min with $CHCl_3$ as an eluent. Polystyrene standards were employed for calibration.

High-Performance Liquid Chromatography

Recyclable preparative high-performance liquid chromatography (HPLC) was performed with Japan Analytical Industry Model LaboACE LC-5060 (JAIGEL-2.5H and 3HH columns) using $CHCl_3$ as an eluent.

Thermal Analysis

Thermogravimetric analysis (TGA) was performed on an EXSTAR TG/DTA6220, Seiko Instrument, Inc., with the heating rate of 10 °C/min up from 40 to 500 °C under nitrogen flowing (200 mL/min). Residual water was removed by keeping on an aluminum pan at 100 °C for 30 min before the curve profiling. The decomposition temperatures (T_d) were determined from the onset of the weight loss. Differential scanning calorimetry (DSC) was carried out on a SII DSC 6220 instrument by using about 5 mg of exactly weighed samples at heating rate of 10 °C/min.

Photophysical Measurements

UV−vis absorption spectra were recorded on a SHIMADZU UV–3600 spectrophotometer. Fluorescence and phosphorescence emission spectra and phosphorescence decay were measured with a HORIBA JOBIN YVON Fluorolog-3 spectrofluorometer and an Oxford Optistat DN cryostat for temperature control. Absolute photoluminescence quantum yields were measured with a Hamamatsu Photonics Quantaurus-QY Plus C13534-01 spectrophotometer and a sample holder for low temperature, A11238-05, was used for the measurements at 77 K. Photoluminescence (PL) lifetimes were measured

by a Horiba FluoroCube spectrofluorometer system with an Oxford Optistat DN cryostat for temperature control and a UV diode laser (NanoLED 375 nm).

X-Ray Diffraction

Wide-angle X-ray diffraction (WAXD) patterns were taken by using Cu Kα radiation with a Rigaku SmartLab X-ray Diffractometer. For polymers, X-ray incident angle was fixed at 1.0° for grazing-incidence measurements. In out-of-plane measurements, diffraction patterns were taken in 2θ range from 3° to 30° by continuous scanning with a step size of 0.01°. In in-plane measurements, diffraction patterns were taken in $2\theta\chi/\varphi$ range from 3° to 30° by continuous scanning with a step size of 0.008°.

Film Thickness Measurement

Film thickness was measured with a Bruker DektakXT profilometer.

Device Fabrication

Glass substrates coated with a 100-nm thin layer of indium tin oxide (ITO) were cleaned by ultrasonication with isopropyl alcohol, purged with nitrogen, and washed with UV ozone for 5 min. The hole-injecting layer was prepared by the ink-jet printing method with a PEDOT:PSS dispersion (2 wt% in isopropyl alcohol), then dried at 80 °C for 5 min. TCTA, *m*CP:**DAI-Tol**, TPBi, LiF, and Al were subsequently deposited by thermal evaporation.

Materials

All reactions were performed under argon atmosphere unless otherwise noted. Phenylacetyl chloride (Tokyo Chemical Industry Co., Ltd.; TCI), $POCl_3$ (Tokyo Chemical Industry Co., Ltd.; TCI), $NaClO_4$ (FUJIFILM Wako Pure Chemicals Corporation; Wako), *p*-tolylacetic acid (TCI), HPF_6 aq. (60 wt%, Wako), NaOH (Wako), aniline (TCI), benzylamine (TCI), 1,1,3,3-tetramethoxypropane (TCI), HCl aq. (1 M, Wako), $BF_3{\cdot}OEt_2$ (Sigma-Aldrich Co. LLC.), deoxygenated toluene (Wako), deoxygenated dimethylformamide (DMF, Wako), dichloromethane (DCM, Wako), 2-propanol (Wako), methanol (Wako), hexane (Wako), chloroform (Wako), and cyclopentyl methyl ether (Wako) were purchased from commercial sources and used as received. Deoxygenated diethyl ether (Wako), and triethyl amine (Kanto Chemical Co., Inc) were purified using a two-column solid-state purification system (Glasscontour System, Joerg Meyer, Irvine, CA). **DKI-4Ph**[1] and **DKI-5Ph**[2] were synthesized according to the literature.

Synthesis of Vin-Ph:

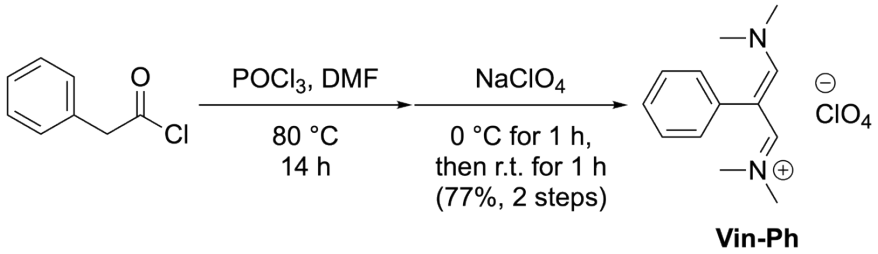

$POCl_3$ (6.1 mL, 65 mmol) was added to DMF (12 mL, 162 mmol) dropwise for 40 min. The deep red Vilsmeier reagent's solution was allowed to cool to 0 °C. Phenylacetyl chloride (5.0 g, 32 mmol) was added dropwise to the solution for 20 min. The reddish orange solution was warmed to 80 °C and stirred for 14 h. The deep brown solution was cooled to 0 °C and diluted with DCM (20 mL). The reaction mixture was added dropwise to the precooled solution of $NaClO_4$ (4.36 g, 36 mmol) in water (140 mL). The precipitate was collected with suction filtration, washed with water and Et_2O, and dried under vacuum, affording the pure product as a pale-yellow powder (7.58 g, 77%). ^{1}H NMR (400 MHz; CD_2Cl_2):

δ = 7.73 (s, 2H, >N–C*H*=C), 7.43–7.41 (m, 3H, Ar), 7.30–7.27 (m, 2H, Ar), 3.31 (s, 6H, NCH_3), 2.46 (s, 6H, NCH_3). $^{13}C\{^1H\}$ NMR (101 MHz; CD_2Cl_2): δ 163.7, 132.5, 132.4, 129.1, 128.8, 106.2, 101.7, 49.1, 39.7. HRMS (ESI) $[M]^+$; Found: 203.1542. Calcd.: 203.1543.

Synthesis of Vin-Tol:

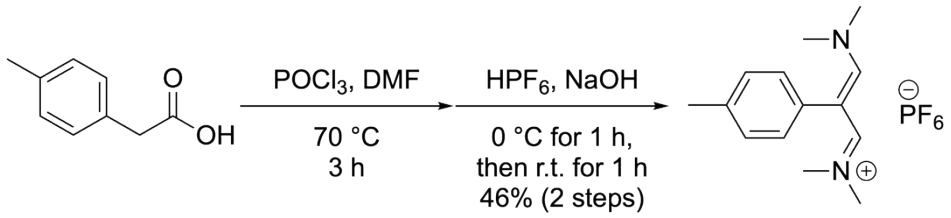

Vin-Tol

To a mixture of *p*-tolylacetic acid (9.8 g, 65 mmol) and DMF (28 mL, 366 mmol) was added $POCl_3$ (6.1 mL, 65 mmol) dropwise over 10 min at 70 °C under nitrogen flow. After stirring at 70 °C for 3 h, the reddish brown solution was allowed to cool to r.t. The reaction mixture and 5 M NaOH aq. (18 mL) were simultaneously added dropwise to a solution of NaOH (7.0 g, 174 mmol) and HPF_6 aq. (60 wt%, 10.4 mL, 70 mmol) in water (130 mL) over 1 h at a temperature below 10 °C. The mixture was stirred at r.t. for 1 h, then filtered and the filtrate washed with water to give a yellow solid. The residue was purified by recrystallization from the mixed solvent of 2-propanol and water (1/4, *v*/*v*) affording the analytically pure product as a yellow solid (10.8 g, 46% yield). ^1H NMR (400 MHz; $CDCl_3$): δ = 7.62 (s, 2H, >N–C*H*=C), 7.20 (d, 2H, Ar, $^3J_{H–H}$ = 8.1 Hz), 7.13 (d, 2H, Ar, $^3J_{H–H}$ = 8.1 Hz), 3.30 (s, 6H, NCH_3), 2.48 (s, 6H, NCH_3), 2.39 (s, 3H, Ar–CH_3). $^{13}C\{^1H\}$ NMR (101 MHz; $CDCl_3$): δ = 163.7, 139.1, 132.0, 129.4, 128.7, 105.8, 49.0, 39.5, 21.1. HRMS (ESI) $[M]^+$; Found: 217.1697. Calcd.: 217.1699.

General procedure for the synthesis of proligands

A solution of a vinamidinium salt and a primary amine (2.2 eq.) in methanol (0.1 M for proligand) was heated to the reflux temperature and stirred for *ca.* 24 h. Further purification was carried as shown in each compound section.

Synthesis of DAI-3Ph_L:

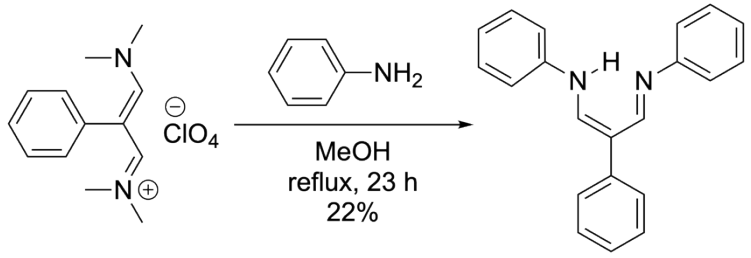

Vin-Ph (1.5 g, 5.0 mmol) and aniline (1.0 mL, 1.0 g, 11 mmol) were used. The suspension was filtered and washed with cold methanol and hexane, then the analytically pure product was obtained as a yellow powder (0.33 g, 22%). ^{1}H NMR (400 MHz; CD_2Cl_2) δ = 12.84 (s, 1H, N*H*), 8.11 (s, 2H, >N–C*H*=C), 7.43—7.35 (m, 8H), 7.24 (tt, *J* = 7.1, 1.6 Hz, 1H), 7.19 (dd, *J* = 8.5, 1.0 Hz, 4H), 7.11 (tt, *J* = 7.4, 1.1 Hz, 2H). ^{13}C{^{1}H} NMR (101 MHz; $CDCl_3$): δ = 149.2, 146.5, 140.2, 129.4, 128.7, 126.0, 125.5, 123.8, 118.4, 109.6. HRMS (ESI) $[M+H]^+$; Found: 299.1546. Calcd.: 299.1543.

Synthesis of DAI-Tol_L:

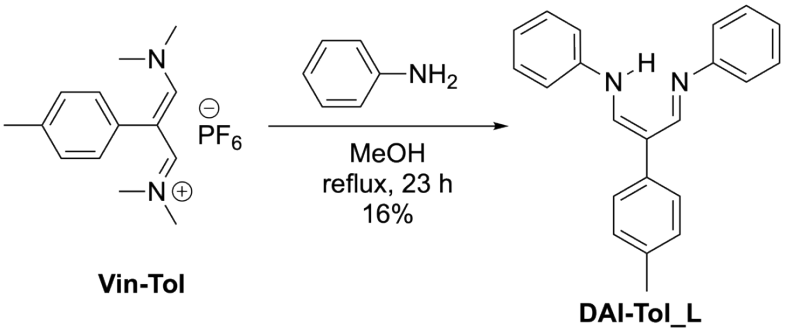

Vin-Tol (5.0 g, 14 mmol) and aniline (2.8 mL, 30 mmol) were used. After cooling to r.t., yellow precipitate appeared. The suspension was filtered and washed with cold methanol and hexane, then the analytically pure product was obtained as a yellow powder (0.68 g, 16% yield). ^{1}H NMR (400 MHz; $CDCl_3$) δ = 12.82 (s, 1H, N*H*), 8.04 (s, 2H, >N–C*H*=C), 7.38–7.33 (m, 4H), 7.30–7.27 (m, 2H), 7.19 (d, *J* = 7.9 Hz, 2H), 7.15 (dt, *J* = 8.5, 1.6 Hz, 4H), 7.10 (tt, *J* = 7.3, 1.0 Hz, 2H), 2.37 (s, 3H, CH_3). ^{13}C{^{1}H}

NMR (101 MHz; $CDCl_3$): δ = 149.1, 146.5, 137.3, 135.2, 129.4, 129.4, 126.0, 123.7, 118.3, 109.5, 21.0. HRMS (ESI) $[M+H]^+$; Found: 313.1701. Calcd.: 313.1701.

Synthesis of DAI-Bn_L:

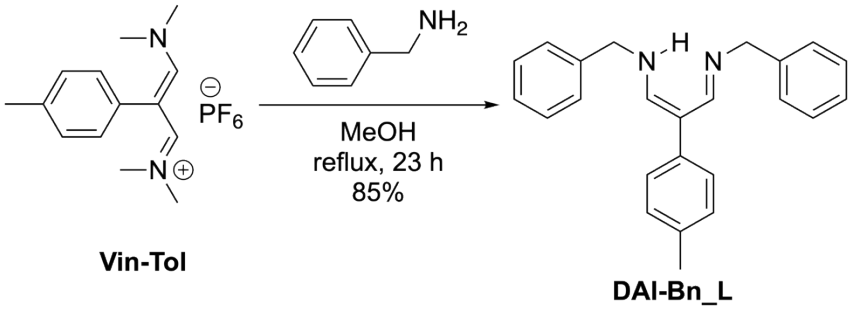

Vin-Tol (1.0 g, 2.8 mmol) and benzylamine (0.66 mL, 0.65 g, 6.1 mmol) were used. After cooling to r.t., the reaction mixture was concentrated with a rotary evaporator. The crude product was purified by a silica gel flash column chromatography with $CHCl_3$/MeOH (20/1, *v*/*v*, *Rf* ~ 0.3 (broad)) as an eluent. The product was obtained as a yellow powder involving unknown impurities (0.80 g, 85% crude yield). The crude product was used for the following synthesis without further purification. ^{1}H NMR (400 MHz; $CDCl_3$) δ = 8.03 (s, 2H, >N–C*H*=C), 7.35–7.23 (m, 12H, Ar), 7.06 (d, *J* = 7.9 Hz, 2H, Ar), 6.51 (s, 1H, N*H*), 4.59 (s, 4H, CH_2), 2.32 (s, 3H, CH_3). ^{13}C{^{1}H} NMR (101 MHz; $CDCl_3$): δ = 162.9, 140.2, 134.8, 131.7, 130.8, 129.4, 129.2, 128.7, 128.0, 108.0, 53.6, 21.2 HRMS (ESI) $[M+H]^+$; Found: 341.2017. Calcd.: 341.2012.

Synthesis of DAI-3Ph-I_L:

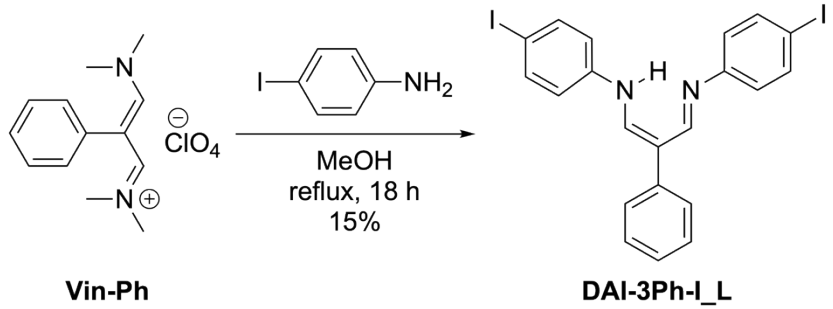

Vin-Ph (1.5 g, 5.0 mmol) and *p*-iodoaniline (2.4 g, 11 mmol) were used. The cooled suspension was filtered and washed with cold methanol. The filtrate were purified by recrystallization from hexane to afford the analytically pure product as an orange powder (0.40 g, 15% yield). ^{1}H NMR (400 MHz; CD_2Cl_2): δ = 12.81 (s, 1 H, N*H*), 8.05 (s, 2H, >N–C*H*=C), 7.4 (d, *J* = 8.79 Hz, 4H, Ar), 7.39–7.38 (m, 4H, Ar), 7.26 (m, 1H, Ar), 6.96 (d, *J* = 8.79 Hz, 4H, Ar). ^{13}C{^{1}H} NMR (101 MHz; $CDCl_3$): 149.16 (N=*C*), 145.95, 139.66, 138.36, 128.84, 126.17, 125.95, 120.36, 110.6, 87.12. HRMS (ESI) $[M+H]^+$; Found: 550.9471, Calcd.: 550.9476.

Synthesis of DAI-2Ph_L:

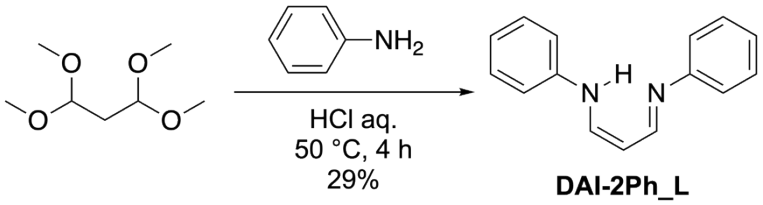

To a solution of 1,1,3,3-tetramethoxypropane (4.0 mL, 4.0 g, 24 mmol) in 0.5 M HCl aq. (63 mL) was added a solution of aniline (4.5 mL, 4.5 g, 49 mmol) in 0.5 M HCl aq. (87 mL) at 50 °C. The orange suspension was stirred at 50 °C for 4 h. The precipitate was collected with suction filtration and washed with water, Et_2O, cyclopentyl methyl ether, and hexane. The crude orange solid was purified with recrystallization from methanol, affording the pure product as an orange powder (1.5 g, 29%). ^{1}H NMR (400 MHz; DMSO-d6) δ = 12.43 (s, 2H, N*H*), 8.80 (d, *J* = 10.3 Hz, 2H, >N–C*H*=C), 7.49 (t, *J* = 7.7 Hz, 5H, Ar), 7.40 (d, *J* = 8.2 Hz, 4H, Ar), 7.27 (t, *J* = 7.2 Hz, 2H, Ar), 6.39 (t, *J* = 11.0 Hz, 1H, –CH=C*H*–CH=). ^{13}C{^{1}H} NMR (101 MHz; DMSO): δ 158.4, 138.7, 129.8, 125.8, 117.4, 98.6. HRMS (APCI) $[M+H]^+$; Found: 223.1226. Calcd.: 223.1230.

General procedure for the synthesis of a boron complex

To a solution of a proligand and triethylamine in toluene (0.1 M for a proligand) was added $BF_3{\cdot}OEt_2$ (10 eq.) and stirred for 6 h at 100 °C. After cooling to r.t., the reaction mixture was poured into water and extracted with toluene until the aqueous layer showed no emission under UV (375 nm) irradiation. The combined organic layer was washed with water and brine, dried over $MgSO_4$, filtered, and then the filtrate was concentrated under reduced pressure to give a crude product. Further purification was carried as shown in each compound section.

Synthesis of DAI-3Ph:

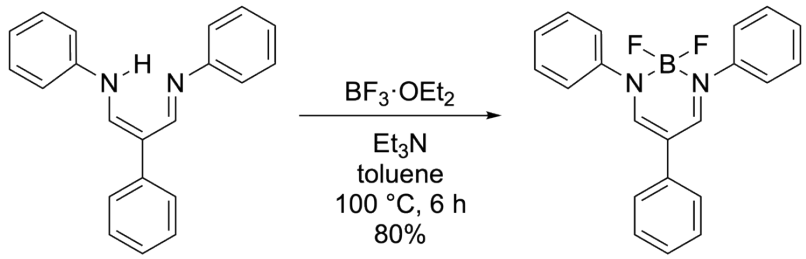

DAI-3Ph_L **DAI-3Ph**

DAI-3Ph_L (0.33 g, 1.1 mmol), triethylamine (0.31 mL, 2.2 mmol) and $BF_3{\cdot}OEt_2$ (1.4 mL, 11 mmol) were used. The crude product was purified by recrystallization from the mixed solvent of CH_2Cl_2 and hexane to afford the analytically pure product as yellow needle-like crystals (0.31 g, 80%). ^{1}H NMR (400 MHz; $CDCl_3$) δ = 8.01–7.96 (m, 2H, >N–C*H*=C), 7.52–7.29 (m, 15H, Ar). $^{13}C\{^1H\}$ NMR (101 MHz; $CDCl_3$): δ = 154.0, 144.0, 136.1, 129.3, 129.1, 127.2, 126.5, 125.3, 124.1, 108.6. $^{11}B\{^1H\}$ NMR (128 MHz; $CDCl_3$): δ = 1.57. HRMS (ESI) $[M+Na]^+$; Found: 369.1346. Calcd.: 369.1345. Anal. Calcd. for $C_{21}H_{17}BF_2N_2$: C, 72.86; H, 4.95; N, 8.09. Found: C, 72.88; H, 4.91; N, 8.11.

Synthesis of DAI-Tol:

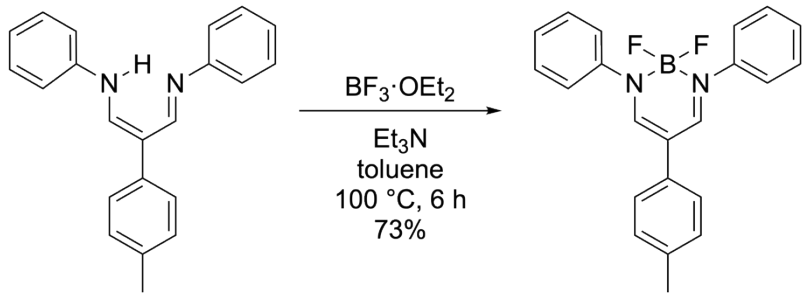

DAI-Tol_L **DAI-Tol**

DAI-Tol_L (0.50 g, 1.6 mmol), triethylamine (0.26 mL, 1.9 mmol) and $BF_3{\cdot}OEt_2$ (0.71 mL, 5.6 mmol) were used. The crude product was dissolved in a small amount of CH_2Cl_2 and the solution was poured into excess MeOH, aged for 30 min at –78 °C, and then the precipitate was collected and washed with cold MeOH. The resulting yellow powder was purified repeatedly by recrystallization from the mixed solvent of CH_2Cl_2 and hexane to afford the analytically pure product as a yellow needle-like crystal (0.42 g, 73%). ^{1}H NMR (400 MHz; $CDCl_3$) δ = 7.98–7.93 (m, 2H, >N–C*H*=C), 7.50 (d, *J* = 7.9 Hz, 4H, Ar), 7.42 (t, *J* = 7.8 Hz, 4H, Ar), 7.33 (t, *J* = 7.3 Hz, 2H, Ar), 7.21 (t, *J* = 9.6 Hz, 4H, Ar), 2.37 (s, 3H, C*H*$_3$). ^{13}C{^{1}H} NMR (101 MHz; $CDCl_3$): δ = 153.9, 144.1, 136.3, 133.2, 129.8, 129.3, 127.2, 125.3, 124.1, 108.6, 21.0. ^{11}B{^{1}H} NMR (128 MHz; $CDCl_3$): δ = 1.57. HRMS (ESI) $[M+Na]^+$; Found: 383.1501. Calcd.: 383.1502. Anal. Calcd. for $C_{22}H_{19}N_2BF_2$: C, 73.36; H, 5.32; N, 7.78. Found: C, 73.52; H, 5.14; N, 7.70.

Synthesis of DAI-Bn:

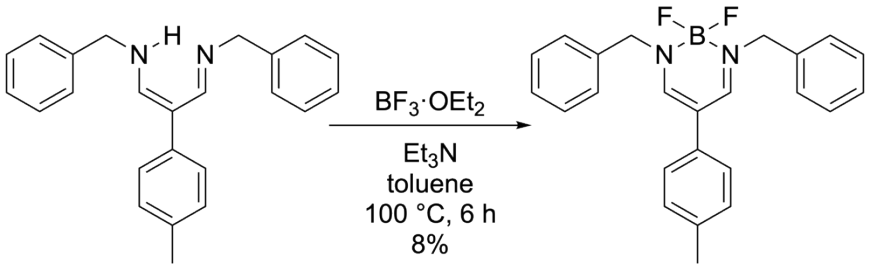

DAI-Bn_L **DAI-Bn**

DAI-Bn_L (0.80 g, 2.3 mmol), triethylamine (0.66 mL, 4.7 mmol) and $BF_3{\cdot}OEt_2$ (2.9 mL, 23 mmol) were used. The colorless product was purified repeatedly by recrystallization from methanol and hexane/EtOAc to afford an analytically pure product as colorless crystals (7.3 mg, 8%). The product was

gradually decomposed in solution under ambient condition. ^{1}H NMR (400 MHz; $CDCl_3$) δ = 7.53 (s, 2H, >N–C*H*=C), 7.37–7.29 (m, 9H, Ar), 7.06 (d, *J* = 8.3 Hz, 2H, Ar), 6.92 (d, *J* = 8.1 Hz, 2H, Ar), 4.73 (s, 4H, CH_2), 2.28 (s, 3H, CH_3). ^{13}C{^{1}H} NMR (101 MHz; $CDCl_3$): δ = 154.7, 137.5, 135.5, 133.7, 129.6, 128.84, 128.78, 127.9, 125.0, 105.7, 53.5, 20.9. ^{11}B{^{1}H} NMR (128 MHz; $CDCl_3$): δ = 1.48. HRMS (ESI) $[M+Na]^+$; Found: 411.1819. Calcd.: 411.1815. Anal. Calcd. for $C_{24}H_{23}N_2BF_2$: C, 74.24; H, 5.97; N, 7.22. Found: C, 74.12; H, 6.09; N, 7.03.

Synthesis of DAI-3Ph-I:

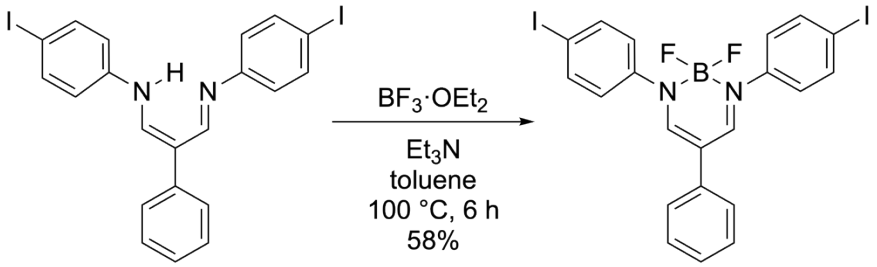

DAI-3Ph_L (0.39 g, 0.71 mmol), triethylamine (0.20 mL, 1.4 mmol) and $BF_3{\cdot}OEt_2$ (0.89 mL, 7.1 mmol) were used. The residue was purified by recrystallization repeatedly from the mixed solvent of CH_2Cl_2 and hexane to afford the analytically pure product as an orange needle-like crystal (0.25 g, 58% yield). ^{1}H NMR (400 MHz; CD_2Cl_2): δ = 7.98 (s, 2H, >N–C*H*=C), 7.78 (d, *J* = 8.79 Hz, 4H, Ar), 7.43–7.35 (m, 4H, Ar), 7.30 (t, *J* = 7.02 Hz, 1H, Ar), 7.25 (d, *J* = 8.79 Hz, 4H, Ar). ^{13}C{^{1}H} NMR (101 MHz; $CDCl_3$): δ = 153.83, 143.51, 138.41, 135.58, 129.25, 126.84, 125.85, 125.49, 109.38, 92.34. ^{11}B{^{1}H} NMR ($CDCl_3$): δ = 1.18 (t, *J* = 24.96 Hz). HRMS (ESI) $[M+Na]^+$; Found: 620.9270. Calcd.: 620.9278.

Synthesis of DAI-2Ph:

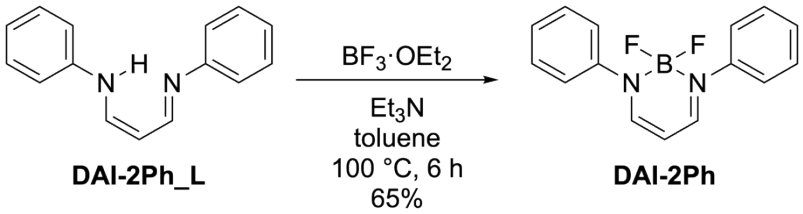

DAI-2Ph_L (0.90 g, 4.0 mmol), triethylamine (1.1 mL, 8.1 mmol) and $BF_3{\cdot}OEt_2$ (5.1 mL, 40 mmol) were used. The brown oil was purified by a silica gel column chromatography with $CHCl_3$/hexane (3/1, *v*/*v*, *Rf* = 0.25) as an eluent. The obtained yellow oil was dissolved in CH_3CN (*ca.* 5 mL) and poured into excess water (*ca.* 50 mL). Yellow precipitate appeared and was collected with suction filtration. The product was purified by recrystallization from hexane/toluene to afford the analytically pure product as a colorless crystal (0.71 g, 65%). ^{1}H NMR (400 MHz; $CDCl_3$) δ = 7.66 (s, 2H, >N–C*H*=C), 7.46–7.38 (m, 8H, Ar), 7.33–7.28 (m, 2H, Ar), 5.49 (t, *J* = 6.0 Hz, 1H, –CH=C*H*-CH=). ^{13}C{^{1}H} NMR (101 MHz; $CDCl_3$): δ = 154.6, 144.0, 129.2, 127.0, 124.0, 93.1. HRMS (ESI) $[M+Na]^+$; Found: 293.1033. Calcd.: 293.1032. Anal. Calcd. for $C_{15}H_{13}BF_2N_2$: C, 66.71; H, 4.85; N, 10.37. Found: C, 66.69; H, 4.83; N, 10.29.

General procedure for the synthesis of polymers

To a two-neck round-bottomed flask equipped with **DAI-3Ph-I**, a boronic acid derivative, $Pd_2(dba)_3$, SPhos and cesium carbonate were added toluene and water. The mixture was stirred at 80 °C for 24 h under nitrogen atmosphere. The resulted solution was diluted with a small amount of toluene and poured into an excess amount of methanol to collect the polymer by suction filtration. The precipitate was dissolved in a small amount of $CHCl_3$, and then the product was reprecipitated in ethanol. The polymer collected by filtration was dried in vacuum to give a corresponding polymer.

Synthesis of PDAI-Ph

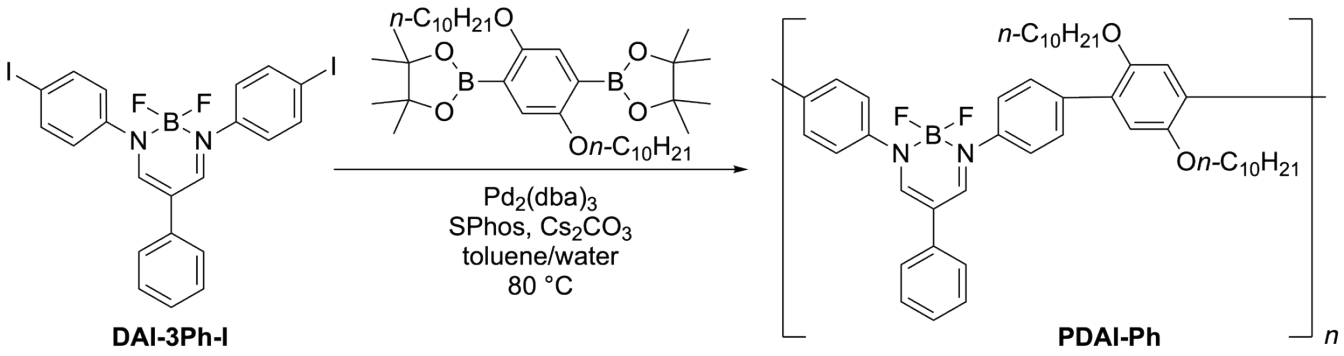

DAI-3Ph-I (0.25 g, 0.42 mmol), 2,5-didecyloxyphenylene-1,4-bis(4,4,5,5-tetramethyl-1,3,2-dioxaborolate) (0.27 g, 0.42 mmol), $Pd_2(dba)_3$ (3.8 mg, 4.2 μmol), SPhos (6.9 mg, 17 μmol) and cesium carbonate (1.4 g, 42 mmol) were added toluene (6.0 mL) and water (6.0 mL) were used. The title compound was obtained as a yellow solid (0.30 g, 98%). SEC ($CHCl_3$, polystyrene standard): M_n = 16,000; M_w = 39,000; $Đ$ = 2.4. ^{1}H NMR (400 MHz; $CDCl_3$): δ = 8.08 (s, 2H, >N–C*H*=C), 7.70 (d, *J* = 8.24 Hz, 4H, Ar), 7.59 (d, *J* = 8.24 Hz, 4H, Ar), 7.43–7.41 (m, 4H, Ar), 7.33–7.30 (m, 1H, Ar), 7.02 (s, 2H, Ar), 3.96 (t, *J* = 6.78 Hz, 4H, O–CH_2), 1.72 (m, 4H, alkyl), 1.39 (m, 4H, alkyl), 1.25 (m, 24H, alkyl), 0.85 (t, *J* = 6.99 Hz, 6H). ^{13}C{^{1}H} NMR (101 MHz; $CDCl_3$): δ = 153.71, 150.30, 142.84, 137.41, 136.25, 130.39, 129.92, 129.18, 126.51, 125.41, 123.52, 116.06, 108.83, 69.64, 31.87, 29.60, 29.59, 29.54, 29.32, 29.29, 26.07, 22.65, 14.08. ^{11}B{^{1}H} NMR ($CDCl_3$): δ = 1.47 (t, *J* = 31.36 Hz).

Synthesis of PDAI-FL

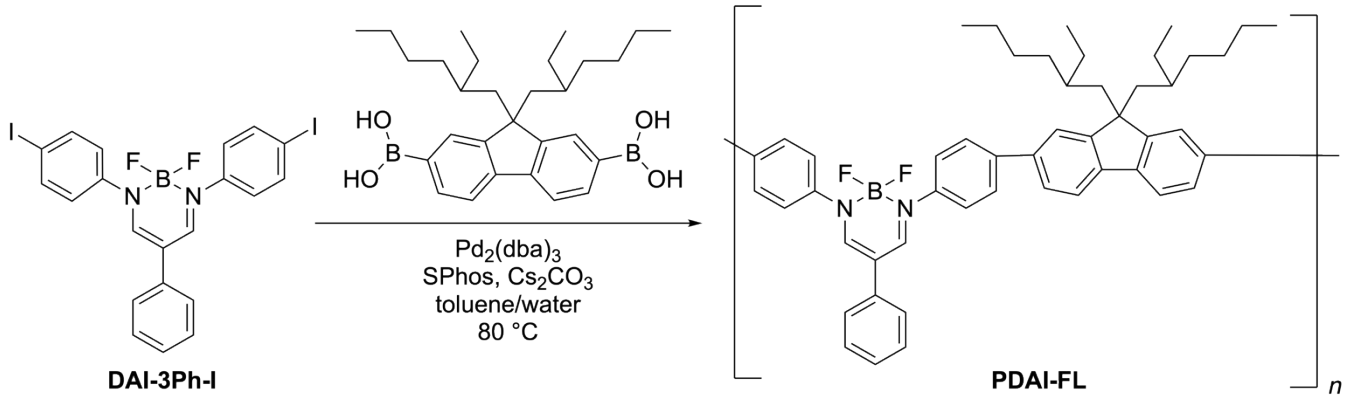

DAI-3Ph-I (0.30 g, 0.50 mmol), [9,9-bis(2-ethylhexyl)-9H-fluorene-2,7-diyl]bisboronic acid (0.24 g, 0.50 mmol), $Pd_2(dba)_3$ (4.6 mg, 5.0 μmol), SPhos (8.2 mg, 20 μmol) and cesium carbonate (1.6 g, 5.0 mmol) were added toluene (5.0 mL) and water (5.0 mL) were used. The title compound was obtained as a yellow solid (0.28 g, 75%). SEC ($CHCl_3$, polystyrene standard): M_n = 7,200; M_w = 16,000; $Đ$ = 1.9. ^{1}H NMR (400 MHz; $CDCl_3$): δ = 8.08 (s, 2H, >N–C*H*=C), 7.80–7.32 (m, 19H, Ar), 2.09 (m, 4H, alkyl), 0.86–0.54 (m, 30H, alkyl). ^{13}C{^{1}H} NMR (101 MHz; $CDCl_3$): δ = 153.65, 151.43, 143.01, 140.86, 140.48, 138.53, 138.39, 136.16, 129.20, 127.93, 126.58, 126.11, 125.43, 124.32, 122.76, 120.08, 55.16, 44.54,

34.74, 33.91, 28.27, 28.24, 27.13, 22.71, 13.96, 10.38, 10.36. $^{11}B\{^{1}H\}$ NMR ($CDCl_3$): δ = 1.48 (t, J = 31.36 Hz).

Synthesis of PDAI-BT

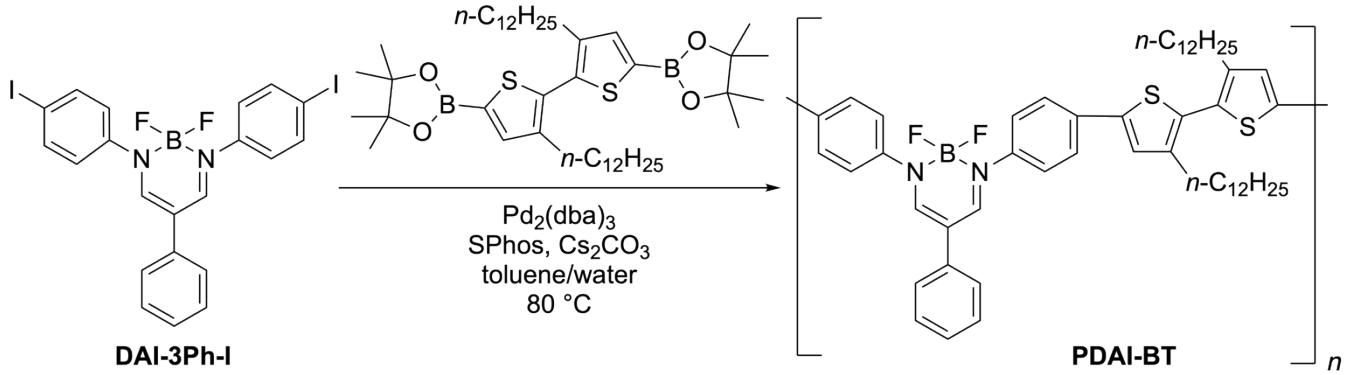

DAI-3Ph-I (0.20 g, 0.33 mmol), 4,4'-didodecyl-2,2'- bithiophene-5,5'-diboronicacid bis(pinacol) ester (0.25 g, 0.33 mmol), $Pd_2(dba)_3$ (3.1 mg, 3.3 μmol), SPhos (5.5 mg, 13 μmol) and cesium carbonate (1.1 g, 3.3 mmol) were added toluene (3.3 mL) and water (3.3 mL) were used. The title compound was obtained as an orange solid (0.28 g, 100%). SEC ($CHCl_3$, polystyrene standard): M_n = 14,000; M_w = 30,000; $Đ$ = 2.1. ^{1}H NMR (400 MHz; $CDCl_3$): δ = 8.01 (s, 2H, >N–C*H*=C), 7.67 (d, J = 8.36 Hz, 4H, Ar), 7.54 (d, J = 8.36 Hz, 4H, Ar), 7.45–7.38 (m, 4H, Ar), 7.34–7.32 (m, 1H, Ar), 7.23 (s, 2H, Ar), 2.59 (t, J = 7.48 Hz, 4H, alkyl), 1.63 (m, 4H, alkyl), 1.25 (m, 36H, alkyl), 0.87 (t, J = 6.90 Hz, 6H). $^{13}C\{^{1}H\}$ NMR (101 MHz; $CDCl_3$): δ = 153.33, 143.72, 143.08, 142.65, 136.03, 133.35, 129.20, 128.63, 126.64, 126.37, 125.48, 125.19, 124.32, 109.15, 31.90, 30.72, 29.68, 9.64, 29.59, 29.47, 29.34, 29.15, 22.67, 14.09. $^{11}B\{^{1}H\}$ NMR ($CDCl_3$): δ = 1.47 (t, J = 30.72 Hz).

Photocyclization of DKI-4Ph

To reveal the existence of a photocyclization path for DKI complexes, we subjected **DKI-4Ph** to a photochemical cyclization condition for 5 h (Scheme S1). As a result, a trace amount of a doubly cyclized compound was detected in the crude mixture by high-resolution mass spectrometry with APCI. Aerial oxidation would occur in this photocyclization process. Therefore, it was experimentally demonstrated that the photocyclization process should be one of actual decay paths of photoexcited DKI complexes. Unfortunately, further purification and isolation of the cyclized compound has not been accomplished probably due to its instability.

Scheme S1. Photochemical cyclization of **DKI-4Ph**

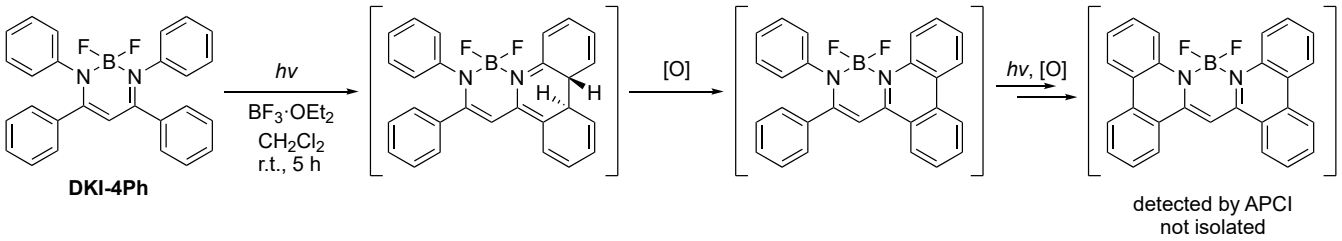

Condition: To a 1000-mL photochemical reaction vessel equipped with a stirrer bar, **DKI-4Ph** (0.10 g, 0.24 mmol) and dry CH_2Cl_2 (200 mL) was added $BF_3{\cdot}OEt_2$ (5.8 mL, 47 mmol). The reaction mixture was irradiated with a high-pressure mercury UV lamp (Sen Lights Corp., HL400BH-8) for 5 h. After concentration with a rotary evaporator, the residue was redissolved in CH_2Cl_2 and washed with saturated $NaHCO_3$ aq. The organic layer was dried over $MgSO_4$, followed by filtration. After concentration, the crude product was analyzed with HRMS. Further purification and isolation of the product have not been accomplished probably due to its instability. HRMS (APCI) $[M+H]^+$; Found: 419.1523. Calcd.: 419.1526.

SEC Profile

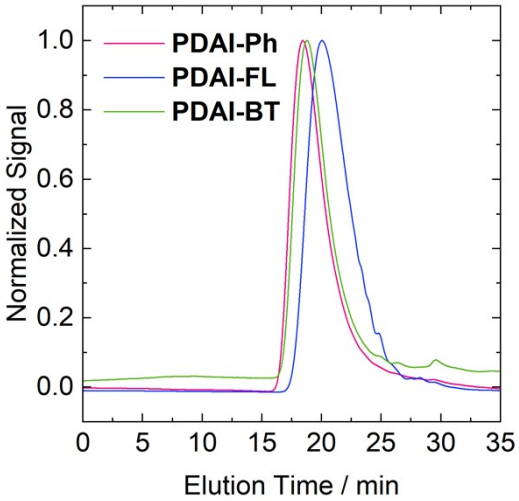

Figure S1. Chromatogram of the synthesized polymers. $CHCl_3$ was used as an eluent.

Photophysical Properties

Photoluminescence lifetime

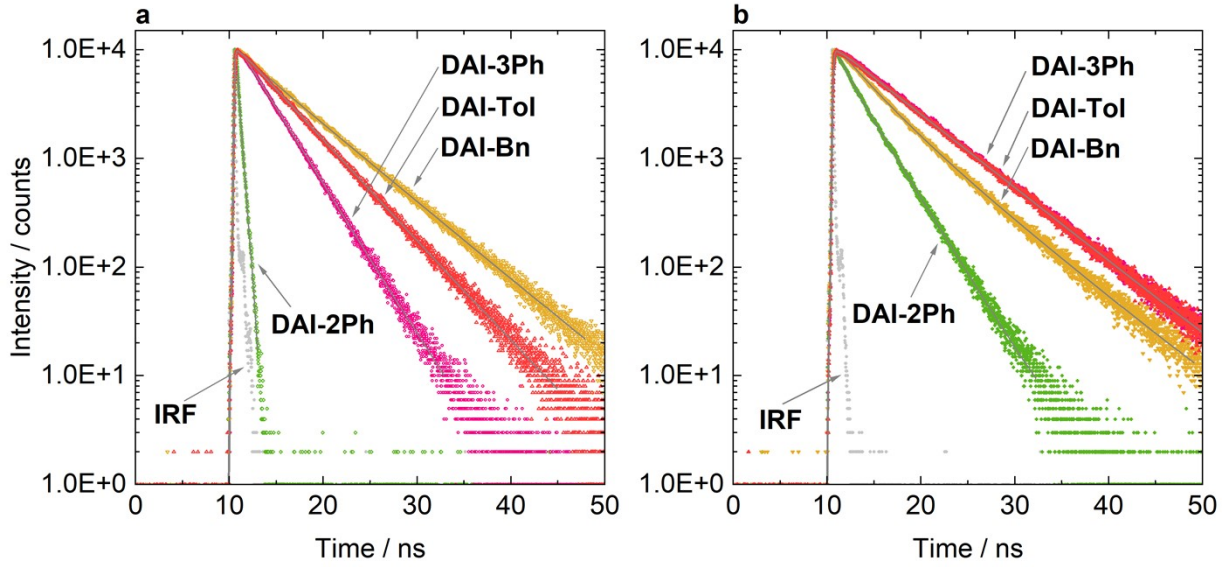

Figure S2. Fluorescence decay curves of DAI complexes in (a) solution and (b) crystalline states. Color symbols and gray solid lines are experimental and fitted data, respectively. IRF denotes the instrument response function.

Photophysical properties of DAI complexes in various solvents

UV–vis absorption and photoluminescence spectra of DAI complexes were measured in $CHCl_3$, toluene, and DMSO. For all solutions, the concentration was 1.0×10^{-5} M (Figure S3). The results indicated that the photophysical properties of these complexes did not significantly depend on solvents.

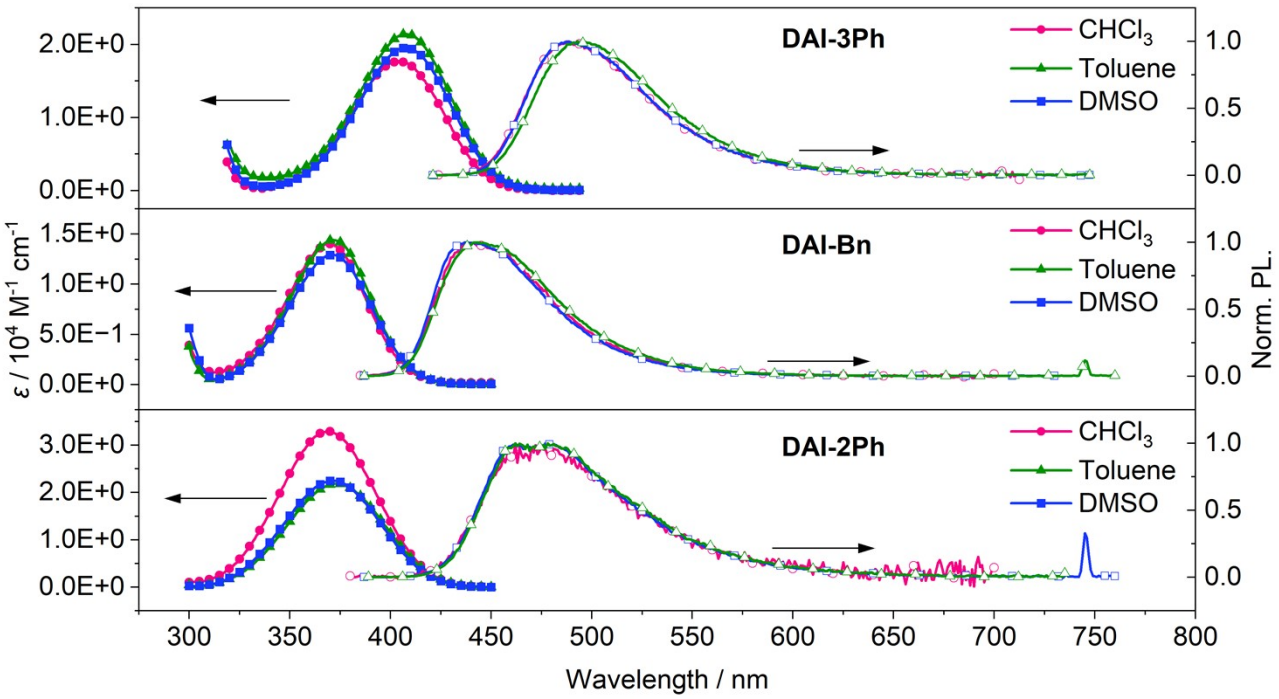

Figure S3. UV–vis absorption and photoluminescence spectra of DAI complexes in $CHCl_3$, toluene, and DMSO.

Photophysical properties of DAI complexes in various molecular environments

Crystal samples were prepared by recrystallization from DCM/hexane mixed solutions. Amorphous samples were prepared by the following melt-quenching method except for **DKI-5Ph**: A crystalline powder placed on a quartz substrate was heated on a hot plate until the sample melted entirely, and then it was immediately taken into a freezer (–20 °C) to give an amorphous solid. For **DKI-5Ph**, which shows remarkably high crystallinity, the crystalline powder was melted on a single-crystal silicon substrate, and then it was immediately taken into room-temperature water in a glass Petri dish to give an amorphous solid. Powder X-ray diffraction data indicated the melt-quenched samples were composed of an amorphous phase (Figure S4).

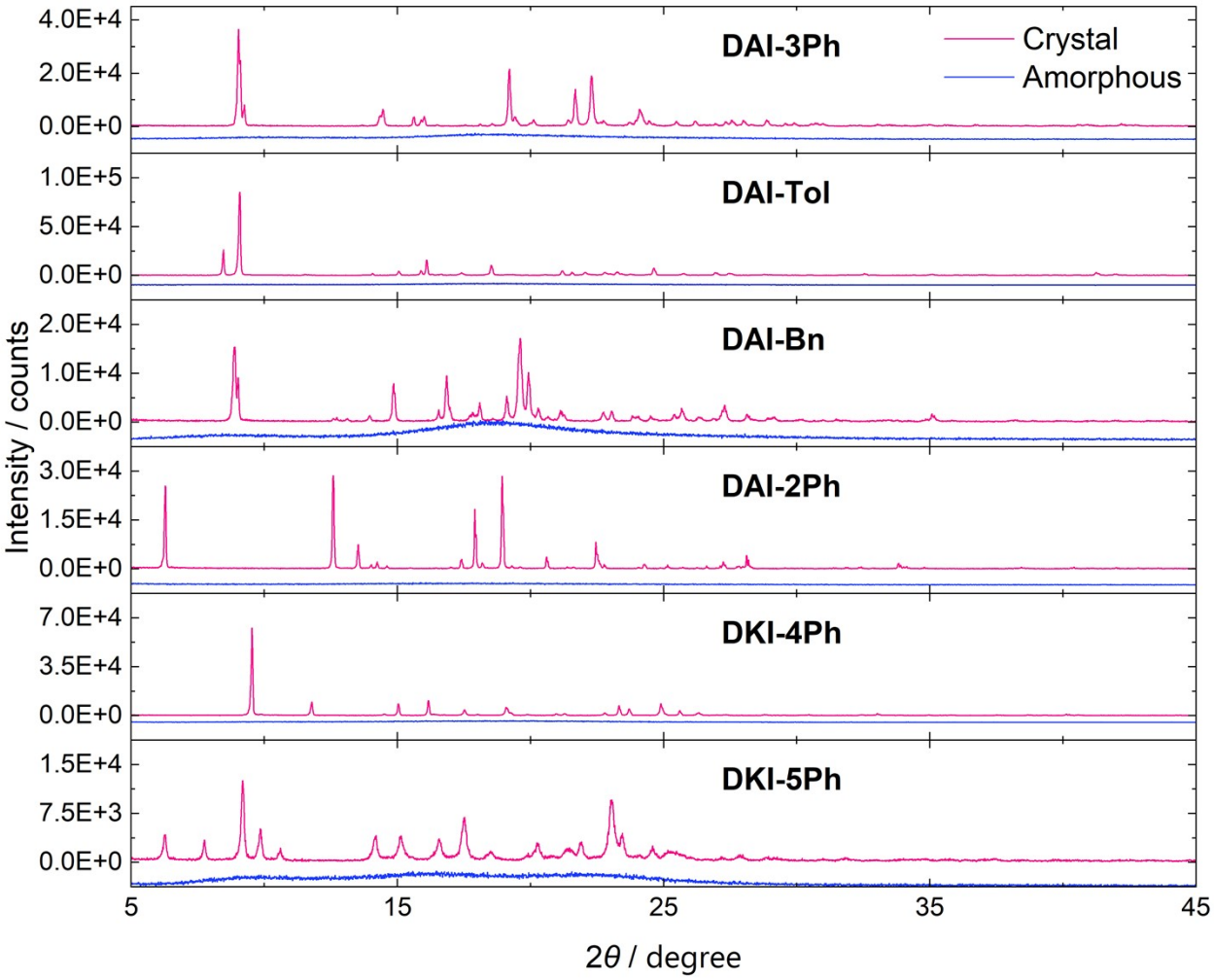

Figure S4. Powder X-ray diffraction profiles of the crystalline powder (magenta) and the amorphous solid (blue) of the synthesized complexes.

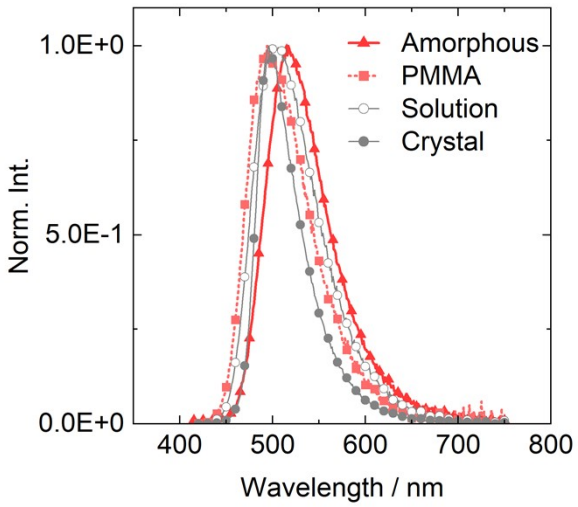

Figure S5. Normalized photoluminescence spectra of **DAI-Tol** in amorphous, PMMA, solution, and crystalline states.

Films of DAI polymers with different thickness

Thin films of DAI polymers were fabricated on a quartz substrate (1 × 1 cm^2). The surface of quartz substrates was modified with octadecyltrimethoxysilane by the following procedure: A pristine quartz substrate was treated with piranha solution (H_2SO_4/H_2O_2 = 3/1, v/v) at 80 °C for 2 h and rinsed with deionized water. It was washed by ultrasonication in deionized water, acetone, and isopropanol for 10 min each. Then, the substrate was subjected to the hot vapor of isopropanol for 3 min in a beaker on a hot plate (180 °C). The pre-cleaned substrate was treated with UV/O_3 for 30 min in a UV/O_3 cleaner (Filgen UV253E). The substrate was immersed into a solution of octadecyltrimethoxysilane (0.01 M in deoxygenated toluene) for 16 h at room temperature. It was washed by ultrasonication in toluene, acetone, and isopropanol for 10 min each. Polymer films were fabricated onto the modified quartz substrates by the spin-coat method (1000 rpm, 30 sec) with 20 μL cm^{-1} of polymer solutions. Concentration of polymer solutions was varied from 0.5, 1, 5, 10, 20 mg mL^{-1} for controlling film thickness. The as-cast films were dried under a vacuum for several hours. Film thickness was measured with a Bruker DektakXT profilometer.

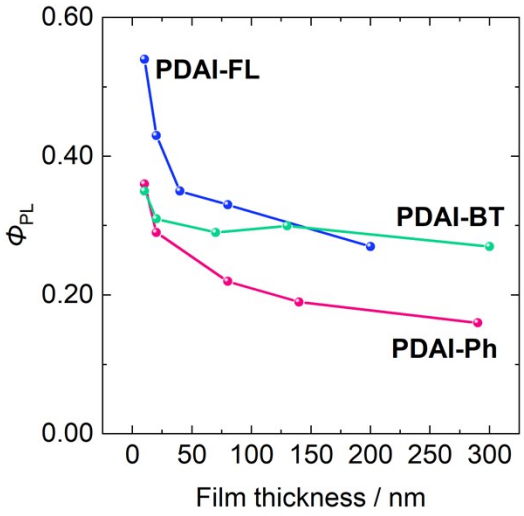

Figure S6. Photoluminescence quantum yields of the films of DAI polymers with different thickness.

Molecular weight dependence on photophysical properties of PDAI-Ph

Pristine **PDAI-Ph** was fractionated into four fractions with high-performance liquid chromatography using $CHCl_3$ as an eluent. All samples were reprecipitated into MeOH and collected by suction filtration. M_n of each fraction was determined with SEC as 45, 27, 15, and 10 kDa (Figure S5 and Table S1). UV–vis absorption and photoluminescence spectra of each fraction were recorded (Figure S6).

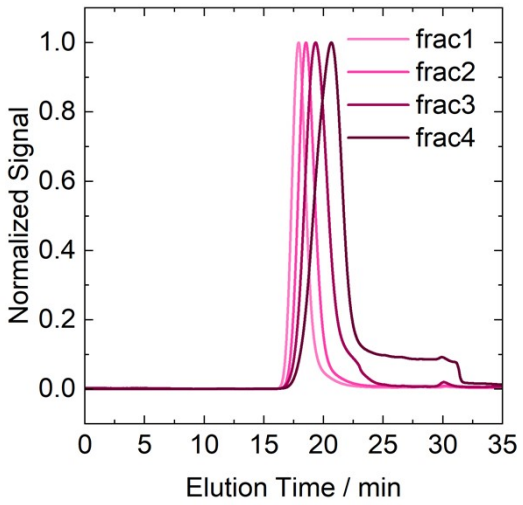

Figure S7. Chromatogram of the fractionated **PDAI-Ph**. $CHCl_3$ was used as an eluent.

Table S1. Properties of fractionated **PDAI-Ph**

Fraction	M_n	$Đ$	X_n
1	45,000	1.4	62
2	27,000	1.4	37
3	15,000	1.5	21
4	10,000	1.4	14

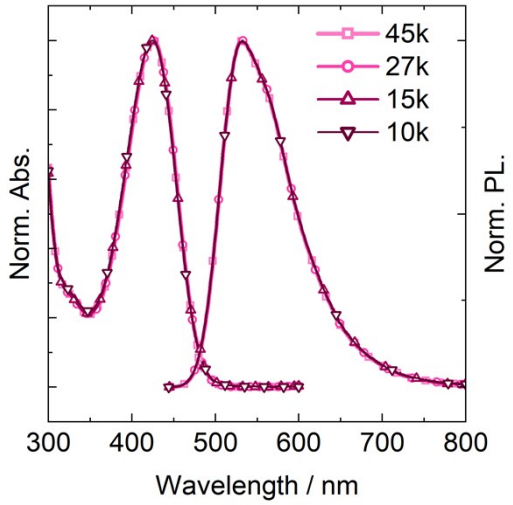

Figure S8. Normalized UV-vis absorption and photoluminescence spectra of PDAI-Ph with different molecular weights (M_n = 45, 27, 15, and 10 kDa).

Lippert–Mataga Plots for DAI Polymers

Absorption and photoluminescence spectra of the DAI polymers were measured in cyclohexane (Cy), toluene (Tol), chloroform, ethyl acetate (AcOEt), dimethyl sulfoxide (DMSO), and methanol (Figure S7). Lippert–Mataga plots were made with the data except for one of **PDAI-Ph** in Cy because of the incomplete solubility of the polymer (Figure S8).

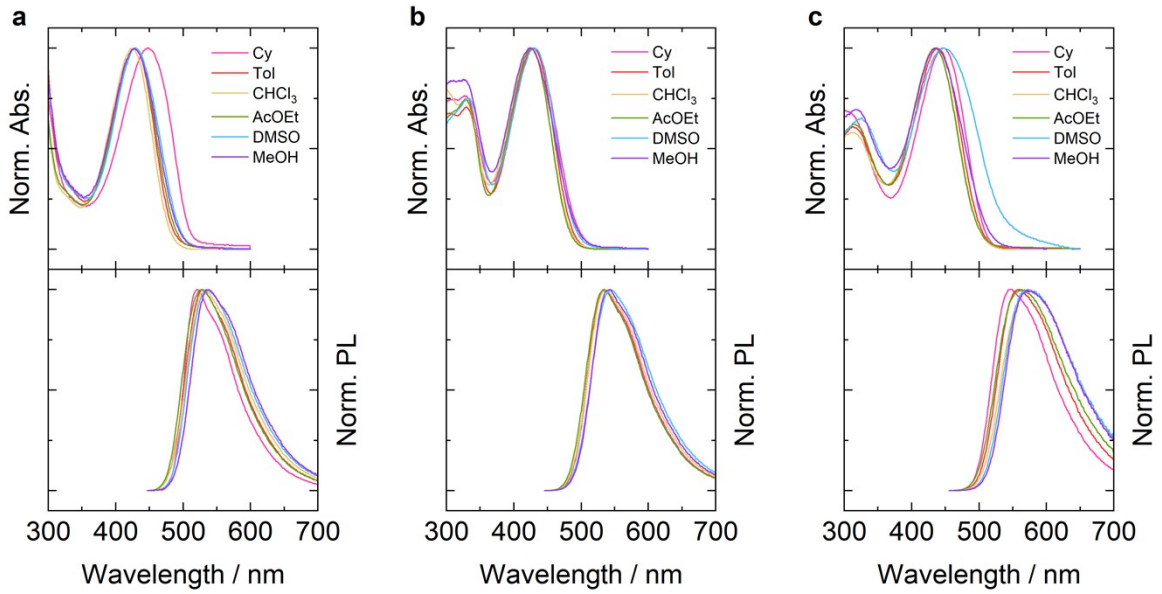

Figure S9. Normalized UV–vis and photoluminescence spectra of (a) **PDAI-Ph**, (b) **PDAI-FL**, and (c) **PDAI-BT** in different solutions.

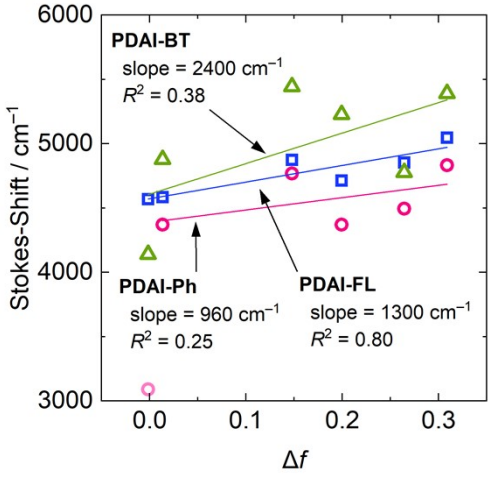

Figure S10. Lippert–Mataga plots for **PDAI-Ph** (magenta, circle), **PDAI-FL** (blue, square), and **PDAI-BT** (green, triangle). Open symbols, measured data; solid lines, fitted line. The data of **PDAI-Ph** in cyclohexane (light magenta) was omitted in the fitting due to the incomplete solubility of the polymer.

Cyclic Voltammetry

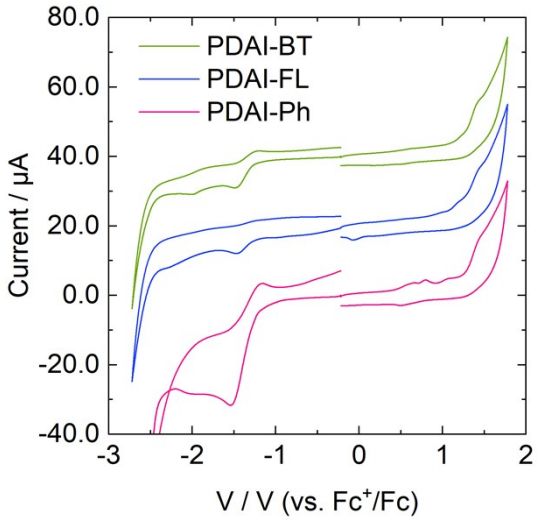

Figure S11. Cyclic voltammogram for DAI polymers.

Theoretical Calculations

Gaussian 16 Rev. C[3] was used for density functional theory (DFT) and time-dependent DFT (TD-DFT) calculations. Firstly, geometry optimization was conducted for each compound in ground singlet (S_0) and excited singlet (S_1) states at the CAM-B3LYP/6-31+G(d,p) level of theory. Optimized structures at S_0 states (S_0^{MIN}) were obtained for all compounds and were confirmed as local minima on each potential energy surface using frequency calculations. It should be noted that these calculations have overestimated the transition energies, especially for **DAI-3Ph** and **DAI-Tol**. This is probably because their HOMO/LUMO overlap is relatively small, leading to small exchange integral, like non-alternant hydrocarbons.[4]

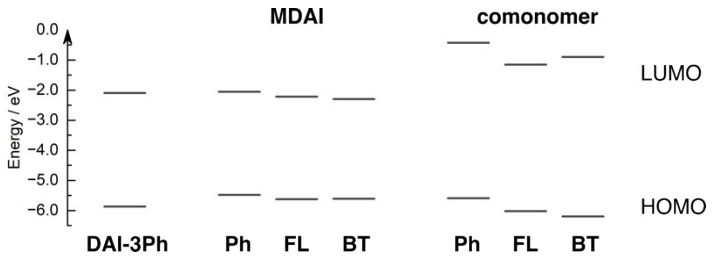

Figure S12. HOMO and LUMO energy diagrams for **DAI-3Ph**, **MDAI-Ph**, **MDAI-FL**, **MDAI-BT**, and the corresponding comonomers.

Two-root (S_0 and S_1) state-averaged restricted active space self-consistent field (SA2-RASSCF) calculations were performed by the Molpro 2021.2 package.[5–7] GaussView 6 and VESTA 3[8] were used for visualization of the calculation results.

Table S2. Defined active space for SA2-RASSCF calculations[a]

	Active space	RAS1[b]	RAS2[c]	RAS3[d]
DAI-2Ph	(12e, 12o)	4o	4o	4o
DAI-3Ph	(16e, 16o)	6o	4o	6o
DKI-4Ph	(26e, 25o)	11o	4o	10o

[a]e, o, and h denote electron, orbital, and hole, respectively. [b]One or two excitations (holes) were allowed from RAS1. [c]Any number of electrons was allowed in RAS2. [d]A maximum of two electrons in RAS3 was allowed.

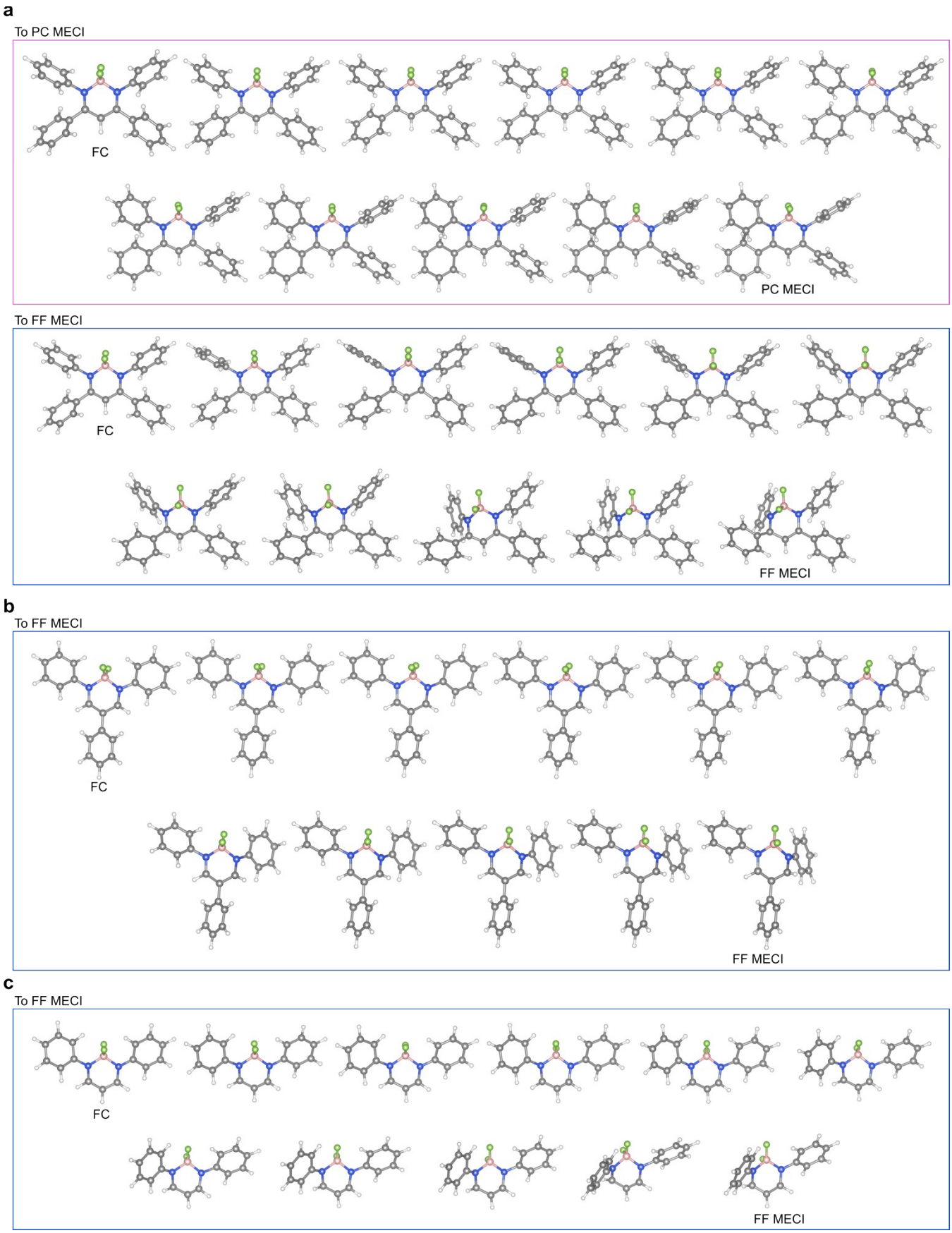

Figure S13. LIIC from FC to each MECI for (a) **DKI-4Ph**, (b) **DAI-3Ph**, and (c) **DAI-2Ph**.

NMR Spectra

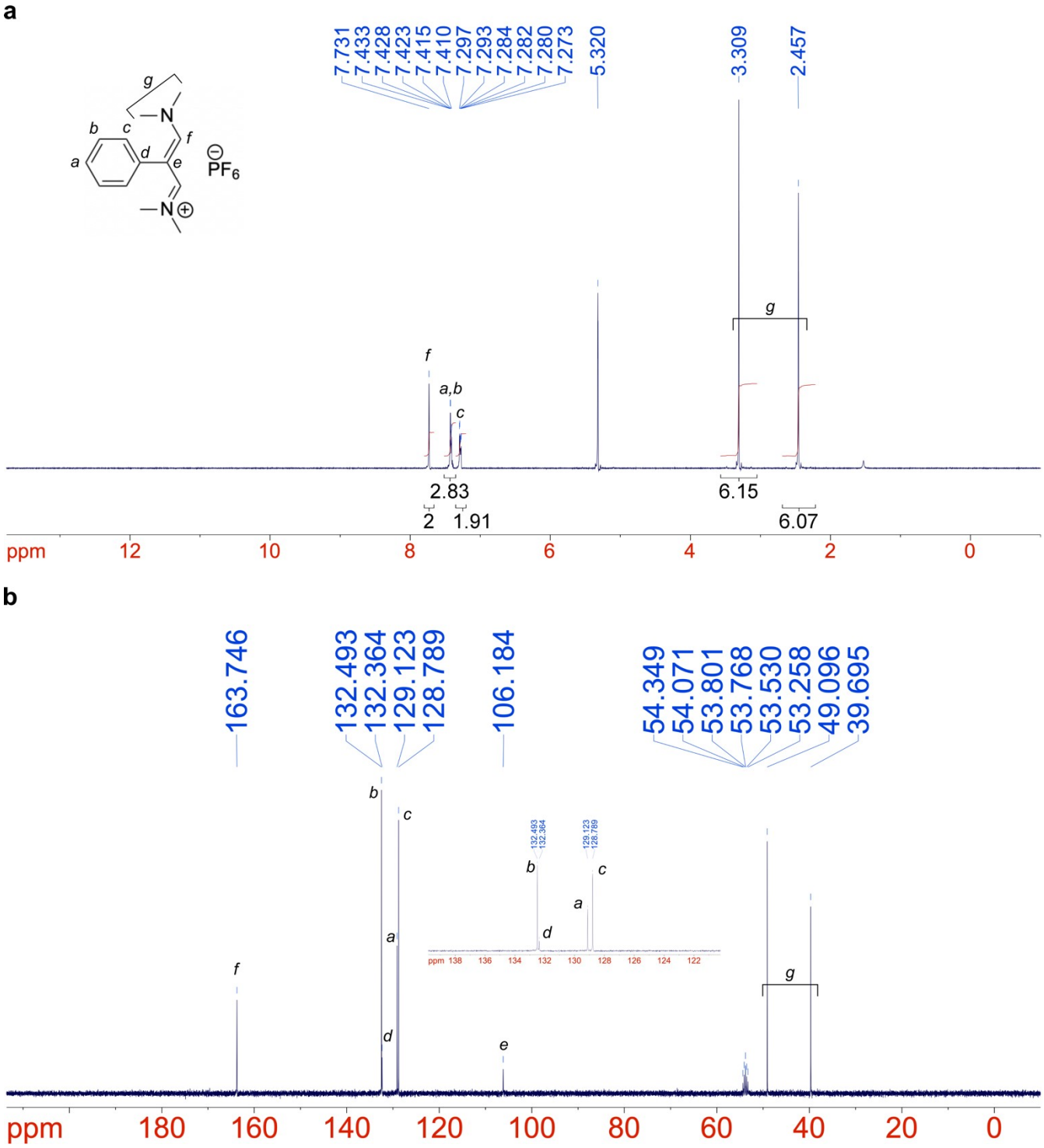

Figure S14. (a) ^{1}H and (b) $^{13}C\{^{1}H\}$ NMR spectra of **Vin-Ph** in CD_2Cl_2.

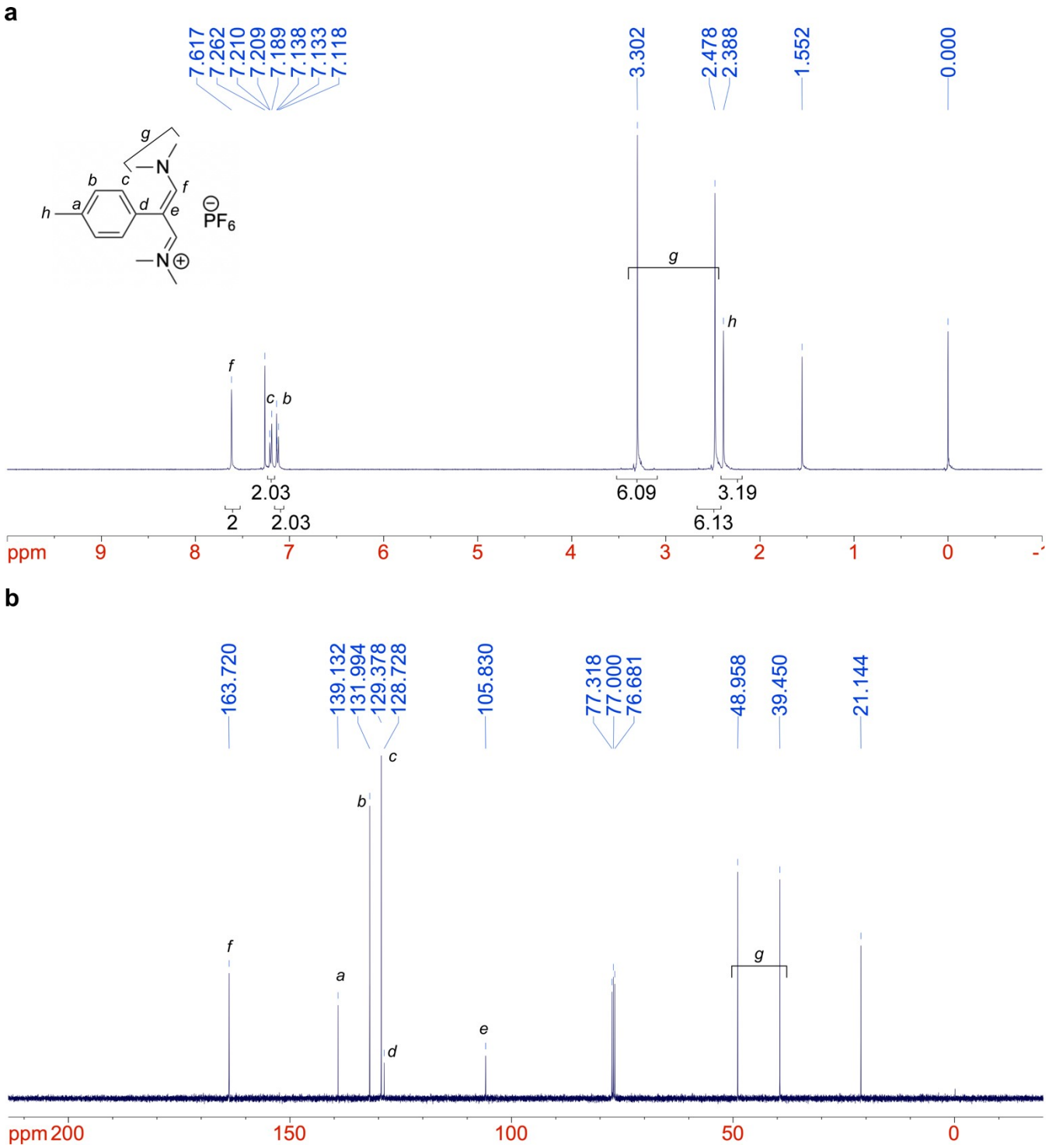

Figure S15. (a) ^{1}H and (b) ^{13}C{^{1}H} NMR spectra of **Vin-Tol** in $CDCl_3$.

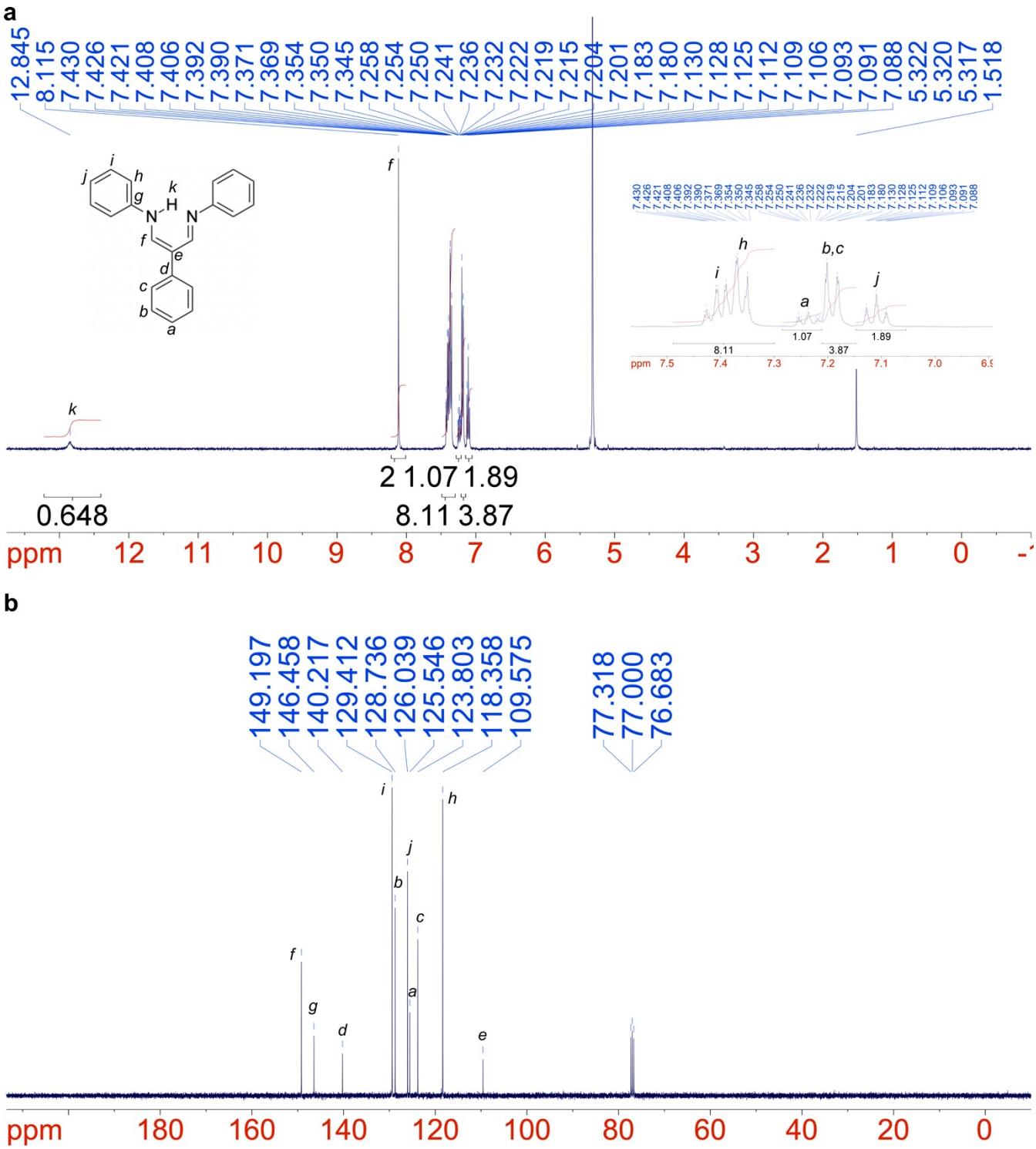

Figure S16. (a) ^{1}H and (b) ^{13}C{^{1}H} NMR spectra of **DAI-3Ph_L** in CD_2Cl_2 and $CDCl_3$, respectively.

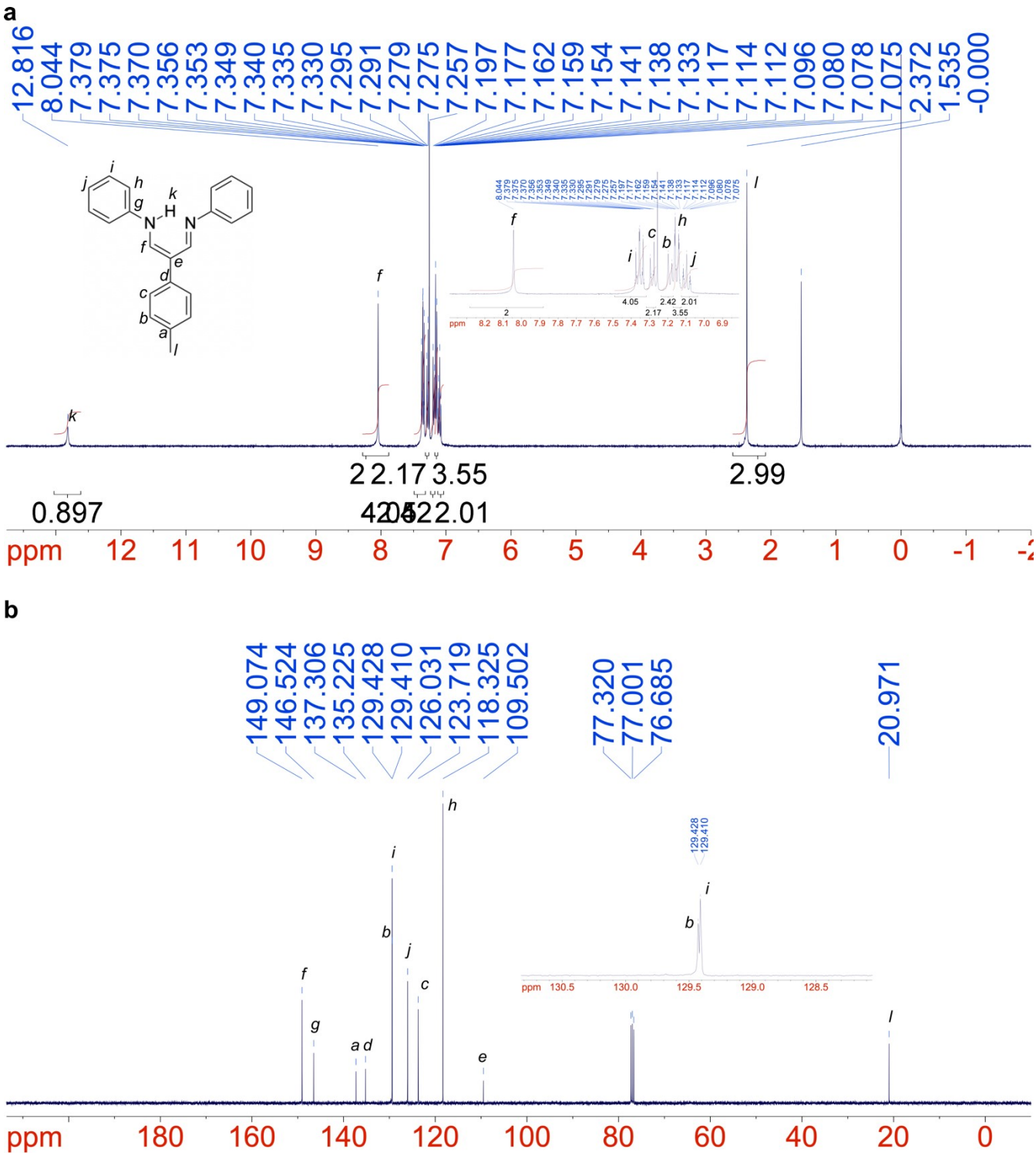

Figure S17. (a) ^{1}H and (b) ^{13}C{^{1}H} NMR spectra of **DAI-Tol_L** in $CDCl_3$.

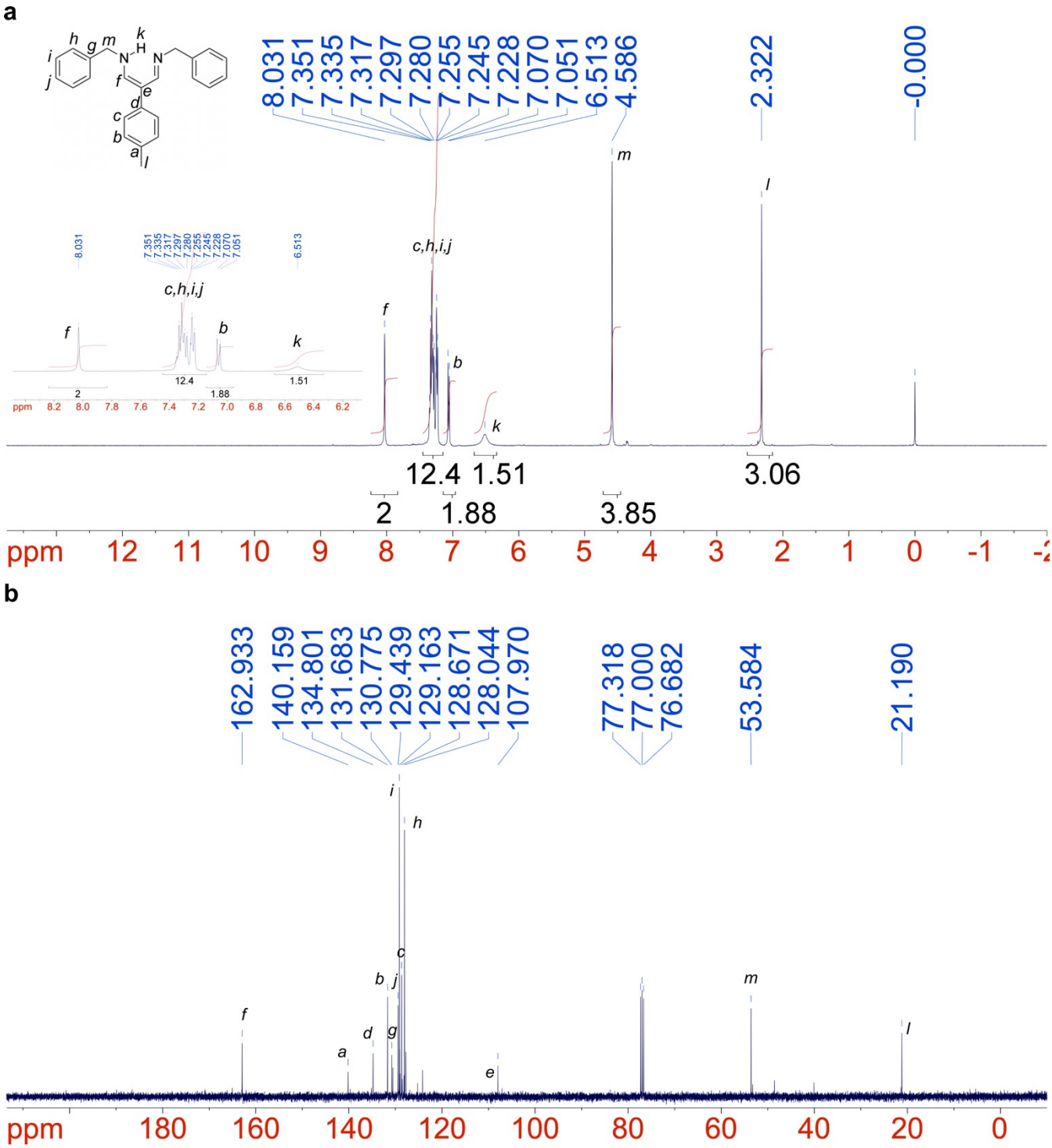

Figure S18. (a) ^{1}H and (b) ^{13}C{^{1}H} NMR spectra of **DAI-Bn_L** in $CDCl_3$.

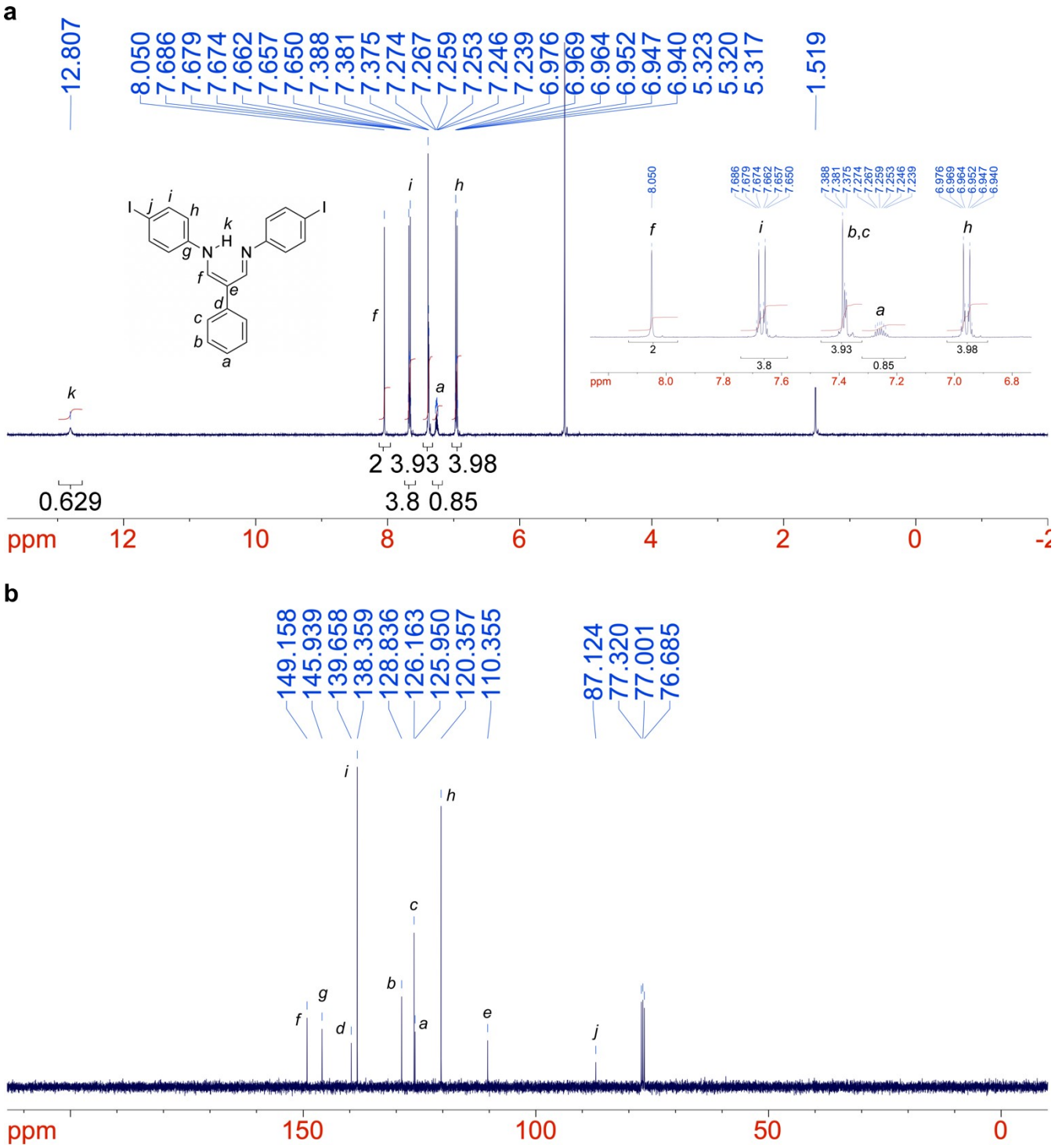

Figure S19. (a) ^{1}H and (b) $^{13}C\{^{1}H\}$ NMR spectra of **DAI-Ph-I_L** in CD_2Cl_2 and $CDCl_3$, respectively.

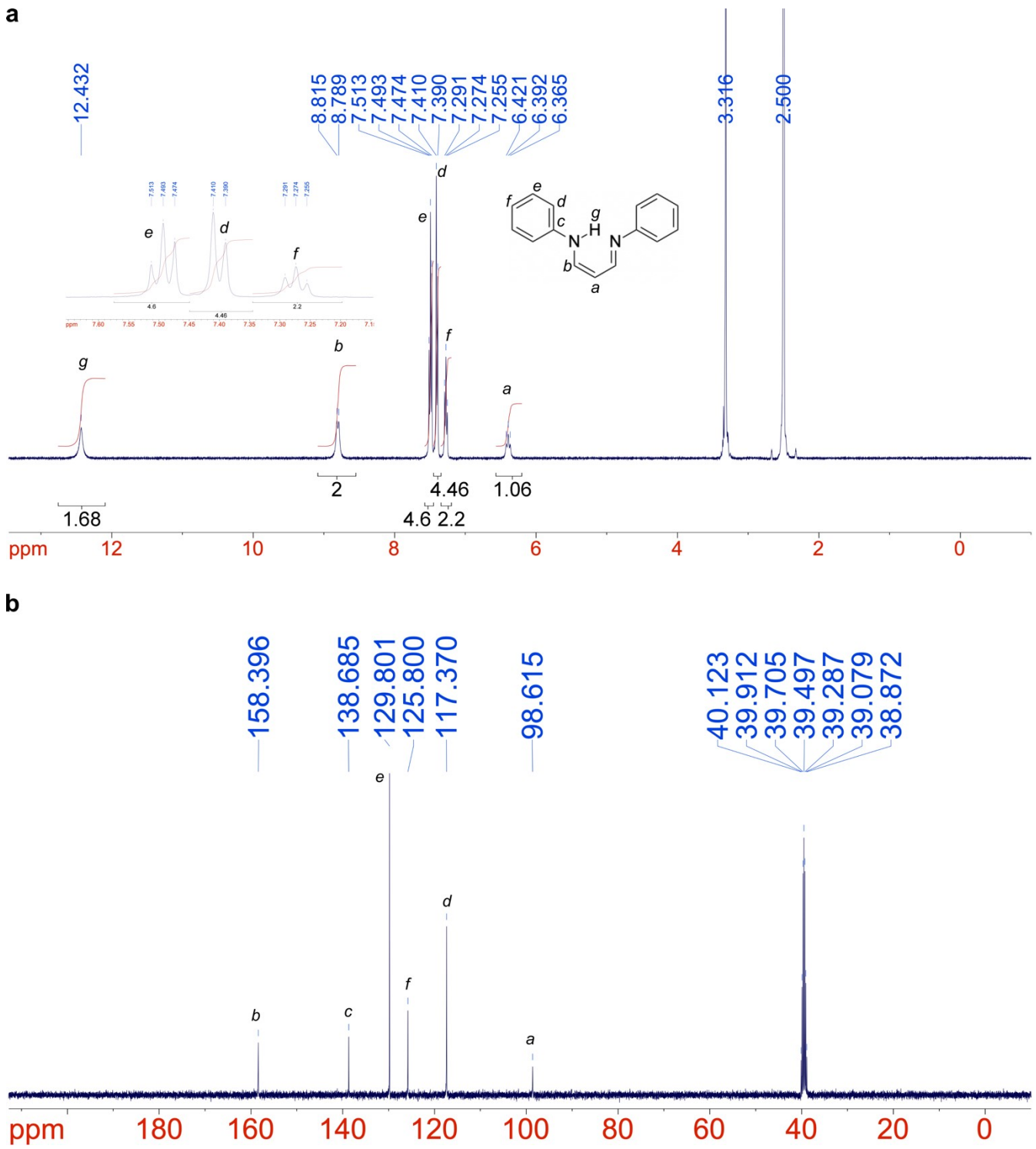

Figure S20. (a) ^{1}H and (b) ^{13}C{^{1}H} NMR spectra of **DAI-2Ph_L** in DMSO-*d*6.

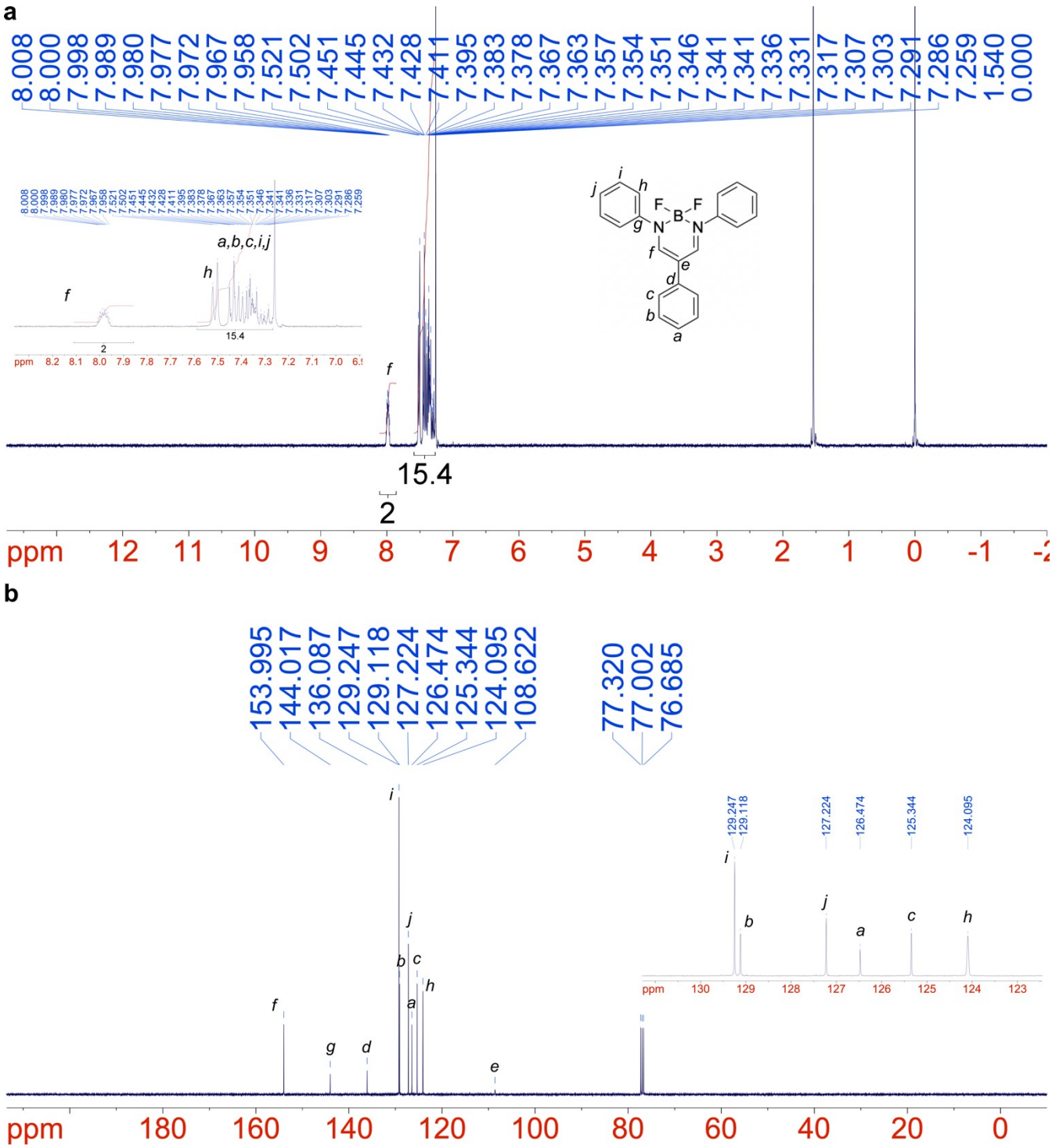

Figure S21. (a) ^{1}H and (b) ^{13}C{^{1}H} NMR spectra of **DAI-3Ph** in $CDCl_3$.

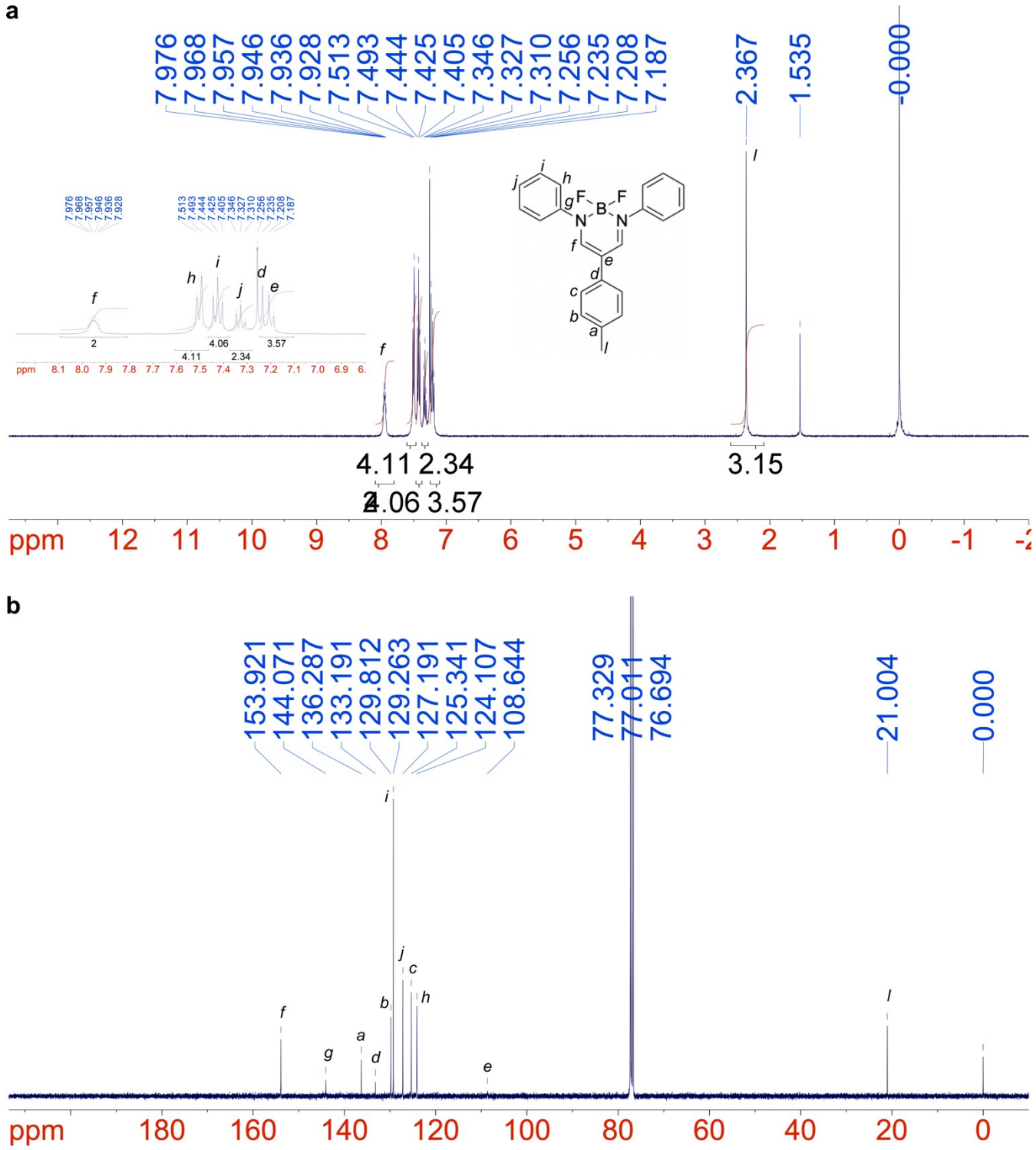

Figure S22. (a) ^{1}H and (b) ^{13}C{^{1}H} NMR spectra of **DAI-Tol** in $CDCl_3$.

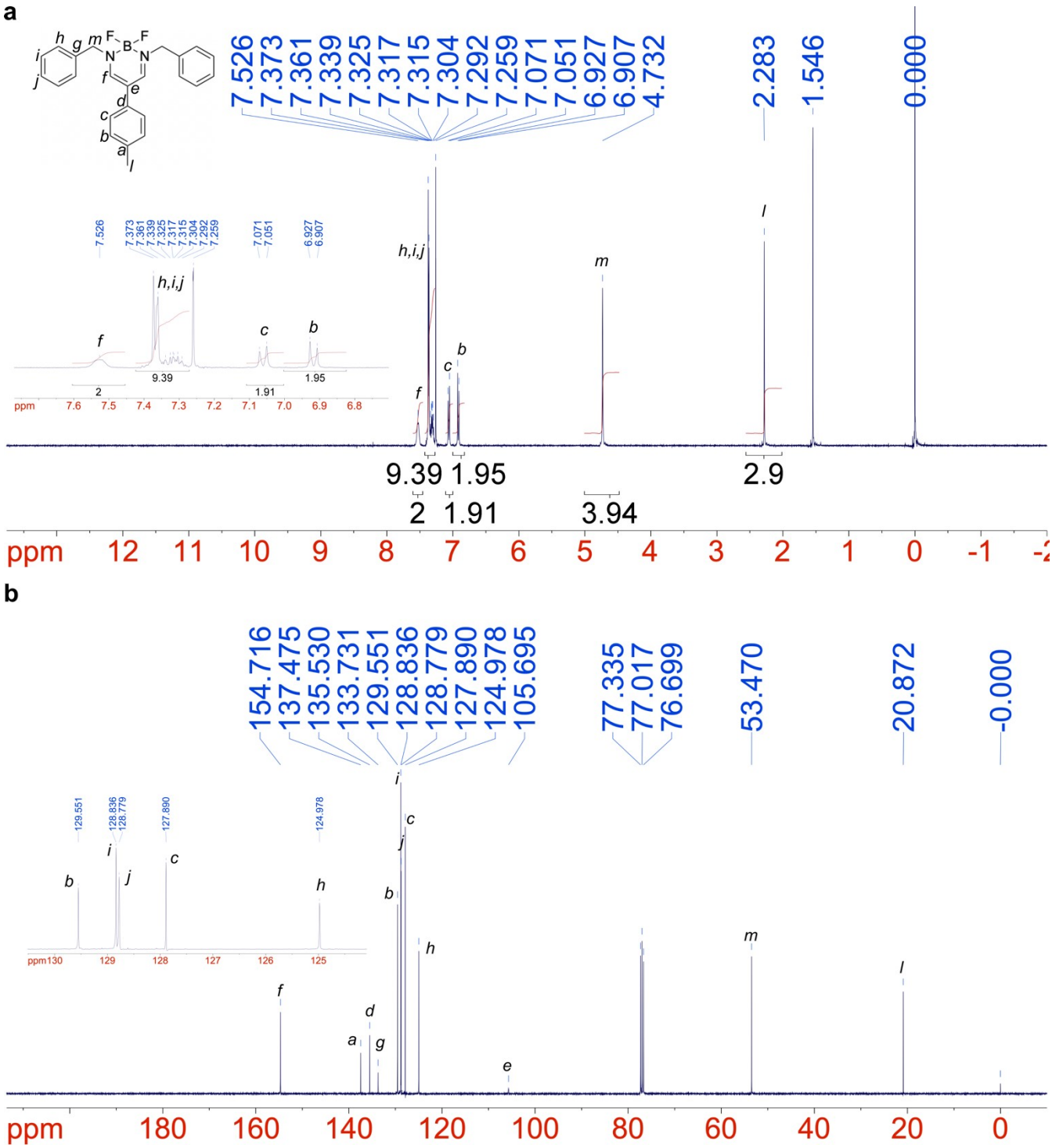

Figure S23. (a) ^{1}H and (b) ^{13}C{^{1}H} NMR spectra of **DAI-Bn** in $CDCl_3$.

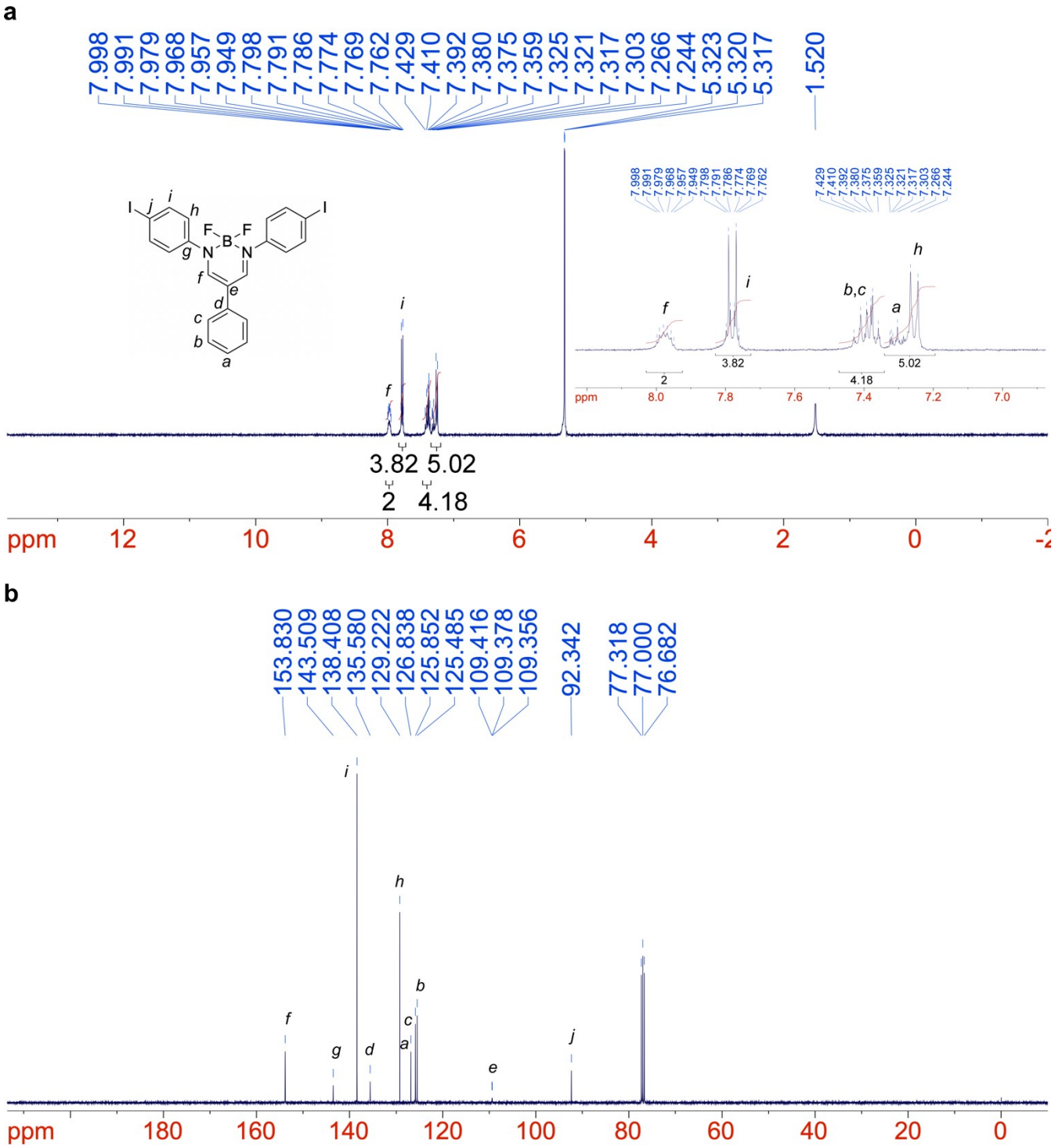

Figure S24. (a) ^{1}H and (b) ^{13}C{^{1}H} NMR spectra of **DAI-3Ph-I** in CD_2Cl_2 and $CDCl_3$, respectively.

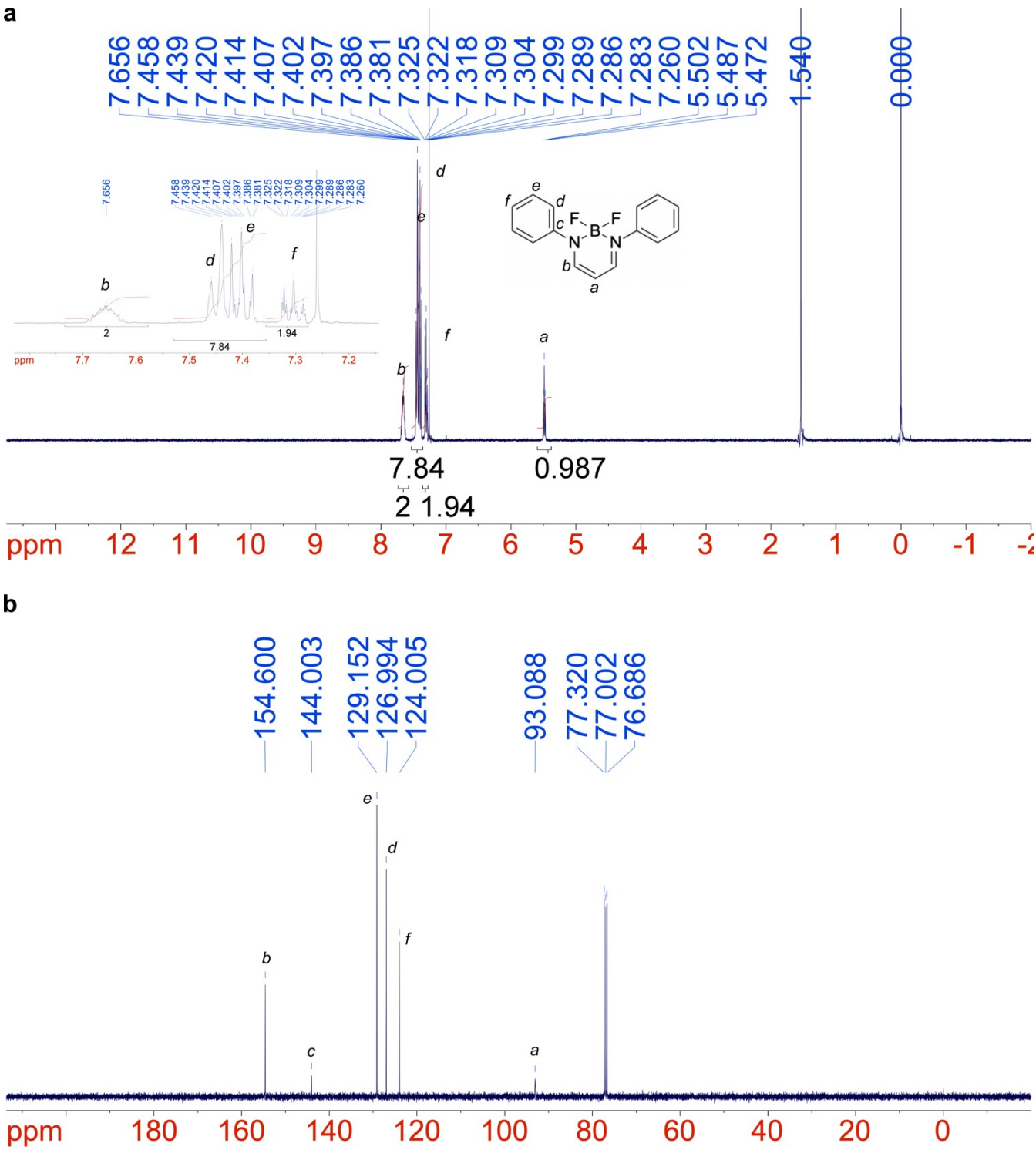

Figure S25. (a) ^{1}H and (b) ^{13}C{^{1}H} NMR spectra of **DAI-2Ph** in $CDCl_3$.

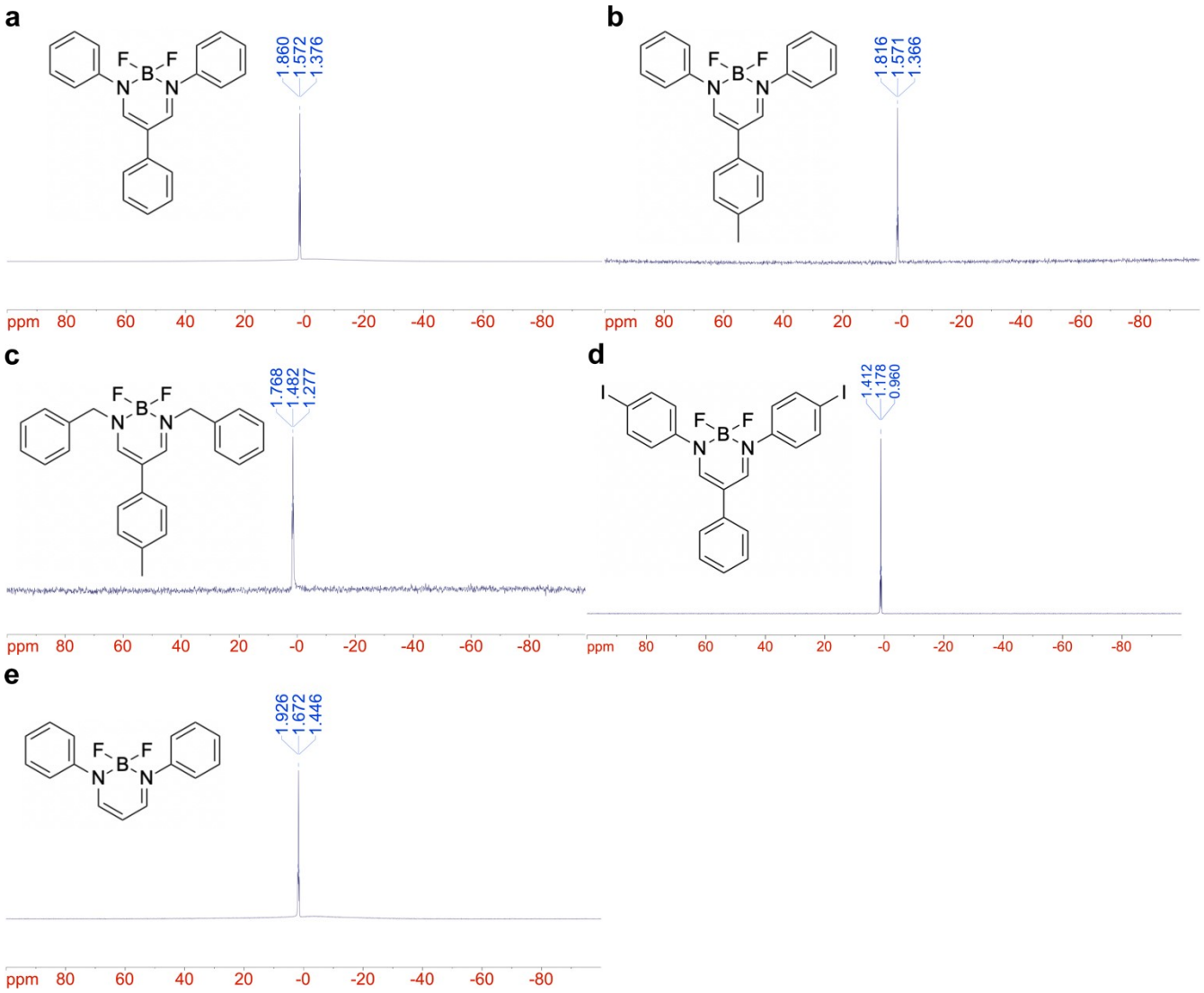

Figure S26. $^{11}B\{^{1}H\}$ NMR spectra of (a) **DAI-3Ph**, (b) **DAI-Tol**, (c) **DAI-Bn**, (d) **DAI-3Ph-I**, and (e) **DAI-2Ph** in $CDCl_3$.

a

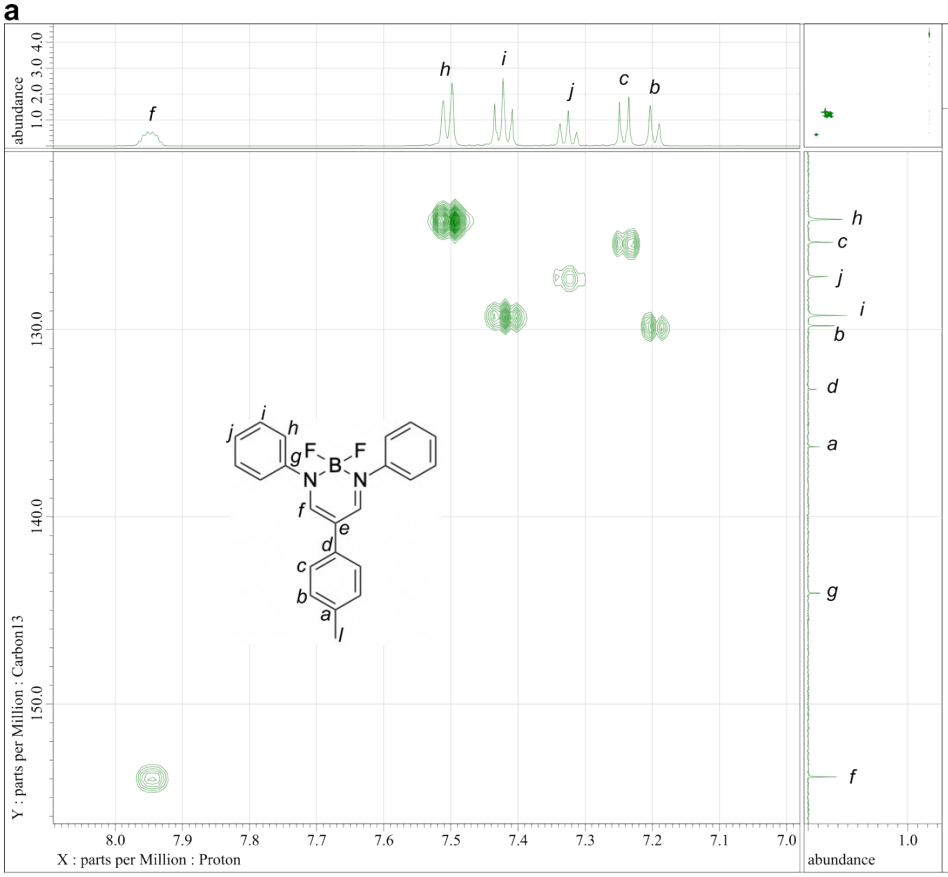


```
Filename            = kusaka-hashizume-DAIBF_30
Author              = delta
Experiment          = hmqc.jxp
Sample_Id           = kusaka-hashizume-DAIBF_30
Solvent             = CHLOROFORM-D
Actual_Start_Time   = 31-JAN-2019 15:49:23
Revision_Time       = 19-FEB-2022 09:47:48

Comment             = gradient enhanced HMQC wi
Data_Format         = 2D REAL REAL
Dim_Size            = 819, 512
X_Domain            = Proton
Y_Domain            = Carbon
Dim_Title           = Proton Carbon13
Dim_Units           = [ppm] [ppm]
Dimensions          = X Y
Spectrometer        = DELTA2_NMR

Field_Strength      = 14.09636928[T] (600[MHz])
X_Acq_Duration      = 0.19980288[s]
X_Domain            = 1H
X_Freq              = 600.1723046[MHz]
X_Offset            = 5.1341[ppm]
X_Points            = 1024
X_Prescans          = 4
X_Resolution        = 5.00493286[Hz]
X_Sweep             = 5.12505125[kHz]
X_Sweep_Clipped     = 4.100041[kHz]
Y_Domain            = 13C
Y_Freq              = 150.91343039[MHz]
Y_Offset            = 88.71462[ppm]
Y_Points            = 256
Y_Prescans          = 0
Y_Resolution        = 96.68935644[Hz]
Y_Sweep             = 24.75247525[kHz]
Tri_Domain          = Proton
Tri_Freq            = 600.1723046[MHz]
Tri_Offset          = 5[ppm]
Clipped             = FALSE
Scans               = 2
Total_Scans         = 512

Relaxation_Delay    = 1.5[s]
Recvr_Gain          = 98
Temp_Get            = 30[dC]
X_Acq_Time          = 0.19980288[s]
X_Atn               = 4.8[dB]
X_Gamma             = 42576375
X_Pulse             = 11.8[us]
Y_Acq_Time          = 10.3424[ms]
Y_Atn               = 8[dB]
Y_Gamma             = 10705836.9
Y_Pulse             = 9.98[us]
Irr_Atn_Dec         = 27.84[dB]
Irr_Noise           = MPF8
Irr_Pwidth          = 98[us]
Tri_Mode            = Off
Dante_Presat        = FALSE
Decoupling          = TRUE
Delay_Time          = 1.5[s]
Grad_1              = 1[ms]
```

b

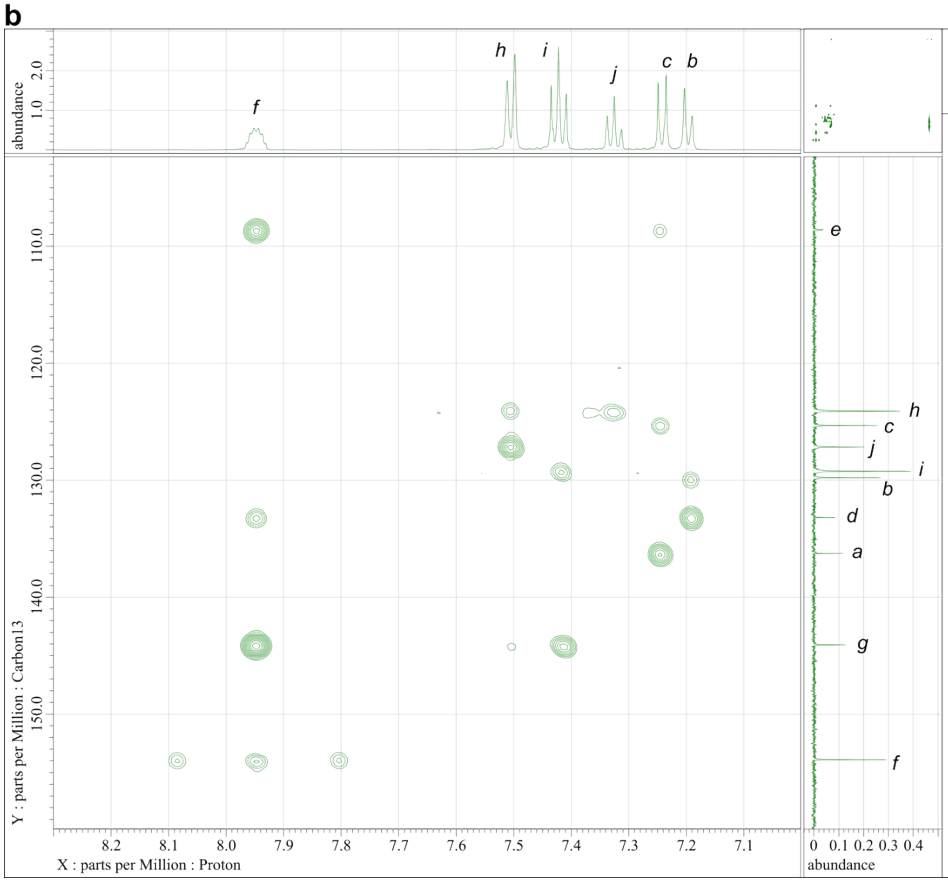


```
Filename            = kusaka-hashizume-DAIBF_30
Author              = delta
Experiment          = hmbc.jxp
Sample_Id           = kusaka-hashizume-DAIBF_30
Solvent             = CHLOROFORM-D
Actual_Start_Time   = 31-JAN-2019 16:04:39
Revision_Time       = 19-FEB-2022 10:15:00

Comment             = gradient enhanced HMBC
Data_Format         = 2D REAL REAL
Dim_Size            = 1638, 512
X_Domain            = Proton
Y_Domain            = Carbon
Dim_Title           = Proton Carbon13
Dim_Units           = [ppm] [ppm]
Dimensions          = X Y
Spectrometer        = DELTA2_NMR

Field_Strength      = 14.09636928[T] (600[MHz])
X_Acq_Duration      = 0.39960576[s]
X_Domain            = 1H
X_Freq              = 600.1723046[MHz]
X_Offset            = 5.1341[ppm]
X_Points            = 2048
X_Prescans          = 4
X_Resolution        = 2.50246643[Hz]
X_Sweep             = 5.12505125[kHz]
X_Sweep_Clipped     = 4.100041[kHz]
Y_Domain            = 13C
Y_Freq              = 150.91343039[MHz]
Y_Offset            = 88.71462[ppm]
Y_Points            = 256
Y_Prescans          = 0
Y_Resolution        = 96.68935644[Hz]
Y_Sweep             = 24.75247525[kHz]
Tri_Domain          = Proton
Tri_Freq            = 600.1723046[MHz]
Tri_Offset          = 5[ppm]
Clipped             = FALSE
Scans               = 4
Total_Scans         = 1024

Relaxation_Delay    = 1.5[s]
Recvr_Gain          = 98
Temp_Get            = 30[dC]
X_Acq_Time          = 0.39960576[s]
X_Atn               = 4.8[dB]
X_Gamma             = 42576375
X_Pulse             = 11.8[us]
Y_Acq_Time          = 10.3424[ms]
Y_Atn               = 8[dB]
Y_Gamma             = 10705836.9
Y_Pulse             = 9.98[us]
Tri_Mode            = Off
Dante_Presat        = FALSE
Delay_Time          = 1.5[s]
Delta               = 62.5[ms]
Delta_1             = 3.83288616[ms]
Delta_2             = 3.43642612[ms]
Delta_3             = 3.11429461[ms]
Grad_1              = 1[ms]
```

Figure S27. (a) HMQC ($^{1}H–^{13}C$) and (b) HMBC ($^{1}H–^{13}C$) spectra of **DAI-Tol** in $CDCl_3$.

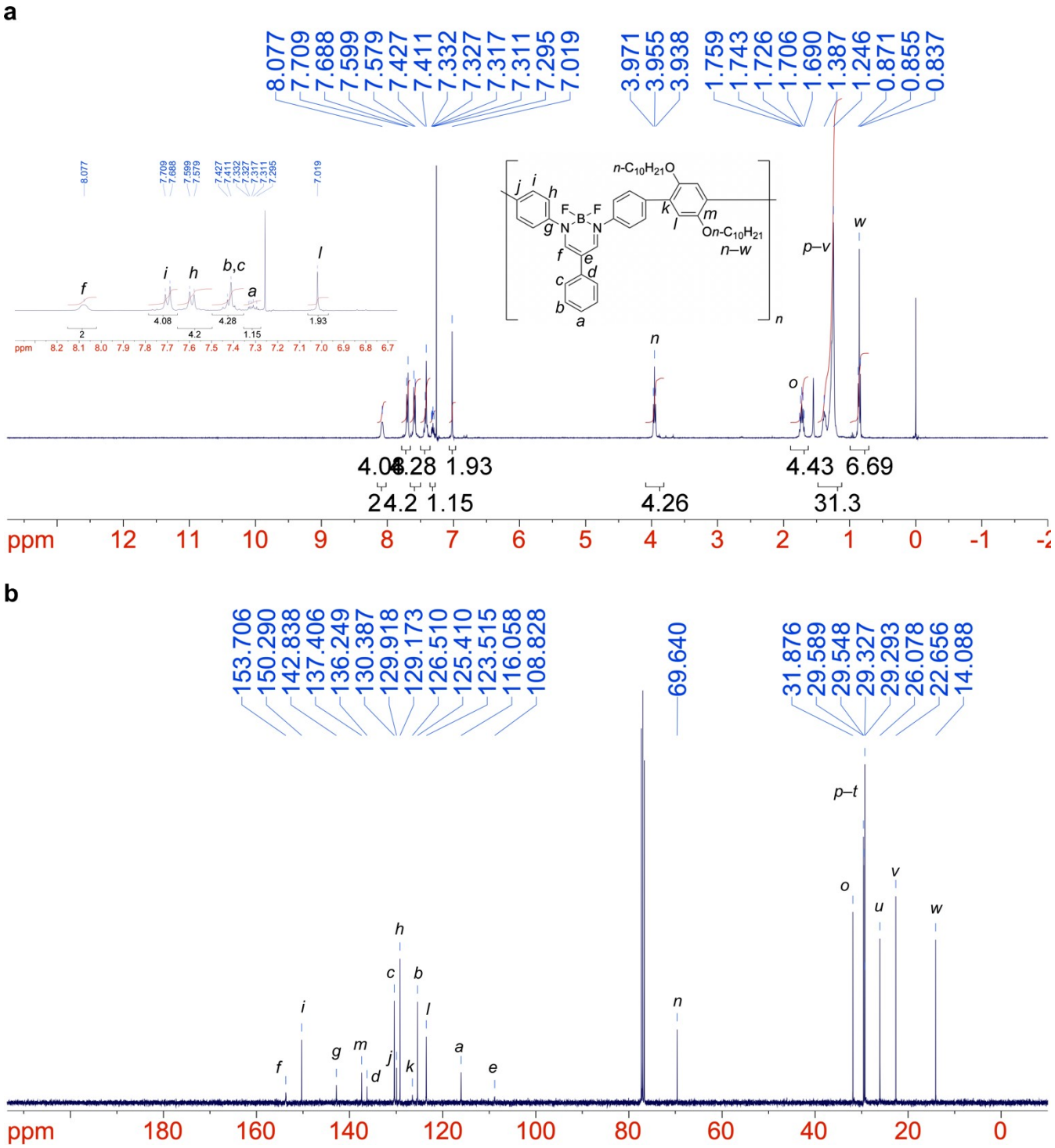

Figure S28. (a) ^{1}H and (b) ^{13}C{^{1}H} NMR spectra of **PDAI-Ph** in $CDCl_3$.

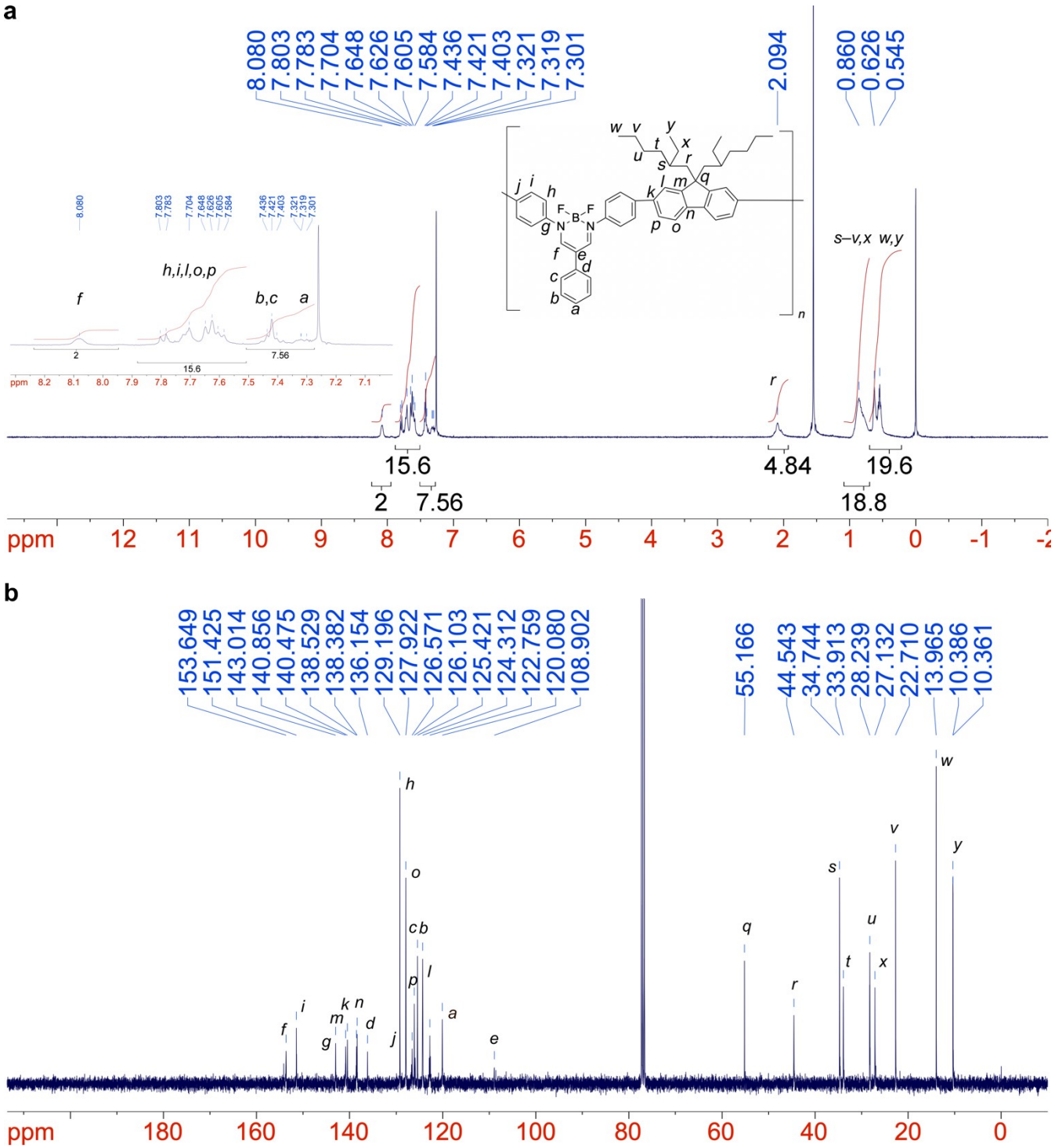

Figure S29. (a) ^{1}H and (b) ^{13}C{^{1}H} NMR spectra of **PDAI-FL** in $CDCl_3$.

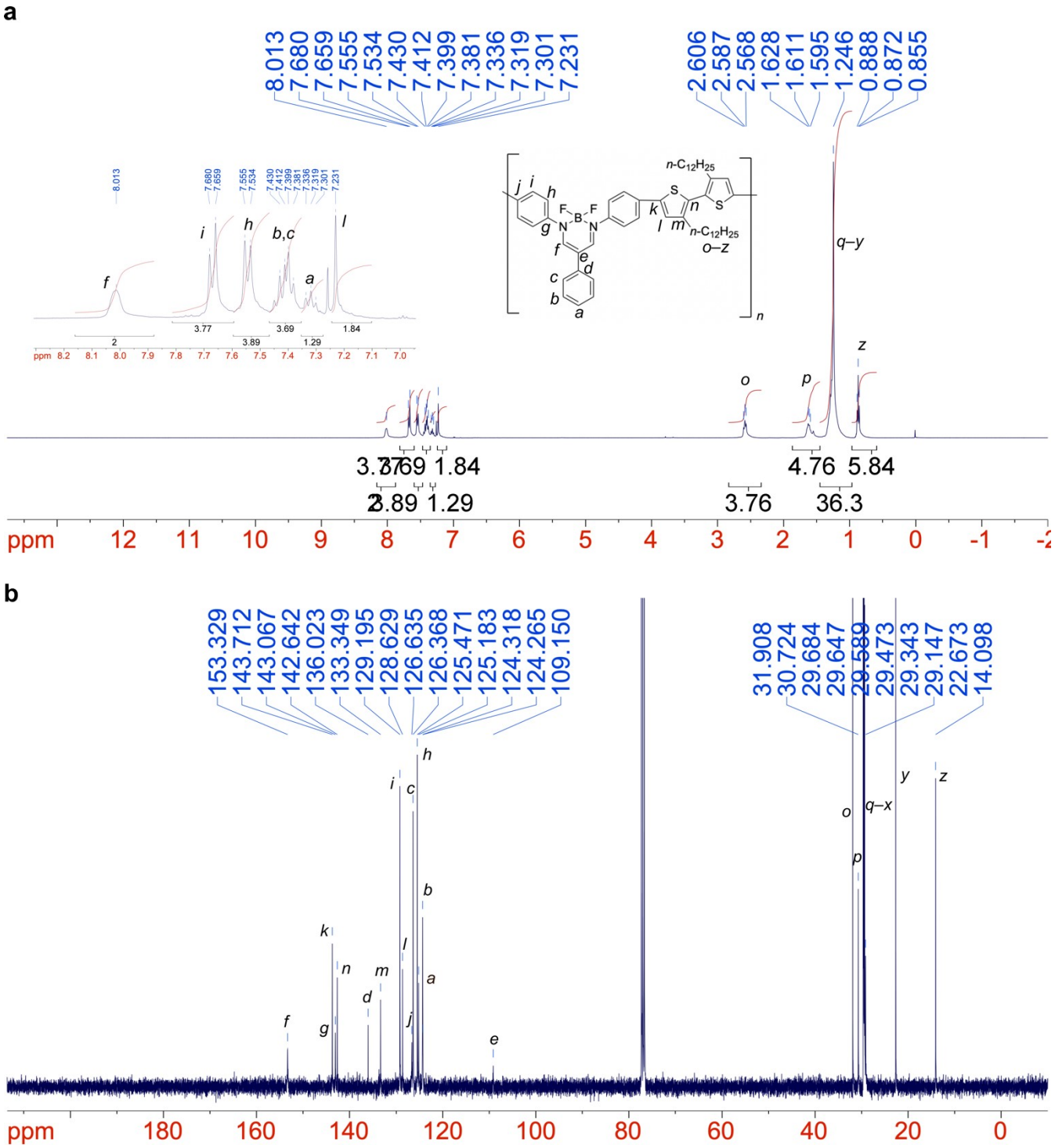

Figure S30. (a) ^{1}H and (b) ^{13}C{^{1}H} NMR spectra of **PDAI-BT** in $CDCl_3$.

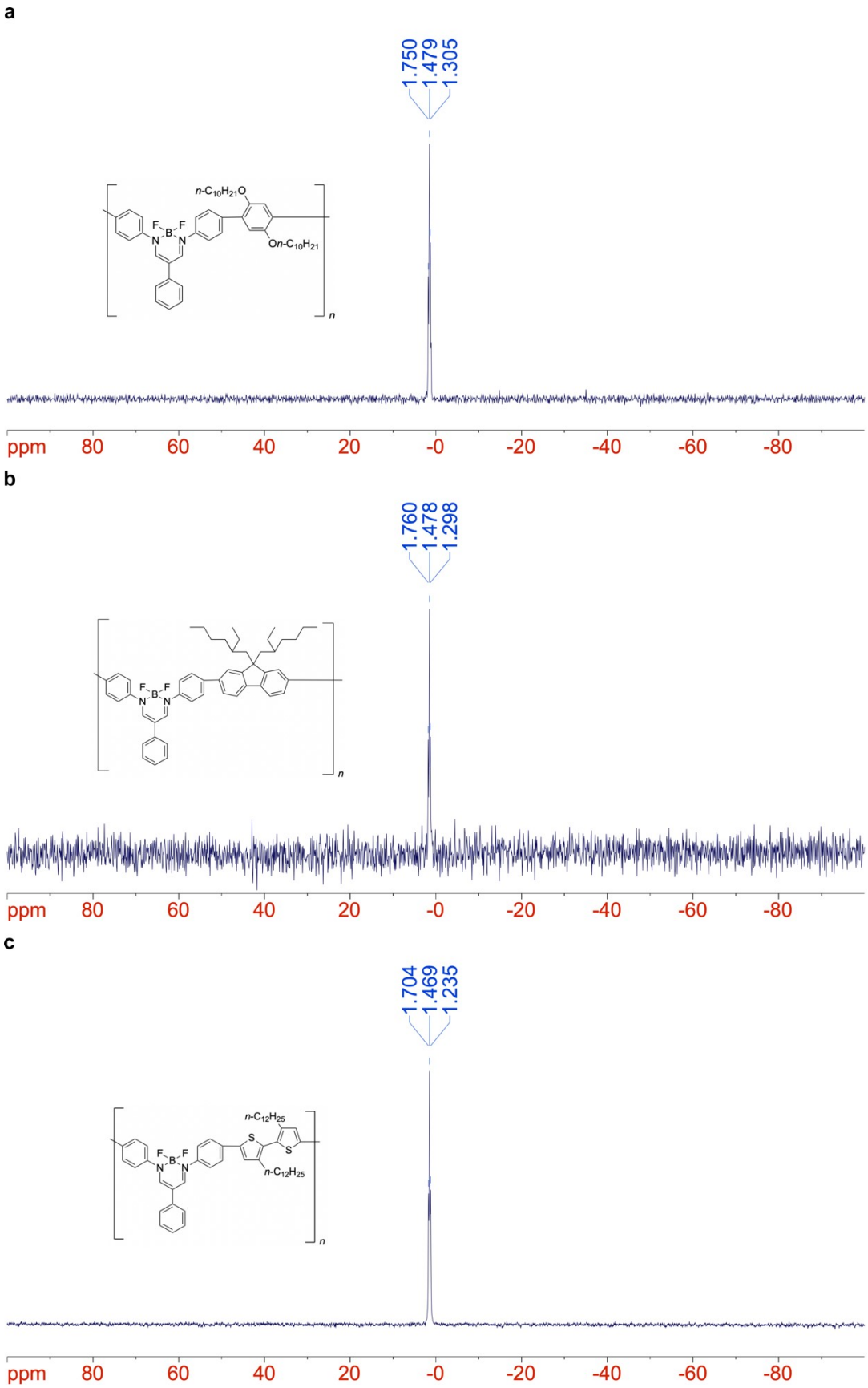

Figure S31. $^{11}B\{^{1}H\}$ NMR spectra of (a) **PDAI-Ph**, (b) **PDAI-FL**, and (c) **PDAI-BT**in $CDCl_3$.

Optimized Geometry and Calculated Properties

DAI-3Ph

Table S3. Optimized geometry of **DAI-3Ph** at S_0 state

Atomic Number	Coordinates (Angstroms)		
	x	y	z
5	-0.000025	-1.474929	-0.000039
9	-0.094689	-2.271558	-1.139924
9	0.094659	-2.271678	1.13971
7	1.258532	-0.555947	-0.073151
7	-1.258538	-0.555931	0.073111
6	-1.191311	0.763828	0.063612
6	0.000012	1.486402	-0.000027
6	1.191334	0.763803	-0.063676
6	0.000034	2.96785	-0.000007
6	-0.85122	3.687794	0.847017
6	-0.858334	5.078391	0.840433
6	0.000065	5.780957	0.000021
6	0.858446	5.078386	-0.84041
6	0.851302	3.687793	-0.847022
1	0.000079	6.866006	0.000031
6	2.552231	-1.17296	-0.030386
6	2.868465	-2.195825	-0.923444
6	4.130583	-2.777223	-0.879754
6	5.078604	-2.34715	0.044589
6	4.754504	-1.333342	0.940255
6	3.491548	-0.751785	0.910295
6	-2.552248	-1.172901	0.030397
6	-2.868559	-2.19562	0.923603
6	-4.130694	-2.776983	0.879965
6	-5.078668	-2.347016	-0.044479
6	-4.7545	-1.333356	-0.940285
6	-3.491525	-0.751836	-0.910369
1	-2.136072	1.300656	0.099276
1	2.136098	1.300628	-0.099311
1	-1.498413	3.154155	1.536768
1	-1.526616	5.614134	1.507263
1	1.526737	5.61413	-1.507231
1	1.498479	3.154152	-1.536787
1	2.125917	-2.526652	-1.638423
1	4.373663	-3.571317	-1.578274
1	6.061638	-2.805637	0.072045
1	5.478706	-1.002713	1.677715
1	3.224095	0.009943	1.635495
1	-2.12605	-2.526366	1.638659
1	-4.373822	-3.570957	1.578604
1	-6.061718	-2.80547	-0.071905
1	-5.478665	-1.002811	-1.677819
1	-3.224027	0.009785	-1.635666

Table S4. Calculated low frequencies for the optimized structure of **DAI-3Ph** at S_0 state

Low Frequencies / cm^{-1}:

-2.0516	-0.6335	-0.0003	-0.0002	-0.0002	1.1394
7.6271	37.6531	39.3847			

Table S5. Calculated electronic transitions for the optimized structure of **DAI-3Ph** at S_0 state

Excited State	Spin Multiplicity	Energy / eV	Wavelength / nm	f	Composition	Coefficient
1	Singlet-A	3.6806	336.86	0.4221	HOMO -> LUMO	0.69478
2	Singlet-A	5.0438	245.82	0.0123	HOMO-5 -> LUMO+1	-0.2711
					HOMO-2 -> LUMO+2	0.18157
					HOMO-2 -> LUMO+3	-0.13167
					HOMO -> LUMO+2	0.50879
					HOMO -> LUMO+3	-0.26562
3	Singlet-A	5.0771	244.2	0.6168	HOMO-2 -> LUMO+1	0.10362
					HOMO-1 -> LUMO	0.23515
					HOMO -> LUMO+1	0.63068
4	Singlet-A	5.1933	238.74	0.0006	HOMO-4 -> LUMO+1	-0.11288
					HOMO-4 -> LUMO+6	-0.16705
					HOMO-4 -> LUMO+8	0.10654
					HOMO-3 -> LUMO	0.38689
					HOMO-3 -> LUMO+7	0.1511
					HOMO-2 -> LUMO+4	0.1724
					HOMO-1 -> LUMO+5	0.26534
					HOMO -> LUMO+4	-0.35264
5	Singlet-A	5.1997	238.45	0.005	HOMO-4 -> LUMO	0.35732
					HOMO-4 -> LUMO+7	0.15247
					HOMO-3 -> LUMO+1	-0.10742
					HOMO-3 -> LUMO+6	-0.16813
					HOMO-3 -> LUMO+8	0.10651
					HOMO-2 -> LUMO+5	0.19594
					HOMO-1 -> LUMO	-0.19621
					HOMO-1 -> LUMO+4	0.24419
					HOMO -> LUMO+5	-0.35359
6	Singlet-A	5.2539	235.99	0.0469	HOMO-2 -> LUMO	0.67856
7	Singlet-A	5.2743	235.07	0.0029	HOMO-4 -> LUMO	0.17824
					HOMO-1 -> LUMO	0.60387
					HOMO -> LUMO+1	-0.22321
8	Singlet-A	5.5619	222.92	0.0061	HOMO-5 -> LUMO+1	0.11142
					HOMO-3 -> LUMO	-0.14577
					HOMO -> LUMO+2	0.34733
					HOMO -> LUMO+3	0.51334
					HOMO -> LUMO+12	0.16295
9	Singlet-A	5.7008	217.49	0.0801	HOMO-3 -> LUMO	0.46866
					HOMO-2 -> LUMO	-0.10706
					HOMO -> LUMO+3	0.11504
					HOMO -> LUMO+4	0.41358
					HOMO -> LUMO+7	-0.17565
10	Singlet-A	5.7094	217.16	0.0001	HOMO-5 -> LUMO	0.63951
					HOMO-4 -> LUMO	-0.22251
					HOMO -> LUMO+5	-0.13506
11	Singlet-A	5.729	216.41	0.0038	HOMO-5 -> LUMO	0.28042
					HOMO-4 -> LUMO	0.4586
					HOMO-1 -> LUMO	-0.11456
					HOMO -> LUMO+5	0.38713
					HOMO -> LUMO+6	0.10349

12	Singlet-A	5.7738	214.74	0.0179	HOMO-4 -> LUMO	-0.17715
					HOMO-4 -> LUMO+4	-0.1093
					HOMO-3 -> LUMO+5	-0.11648
					HOMO-1 -> LUMO+7	0.12987
					HOMO -> LUMO+6	0.56555
					HOMO -> LUMO+8	-0.22141
13	Singlet-A	5.798	213.84	0.0343	HOMO-4 -> LUMO+5	0.10586
					HOMO-3 -> LUMO	0.21922
					HOMO-3 -> LUMO+4	0.10955
					HOMO-1 -> LUMO+6	0.11192
					HOMO -> LUMO+7	0.52064
					HOMO -> LUMO+9	-0.24804
14	Singlet-A	5.993	206.88	0.0223	HOMO-7 -> LUMO	0.18886
					HOMO-6 -> LUMO	0.62145
15	Singlet-A	6.0559	204.73	0.0406	HOMO-6 -> LUMO	0.11523
					HOMO-6 -> LUMO+2	0.19272
					HOMO-6 -> LUMO+3	-0.10584
					HOMO-5 -> LUMO+1	0.40636
					HOMO-3 -> LUMO	0.10124
					HOMO-2 -> LUMO+2	-0.12251
					HOMO-2 -> LUMO+4	-0.12437
					HOMO -> LUMO+2	0.22507
					HOMO -> LUMO+3	-0.28374
					HOMO -> LUMO+7	-0.13457
16	Singlet-A	6.0939	203.46	0.0003	HOMO-1 -> LUMO+9	0.10112
					HOMO -> LUMO+6	0.25461
					HOMO -> LUMO+8	0.44135
					HOMO -> LUMO+10	-0.32478
					HOMO -> LUMO+11	-0.19369
					HOMO -> LUMO+15	-0.13241
17	Singlet-A	6.2044	199.83	0.0255	HOMO-6 -> LUMO+4	0.14385
					HOMO-5 -> LUMO+1	0.17245
					HOMO-4 -> LUMO+6	-0.16401
					HOMO-4 -> LUMO+8	0.10094
					HOMO-3 -> LUMO	-0.15723
					HOMO-3 -> LUMO+7	0.20249
					HOMO-3 -> LUMO+9	-0.10504
					HOMO-2 -> LUMO+4	0.17276
					HOMO-1 -> LUMO+5	0.20047
					HOMO -> LUMO+3	-0.1052
					HOMO -> LUMO+4	0.38396
					HOMO -> LUMO+7	0.15823
18	Singlet-A	6.2122	199.58	0.0032	HOMO-4 -> LUMO+7	0.1342
					HOMO-3 -> LUMO+6	-0.12282
					HOMO-2 -> LUMO+5	0.11882
					HOMO-1 -> LUMO+4	0.10722
					HOMO -> LUMO+5	0.2019
					HOMO -> LUMO+8	0.28101
					HOMO -> LUMO+10	0.42837
					HOMO -> LUMO+11	-0.20442
					HOMO -> LUMO+16	-0.14805
19	Singlet-A	6.2441	198.56	0.0425	HOMO-6 -> LUMO+5	0.13657

					HOMO-4 -> LUMO	-0.13863
					HOMO-4 -> LUMO+7	0.17309
					HOMO-4 -> LUMO+9	-0.11038
					HOMO-3 -> LUMO+6	-0.15691
					HOMO-3 -> LUMO+8	0.10342
					HOMO-2 -> LUMO+5	0.17012
					HOMO-1 -> LUMO+4	0.19145
					HOMO -> LUMO+5	0.35846
					HOMO -> LUMO+10	-0.3474
20	Singlet-A	6.2995	196.82	0.0069	HOMO-2 -> LUMO+2	0.13284
					HOMO-2 -> LUMO+3	0.15974
					HOMO-1 -> LUMO+8	0.12821
					HOMO -> LUMO+7	0.23549
					HOMO -> LUMO+9	0.51072
					HOMO -> LUMO+12	-0.1631

Table S6. Optimized geometry of **DAI-3Ph** at S_1 state

Atomic Number	Coordinates (Angstroms)		
	x	y	z
5	0.00172	-1.427874	-0.000031
9	0.136105	-2.218421	1.140796
9	-0.13072	-2.218878	-1.140669
7	-1.286696	-0.54268	0.118539
7	1.288168	-0.539604	-0.11864
6	1.205969	0.808456	-0.207846
6	-0.001651	1.50069	0.000011
6	-1.207737	0.805407	0.207841
6	-0.003579	2.965313	0.000072
6	0.923574	3.69375	-0.768148
6	0.918145	5.080966	-0.769889
6	-0.007158	5.781844	0.000286
6	-0.930688	5.078494	0.770341
6	-0.9326	3.691266	0.768389
1	-0.008541	6.866863	0.000359
6	-2.536731	-1.160153	0.032006
6	-2.676684	-2.529345	0.344267
6	-3.919094	-3.136505	0.283577
6	-5.052593	-2.416599	-0.093806
6	-4.920965	-1.069821	-0.425079
6	-3.685032	-0.444881	-0.369235
6	2.539576	-1.1541	-0.032174
6	2.682473	-2.523347	-0.3431
6	3.926229	-3.127688	-0.282483
6	5.058315	-2.404887	0.093542
6	4.923901	-1.058093	0.423566
6	3.686578	-0.435961	0.367782
1	2.116152	1.355801	-0.397567
1	-2.119201	1.35063	0.397606
1	1.631593	3.167273	-1.398419
1	1.635626	5.618558	-1.381274
1	-1.649539	5.614159	1.381804
1	-1.639316	3.162942	1.398572
1	-1.811553	-3.097217	0.656112
1	-4.003903	-4.187937	0.538817
1	-6.022256	-2.901076	-0.139241

1	-5.78741	-0.501752	-0.748937
1	-3.604947	0.586276	-0.690097
1	1.818471	-3.093431	-0.653889
1	4.013243	-4.179155	-0.536692
1	6.029077	-2.887164	0.138926
1	5.789247	-0.487828	0.746376
1	3.604398	0.595263	0.687747

Table S7. Calculated low frequencies for the optimized structure of **DAI-3Ph** at S_1 state

Low Frequencies:					
-7.1737	-6.1231	0.0004	0.0006	0.0008	2.0195
36.5769	42.5114	43.0882			

Table S8. Calculated electronic transition for the optimized structure of **DAI-3Ph** at S_1 state

Excited State	Spin Multiplicity	Energy / eV	Wavelength / nm	f	Composition	Coefficient
1	Singlet-A	2.9009	427.4	0.4408	HOMO -> LUMO	0.69813

Table S9. Optimized geometry of **DAI-3Ph** at FF MECI

Element	Coordinates (Angstroms)		
	x	y	z
F	-2.5387469	0.89560858	1.39324881
F	-0.926364	-0.2185603	2.6200481
N	-1.0665871	-0.6503568	0.18479144
N	-0.0766382	1.3917239	1.0310345
C	1.18508282	0.73381212	1.186775
C	1.36036486	-0.3260362	0.24553682
C	0.22309663	-0.9375099	-0.2330065
C	2.7147289	-0.8382411	-0.0964593
C	3.66363075	-1.0869945	0.90435636
C	4.92657701	-1.5663012	0.5819109
C	5.26503495	-1.811226	-0.7467451
C	4.33761274	-1.5704019	-1.7427257
C	3.07392495	-1.0815676	-1.42405
H	6.24022976	-2.1843209	-0.9939603
C	-2.1038187	-1.5809726	-0.1449165
C	-3.2561851	-1.1357442	-0.7943579
C	-4.263987	-2.034374	-1.1204061
C	-4.1266424	-3.3853405	-0.8108013
C	-2.9868839	-3.8290805	-0.1661268
C	-1.9796683	-2.9316091	0.17592235
C	-0.1631119	2.48289544	0.23041866
C	-1.4257776	2.99868721	-0.1726867
C	-1.4848767	4.10760598	-0.994012
C	-0.316098	4.7376995	-1.4318343
C	0.92326892	4.25496303	-1.0251254
C	1.0115593	3.15712666	-0.2015377
H	1.67216752	0.8150702	2.13551752
H	0.31583715	-1.7521106	-0.9232434
H	3.40874881	-0.9258716	1.93475537
H	5.638849	-1.7569126	1.36170947
H	4.59126906	-1.751925	-2.7697132
H	2.37094083	-0.8765568	-2.2088265
H	-3.3517442	-0.0961314	-1.0317077

H	-5.1486442	-1.6846741	-1.6170073
H	-4.9054072	-4.0775832	-1.0675444
H	-2.8795996	-4.866758	0.08580108
H	-1.1101671	-3.2712056	0.70504214
H	-2.3192949	2.52623403	0.16659814
H	-2.44112	4.48712115	-1.2954486
H	-0.3754864	5.59957871	-2.0668508
H	1.82036524	4.74911553	-1.3424959
H	1.9684361	2.81335402	0.13045498

DAI-Tol

Table S10. Optimized geometry of **DAI-Tol** at S_0 state

Atomic Number	Coordinates (Angstroms)		
	x	y	z
5	-1.796182	0.005933	-0.006946
9	-2.585073	0.104089	-1.152455
9	-2.602032	-0.085647	1.12694
7	-0.882132	-1.256168	-0.073863
7	-0.872892	1.260582	0.072472
6	0.447053	1.188238	0.063372
6	1.165352	-0.005381	0.000534
6	0.438339	-1.193703	-0.061836
6	2.646977	-0.010472	0.001703
6	3.373791	0.825619	0.85614
6	4.763713	0.823769	0.85064
6	5.484239	-0.022336	0.006243
6	4.759376	-0.866026	-0.836658
6	3.369434	-0.854476	-0.848376
6	6.99067	-0.006654	-0.013128
6	-1.503928	-2.54723	-0.029929
6	-2.529644	-2.859681	-0.921177
6	-3.116091	-4.119399	-0.876416
6	-2.688294	-5.069218	0.047155
6	-1.671657	-4.749051	0.941014
6	-1.085143	-3.488404	0.910056
6	-1.484581	2.556646	0.031514
6	-2.506766	2.875752	0.924412
6	-3.083065	4.140274	0.882513
6	-2.648584	5.088184	-0.039878
6	-1.635465	4.761434	-0.935372
6	-1.059079	3.496073	-0.90719
1	0.987678	2.130799	0.100751
1	0.97196	-2.140371	-0.09522
1	2.846843	1.468373	1.555388
1	5.298076	1.481721	1.530677
1	5.290316	-1.535637	-1.507932
1	2.839321	-1.49851	-1.544068
1	7.367036	0.72312	-0.738543
1	7.398647	0.263411	0.964362
1	7.395872	-0.983131	-0.290683
1	-2.858596	-2.115872	-1.63572
1	-3.91238	-4.359243	-1.573577
1	-3.150685	-6.050408	0.075429
1	-1.342644	-5.474501	1.677995
1	-0.321206	-3.224077	1.634065
1	-2.841121	2.13328	1.637804
1	-3.876657	4.385334	1.580934
1	-3.103083	6.073117	-0.065959
1	-1.301361	5.485538	-1.671385
1	-0.297878	3.226764	-1.632244

Table S11. Calculated low frequencies for the optimized structure of **DAI-Tol** at S_0 state

Low Frequencies:					
-2.0216	-0.1932	0.0004	0.0005	0.0006	1.3985
7.4507	18.6696	36.6391			

Table S12. Calculated electronic transitions for the optimized structure of **DAI-Tol** at S_0 state

Excited State	Spin Multiplicity	Energy / eV	Wavelength / nm	f	Composition	Coefficient
1	Singlet-A	3.6532	339.39	0.4117	HOMO -> LUMO	0.693
2	Singlet-A	4.9592	250.01	0.0126	HOMO-5 -> LUMO+1	-0.24119
					HOMO-1 -> LUMO+2	-0.19718
					HOMO-1 -> LUMO+3	0.13394
					HOMO -> LUMO+2	0.52267
					HOMO -> LUMO+3	-0.25785
3	Singlet-A	5.0798	244.07	0.6838	HOMO-2 -> LUMO	0.23115
					HOMO -> LUMO+1	0.62471
4	Singlet-A	5.1543	240.55	0.064	HOMO-1 -> LUMO	0.68001
5	Singlet-A	5.1874	239.01	0.0037	HOMO-4 -> LUMO+1	0.10887
					HOMO-4 -> LUMO+6	0.15231
					HOMO-4 -> LUMO+8	0.1023
					HOMO-3 -> LUMO	0.36696
					HOMO-3 -> LUMO+7	-0.11329
					HOMO-3 -> LUMO+9	0.11451
					HOMO-2 -> LUMO+5	-0.26359
					HOMO-1 -> LUMO+4	-0.17356
					HOMO -> LUMO+2	0.11215
					HOMO -> LUMO+4	-0.34353
6	Singlet-A	5.1961	238.61	0.0054	HOMO-4 -> LUMO	-0.33885
					HOMO-4 -> LUMO+7	0.11678
					HOMO-4 -> LUMO+9	-0.12183
					HOMO-3 -> LUMO+1	-0.10219
					HOMO-3 -> LUMO+6	-0.16322
					HOMO-2 -> LUMO	-0.18212
					HOMO-2 -> LUMO+4	0.24364
					HOMO-1 -> LUMO+5	0.19612
					HOMO -> LUMO+5	0.35169
7	Singlet-A	5.2803	234.8	0.0033	HOMO-4 -> LUMO	-0.16329
					HOMO-2 -> LUMO	0.60872
					HOMO -> LUMO+1	-0.21712
8	Singlet-A	5.5068	225.15	0.0052	HOMO-3 -> LUMO	-0.11366
					HOMO -> LUMO+2	0.31092
					HOMO -> LUMO+3	0.53027
					HOMO -> LUMO+4	0.12143
					HOMO -> LUMO+11	-0.17665
9	Singlet-A	5.6817	218.22	0.0003	HOMO-5 -> LUMO	0.63589
					HOMO-4 -> LUMO	0.25238
					HOMO -> LUMO+6	-0.10963
10	Singlet-A	5.686	218.05	0.0831	HOMO-3 -> LUMO	0.46198
					HOMO -> LUMO+2	-0.11198
					HOMO -> LUMO+4	0.41141
					HOMO -> LUMO+7	0.17502
					HOMO -> LUMO+9	-0.14462
11	Singlet-A	5.7171	216.87	0.0001	HOMO-5 -> LUMO	-0.2636
					HOMO-4 -> LUMO	0.3433
					HOMO-2 -> LUMO	0.12044
					HOMO -> LUMO+5	0.37697
					HOMO -> LUMO+6	-0.31547
					HOMO -> LUMO+8	-0.10208

12	Singlet-A	5.746	215.77	0.023	HOMO-4 -> LUMO	0.34828
					HOMO -> LUMO+5	0.15262
					HOMO -> LUMO+6	0.48027
					HOMO -> LUMO+8	0.19029
13	Singlet-A	5.7768	214.63	0.0278	HOMO-3 -> LUMO	-0.2599
					HOMO-3 -> LUMO+4	-0.10599
					HOMO-2 -> LUMO+6	-0.10147
					HOMO -> LUMO+7	0.40032
					HOMO -> LUMO+8	0.13761
					HOMO -> LUMO+9	-0.37654
14	Singlet-A	5.8954	210.31	0.0147	HOMO-7 -> LUMO	0.16495
					HOMO-6 -> LUMO	0.63842
15	Singlet-A	6.033	205.51	0.0008	HOMO -> LUMO+6	-0.23564
					HOMO -> LUMO+7	-0.13416
					HOMO -> LUMO+8	0.38554
					HOMO -> LUMO+10	-0.3843
					HOMO -> LUMO+12	-0.1566
					HOMO -> LUMO+15	-0.13424
16	Singlet-A	6.039	205.31	0.0255	HOMO-6 -> LUMO+2	0.19297
					HOMO-5 -> LUMO+1	0.362
					HOMO-3 -> LUMO	0.12711
					HOMO-2 -> LUMO+5	0.10461
					HOMO-1 -> LUMO+2	0.17932
					HOMO-1 -> LUMO+4	0.14786
					HOMO -> LUMO+2	0.23205
					HOMO -> LUMO+3	-0.24075
					HOMO -> LUMO+7	0.12715
					HOMO -> LUMO+8	0.10413
					HOMO -> LUMO+20	-0.10038
17	Singlet-A	6.1637	201.15	0.0138	HOMO -> LUMO+4	0.13806
					HOMO -> LUMO+7	-0.18411
					HOMO -> LUMO+8	0.23812
					HOMO -> LUMO+10	0.40644
					HOMO -> LUMO+12	-0.23597
					HOMO -> LUMO+16	0.1577
18	Singlet-A	6.1725	200.87	0.0239	HOMO-6 -> LUMO+4	0.12945
					HOMO-5 -> LUMO+1	0.16852
					HOMO-4 -> LUMO+6	0.11284
					HOMO-3 -> LUMO	-0.14898
					HOMO-3 -> LUMO+7	-0.13412
					HOMO-3 -> LUMO+9	0.12402
					HOMO-2 -> LUMO+5	-0.16702
					HOMO-1 -> LUMO+3	-0.11709
					HOMO-1 -> LUMO+4	-0.13032
					HOMO -> LUMO+3	-0.12966
					HOMO -> LUMO+4	0.31114
					HOMO -> LUMO+7	-0.15553
					HOMO -> LUMO+8	-0.15351
					HOMO -> LUMO+10	-0.19619
					HOMO -> LUMO+12	0.10611
19	Singlet-A	6.2078	199.72	0.0365	HOMO-6 -> LUMO+5	0.17561
					HOMO-4 -> LUMO	-0.16935

					HOMO-4 -> LUMO+7	-0.15341
					HOMO-4 -> LUMO+9	0.16322
					HOMO-3 -> LUMO+6	0.18003
					HOMO-3 -> LUMO+8	0.11077
					HOMO-2 -> LUMO+4	-0.22243
					HOMO-1 -> LUMO+5	-0.17049
					HOMO -> LUMO+5	0.38835
					HOMO -> LUMO+10	-0.21052
20	Singlet-A	6.2349	198.86	0.0022	HOMO-6 -> LUMO+4	0.11662
					HOMO-2 -> LUMO+5	-0.13793
					HOMO-1 -> LUMO+2	0.13346
					HOMO-1 -> LUMO+3	0.1719
					HOMO -> LUMO+4	0.14535
					HOMO -> LUMO+7	0.29967
					HOMO -> LUMO+9	0.42609
					HOMO -> LUMO+14	-0.11646

Table S13. Optimized geometry of **DAI-3Ph** at S_1 state

Atomic Number	Coordinates (Angstroms)		
	x	y	z
5	-1.749762	0.005983	-0.000812
9	-2.539261	0.143418	-1.142307
9	-2.543388	-0.124948	1.138575
7	-0.867531	-1.284082	-0.118576
7	-0.857233	1.288741	0.119328
6	0.489059	1.203388	0.21136
6	1.180375	-0.006131	0.00237
6	0.479625	-1.209932	-0.20772
6	2.641148	-0.011489	0.00322
6	3.378557	0.943251	0.729774
6	4.763626	0.930812	0.732769
6	5.484115	-0.022104	0.006065
6	4.758028	-0.972774	-0.717732
6	3.372771	-0.973346	-0.719484
6	6.987593	-0.008164	-0.017526
6	-1.488967	-2.53407	-0.033822
6	-2.854522	-2.672682	-0.35844
6	-3.464334	-3.914224	-0.299284
6	-2.750004	-5.047576	0.088412
6	-1.406559	-4.916611	0.431996
6	-0.779518	-3.681223	0.378043
6	-1.468155	2.543823	0.03351
6	-2.833393	2.693499	0.354557
6	-3.432858	3.940016	0.294346
6	-2.708247	5.067655	-0.090925
6	-1.365011	4.92583	-0.430992
6	-0.748256	3.685321	-0.375956
1	1.036295	2.11329	0.402166
1	1.019567	-2.124438	-0.397232
1	2.860387	1.680199	1.332857
1	5.299509	1.672104	1.318676
1	5.289547	-1.723981	-1.29491
1	2.850435	-1.710812	-1.318297
1	7.357308	0.626001	-0.83131
1	7.397431	0.385674	0.915885

1	7.393621	-1.010638	-0.173654
1	-3.417965	-1.807431	-0.677979
1	-4.513499	-3.998115	-0.564008
1	-3.236413	-6.01635	0.132485
1	-0.842683	-5.782596	0.764337
1	0.248538	-3.600658	0.708896
1	-3.404759	1.832763	0.672201
1	-4.482004	4.032374	0.556316
1	-3.186582	6.040402	-0.135829
1	-0.793168	5.787318	-0.761402
1	0.279992	3.596526	-0.704078

Table S14. Calculated low frequencies for the optimized structure of **DAI-Tol** at S_1 state

Low Frequencies:					
-15.1884	-2.3573	-0.0009	0.0004	0.0007	5.7106
21.3749	29.7196	34.5613			

Table S15. Calculated electronic transitions for the optimized structure of **DAI-Tol** at S_1 state

Excited State	Spin Multiplicity	Energy / eV	Wavelength / nm	f	Composition	Coefficient
1	Singlet-A	2.8703	431.96	0.4147		
					HOMO -> LUMO	0.69761

DAI-Bn

Table S16. Optimized geometry of **DAI-Bn** at S_0 state

Atomic Number	Coordinates (Angstroms)		
	x	y	z
9	0.030728	-2.856047	-0.446496
9	-0.003378	-2.396899	-2.67736
7	-1.25482	-0.956913	-1.197728
7	1.23433	-0.915798	-1.229472
6	-0.053023	2.487747	-0.37079
6	-0.036963	1.049577	-0.724303
6	1.163147	0.362079	-0.917543
1	2.104893	0.899567	-0.820388
6	3.421891	-1.529931	-0.198264
6	0.837367	3.010449	0.573597
1	1.530955	2.347014	1.081978
6	-0.979274	4.719048	-0.621523
1	-1.698525	5.378654	-1.099667
6	-0.082085	5.242403	0.310518
6	-1.218509	0.321809	-0.882772
1	-2.17431	0.818341	-0.724243
6	-3.3734	-1.651319	-0.069541
6	-0.959496	3.372219	-0.964869
1	-1.648311	3.007606	-1.721472
6	0.82655	4.361613	0.899309
1	1.527856	4.734252	1.641147
6	4.673136	-0.91673	-0.208092
1	5.025772	-0.429461	-1.113456
6	-2.864485	-2.258518	1.082248
1	-1.872983	-2.700478	1.053387
6	2.981812	-2.157265	0.971089
1	2.006841	-2.635618	0.980287
6	-4.646048	-1.085164	-0.030646
1	-5.052282	-0.614173	-0.922099
6	5.034647	-1.55113	2.088744
1	5.65894	-1.561001	2.976568
6	-2.559082	-1.625246	-1.343801
1	-2.34991	-2.640891	-1.68354
1	-3.126027	-1.132156	-2.139926
6	5.479497	-0.927654	0.929154
1	6.45249	-0.447071	0.905864
6	3.782988	-2.165647	2.10606
1	3.432525	-2.657451	3.0081
6	-0.077268	6.710335	0.650163
1	0.600708	7.264606	-0.008388
1	0.253903	6.879985	1.678034
1	-1.072549	7.148406	0.539094
6	2.555554	-1.531377	-1.438057
1	3.068258	-1.012785	-2.254404
1	2.372315	-2.553122	-1.774404
6	-5.405739	-1.122235	1.137607
1	-6.395806	-0.677561	1.152377
6	-4.892444	-1.725237	2.279533
1	-5.479932	-1.754766	3.191688
6	-3.619248	-2.29291	2.248062
1	-3.215162	-2.768172	3.136431
5	0.002094	-1.817946	-1.402633

Table S17. Calculated low frequencies for the optimized structure of **DAI-Tol** at S_0 state

Low Frequencies:					
-1.4036	0.0006	0.0007	0.0008	1.4809	2.6743
12.2454	18.2543	21.2157			

Table S18. Calculated electronic transitions for the optimized structure of **DAI-Tol** at S_0 state

Excited State	Spin Multiplicity	Energy / eV	Wavelength / nm	f	Composition	Coefficient
1	Singlet-A	3.8693	320.43	0.2556	HOMO-6 -> LUMO	-0.11051
					HOMO -> LUMO	0.69154
2	Singlet-A	4.9633	249.8	0.0143	HOMO-6 -> LUMO+4	0.13692
					HOMO-4 -> LUMO+1	0.16437
					HOMO-4 -> LUMO+3	-0.18498
					HOMO -> LUMO+1	0.12464
					HOMO -> LUMO+2	-0.19759
					HOMO -> LUMO+4	0.51707
					HOMO -> LUMO+6	0.12605
					HOMO -> LUMO+7	0.18847
3	Singlet-A	5.11	242.63	0.4323	HOMO -> LUMO+1	0.49519
					HOMO -> LUMO+3	-0.41606
					HOMO -> LUMO+5	0.12982

Table S19. Optimized geometry of **DAI-Tol** at S_1 state

Atomic Number	Coordinates (Angstroms)		
	x	y	z
9	0.125413	-2.831846	-0.392513
9	0.114409	-2.396878	-2.633809
7	-1.223233	-1.006353	-1.191117
7	1.297544	-0.881918	-1.1874
6	-0.130515	2.447034	-0.381593
6	-0.062277	1.050276	-0.715751
6	1.202827	0.411533	-0.868777
1	2.124914	0.97401	-0.80461
6	3.498171	-1.427464	-0.161919
6	1.009263	3.159927	0.072409
1	1.951052	2.644694	0.206978
6	-1.399859	4.521048	-0.161638
1	-2.343608	5.049845	-0.255796
6	-0.265939	5.213527	0.28344
6	-1.259732	0.296212	-0.897593
1	-2.229373	0.731277	-0.69372
6	-3.336691	-1.745948	-0.099423
6	-1.341969	3.1784	-0.483052
1	-2.238075	2.692655	-0.845522
6	0.93524	4.500692	0.397646
1	1.825115	5.010912	0.753932
6	4.751227	-0.81912	-0.192475
1	5.098567	-0.351957	-1.110609
6	-2.824413	-2.262582	1.094039
1	-1.804666	-2.635612	1.112804
6	3.062472	-2.026727	1.023327
1	2.084588	-2.498535	1.047858

6	-4.644182	-1.265255	-0.123273
1	-5.051139	-0.863652	-1.047929
6	5.12578	-1.407817	2.114831
1	5.756039	-1.402181	2.998578
6	-2.481123	-1.726314	-1.351454
1	-2.229804	-2.744706	-1.653428
1	-3.051656	-1.275603	-2.175359
6	5.565203	-0.810125	0.939377
1	6.540453	-0.334769	0.89975
6	3.871308	-2.015742	2.152923
1	3.524229	-2.486476	3.067567
6	-0.329303	6.679003	0.601937
1	-0.105457	7.276233	-0.289842
1	0.398729	6.952856	1.369394
1	-1.323795	6.970035	0.948728
6	2.620767	-1.455811	-1.398785
1	3.123372	-0.916136	-2.21359
1	2.473942	-2.483489	-1.73615
6	-5.436223	-1.30123	1.023451
1	-6.454035	-0.925088	0.989212
6	-4.92039	-1.816019	2.206987
1	-5.533292	-1.844708	3.102406
6	-3.611549	-2.296262	2.238381
1	-3.204678	-2.702126	3.15944
5	0.08029	-1.809697	-1.364334

Table S20. Calculated low frequencies for the optimized structure of **DAI-Tol** at S_1 state

Low Frequencies:					
-4.5381	-2.8024	-0.0007	-0.0003	0.0001	4.0479
11.6641	16.177	22.7233			

Table S21. Calculated electronic transitions for the optimized structure of **DAI-Tol** at S_1 state

Excited State	Spin Multiplicity	Energy / eV	Wavelength / nm	f	Composition	Coefficient
1	Singlet-A	3.3177	373.71	0.1557	HOMO -> LUMO	0.69767
2	Singlet-A	4.4532	278.42	0.5182	HOMO -> LUMO+1	0.67151
					HOMO -> LUMO+2	0.10326
3	Singlet-A	4.7762	259.59	0.0759	HOMO-6 -> LUMO	0.11902
					HOMO-6 -> LUMO+8	0.10283
					HOMO-3 -> LUMO+1	0.25243
					HOMO -> LUMO+6	-0.13901
					HOMO -> LUMO+7	0.20163
					HOMO -> LUMO+8	0.55682

DAI-2Ph

Table S22. Optimized geometry of **DAI-2Ph** at S_0 state

Atomic Number	Coordinates (Angstroms)		
	x	y	z
5	0.000005	-0.18648	0.000252
9	0.107624	-0.983367	1.139069
9	-0.10759	-0.984011	-1.138102
7	-1.262547	0.729203	0.088517
7	1.262533	0.729187	-0.088502
6	1.19525	2.049778	-0.078295
6	0.000004	2.752861	-0.000041
6	-1.195252	2.049795	0.0782
1	0.000008	3.833126	-0.000085
6	-2.555014	0.109203	0.078683
6	-2.854435	-0.902379	0.990268
6	-4.116725	-1.485025	0.976887
6	-5.081994	-1.067141	0.064863
6	-4.775117	-0.064535	-0.84928
6	-3.512068	0.517704	-0.849661
6	2.555005	0.109187	-0.078784
6	2.85438	-0.902327	-0.990457
6	4.116676	-1.484965	-0.977188
6	5.08199	-1.067138	-0.065185
6	4.775158	-0.064597	0.849044
6	3.512106	0.517636	0.849533
1	2.137483	2.588373	-0.142388
1	-2.137485	2.588404	0.14215
1	-2.098672	-1.223794	1.695536
1	-4.346438	-2.270346	1.689725
1	-6.065061	-1.526388	0.061345
1	-5.513041	0.256351	-1.577421
1	-3.257857	1.270091	-1.589288
1	2.098578	-1.223703	-1.695699
1	4.346357	-2.270234	-1.690093
1	6.06506	-1.526379	-0.061752
1	5.513121	0.256245	1.577165
1	3.257926	1.269977	1.589218

Table S23. Calculated low frequencies for the optimized structure of **DAI-2Ph** at S_0 state

Low Frequencies:					
-1.4415	-0.0003	-0.0003	0.0004	0.4735	1.564
7.6	37.8965	43.4391			

Table S24. Calculated electronic transitions for the optimized structure of **DAI-2Ph** at S_0 state

Excited State	Spin Multiplicity	Energy / eV	Wavelength / nm	f	Composition	Coefficient
1	Singlet-A	3.9195	316.33	0.5631	HOMO -> LUMO	0.69339
2	Singlet-A	5.224	237.33	0.0016	HOMO-4 -> LUMO+2	-0.14089
					HOMO-3 -> LUMO+4	-0.22249
					HOMO-2 -> LUMO	0.39461
					HOMO-2 -> LUMO+6	-0.17439
					HOMO-1 -> LUMO+3	-0.27856
					HOMO -> LUMO+2	0.37031
3	Singlet-A	5.2293	237.09	0.0013	HOMO-4 ->	-0.14726

					LUMO+3	
					HOMO-3 -> LUMO	0.3713
					HOMO-3 -> LUMO+6	-0.18342
					HOMO-2 -> LUMO+4	-0.22204
					HOMO-1 -> LUMO	-0.17023
					HOMO-1 -> LUMO+2	-0.27086
					HOMO -> LUMO+3	0.3609
4	Singlet-A	5.2832	234.67	0.0794	HOMO-3 -> LUMO	0.17931
					HOMO-1 -> LUMO	0.65547
5	Singlet-A	5.641	219.79	0.0048	HOMO-5 -> LUMO	-0.1069
					HOMO-4 -> LUMO	0.65589
					HOMO-2 -> LUMO	-0.11983
6	Singlet-A	5.6523	219.35	0.0156	HOMO-4 -> LUMO+1	0.11877
					HOMO -> LUMO+1	0.64261
					HOMO -> LUMO+7	0.17359
7	Singlet-A	5.7812	214.46	0.0655	HOMO-4 -> LUMO	0.11926
					HOMO-2 -> LUMO	0.54149
					HOMO-2 -> LUMO+6	0.11488
					HOMO-1 -> LUMO+3	0.13848
					HOMO -> LUMO+2	-0.37807
8	Singlet-A	5.7995	213.78	0.0074	HOMO-3 -> LUMO	0.54675
					HOMO-3 -> LUMO+6	0.12969
					HOMO-1 -> LUMO	-0.11276
					HOMO-1 -> LUMO+2	0.15811
					HOMO -> LUMO+3	-0.35836
9	Singlet-A	5.8731	211.1	0.0333	HOMO-3 -> LUMO+2	0.15991
					HOMO-2 -> LUMO+3	0.16049
					HOMO-1 -> LUMO+6	-0.20367
					HOMO -> LUMO+4	0.58919
					HOMO -> LUMO+5	0.14018
10	Singlet-A	5.9233	209.32	0.036	HOMO-3 -> LUMO+3	0.16654
					HOMO-2 -> LUMO+2	0.17515
					HOMO-1 -> LUMO+4	-0.1901
					HOMO -> LUMO+6	0.58359
					HOMO -> LUMO+7	0.11242
11	Singlet-A	6.2371	198.79	0.0009	HOMO-1 -> LUMO+1	-0.17149
					HOMO -> LUMO+4	-0.17783
					HOMO -> LUMO+5	0.55861
					HOMO -> LUMO+8	-0.17044
					HOMO -> LUMO+9	0.20456
12	Singlet-A	6.3039	196.68	0.0108	HOMO-4 -> LUMO+2	0.22534
					HOMO-3 -> LUMO+4	0.19894
					HOMO-2 -> LUMO	0.1319
					HOMO-2 -> LUMO+6	0.22758
					HOMO-1 -> LUMO+3	0.15805
					HOMO-1 -> LUMO+4	-0.11046
					HOMO -> LUMO+1	-0.11118
					HOMO -> LUMO+2	0.36
					HOMO -> LUMO+7	0.2428
					HOMO -> LUMO+11	0.18635
					HOMO -> LUMO+15	-0.1087
13	Singlet-A	6.4145	193.29	0.0352	HOMO-4 ->	0.25374

					LUMO+3	
					HOMO-3 -> LUMO	0.11085
					HOMO-3 -> LUMO+6	0.25639
					HOMO-2 -> LUMO+4	0.26187
					HOMO-1 -> LUMO+2	0.18358
					HOMO -> LUMO+3	0.44281
14	Singlet-A	6.4662	191.74	0.0146	HOMO-17 -> LUMO	-0.10146
					HOMO-7 -> LUMO	0.1229
					HOMO-5 -> LUMO	0.53655
					HOMO-1 -> LUMO+5	-0.13283
					HOMO -> LUMO+7	-0.28671
15	Singlet-A	6.5003	190.74	0.0229	HOMO-5 -> LUMO	0.32378
					HOMO-4 -> LUMO+1	0.13917
					HOMO-4 -> LUMO+2	-0.12182
					HOMO-3 -> LUMO+4	-0.11662
					HOMO-2 -> LUMO+6	-0.10165
					HOMO-1 -> LUMO+3	-0.13037
					HOMO-1 -> LUMO+5	0.18229
					HOMO -> LUMO+2	-0.16638
					HOMO -> LUMO+6	-0.17354
					HOMO -> LUMO+7	0.39629
16	Singlet-A	6.5612	188.97	0.124	HOMO-4 -> LUMO+4	-0.23421
					HOMO-3 -> LUMO+2	0.35807
					HOMO-2 -> LUMO+3	0.36075
					HOMO-1 -> LUMO+1	0.10408
					HOMO-1 -> LUMO+6	-0.20008
					HOMO -> LUMO+4	-0.24092
					HOMO -> LUMO+5	-0.1702
17	Singlet-A	6.5693	188.73	0.2455	HOMO-5 -> LUMO	-0.11281
					HOMO-4 -> LUMO+6	-0.21545
					HOMO-3 -> LUMO+3	0.36547
					HOMO-2 -> LUMO+2	0.36174
					HOMO-1 -> LUMO+4	-0.18688
					HOMO -> LUMO+6	-0.28137
18	Singlet-A	6.5817	188.38	0.0503	HOMO -> LUMO+8	0.45064
					HOMO -> LUMO+9	0.42401
					HOMO -> LUMO+12	0.23721
19	Singlet-A	6.7	185.05	0.0431	HOMO-4 -> LUMO+5	0.19134
					HOMO-1 -> LUMO+1	0.15831
					HOMO-1 -> LUMO+7	-0.24629
					HOMO -> LUMO+5	-0.12366
					HOMO -> LUMO+8	-0.33491
					HOMO -> LUMO+9	0.4145
20	Singlet-A	6.8229	181.72	0.0234	HOMO-3 -> LUMO+4	-0.19613
					HOMO-3 -> LUMO+5	0.28371
					HOMO-2 -> LUMO+1	0.35997
					HOMO-2 -> LUMO+7	-0.2154
					HOMO-1 -> LUMO+5	-0.20533
					HOMO -> LUMO+11	0.28167
					HOMO -> LUMO+15	-0.13903

Table S25. Optimized geometry of **DAI-2Ph** at S_1 state

Atomic Number	Coordinates (Angstroms)		
	x	y	z
5	0.000026	-0.133724	0.000148
9	-0.143912	-0.925239	-1.139612
9	0.143953	-0.925389	1.139802
7	1.295038	0.745455	-0.132514
7	-1.295	0.745463	0.13296
6	-1.209122	2.105241	0.203471
6	0.000055	2.764181	0.000249
6	1.209204	2.105345	-0.203107
1	-0.000006	3.847742	0.000288
6	2.53635	0.128717	-0.074447
6	2.660456	-1.256486	-0.341173
6	3.900196	-1.867266	-0.307878
6	5.051868	-1.139589	-0.003839
6	4.940692	0.220851	0.28085
6	3.708682	0.851539	0.252044
6	-2.536417	0.128736	0.074589
6	-2.66066	-1.256355	0.341624
6	-3.90041	-1.867112	0.307989
6	-5.051932	-1.139478	0.003329
6	-4.940552	0.220845	-0.281735
6	-3.708518	0.851516	-0.252621
1	-2.101105	2.664464	0.44619
1	2.101112	2.664489	-0.446259
1	1.781802	-1.830833	-0.597204
1	3.970672	-2.927784	-0.526789
1	6.020476	-1.627671	0.019764
1	5.823394	0.794544	0.544892
1	3.648925	1.895054	0.532238
1	-1.78209	-1.830615	0.598134
1	-3.971014	-2.927574	0.52714
1	-6.020552	-1.627519	-0.020533
1	-5.823116	0.79451	-0.546313
1	-3.648624	1.894927	-0.533177

Table S26. Calculated low frequencies for the optimized structure of **DAI-2Ph** at S_1 state

Low Frequencies:					
-21.0371	-2.3042	-0.001	-0.0006	-0.0002	3.1219
20.6223	48.5862	70.1019			

Table S27. Calculated electronic transitions for the optimized structure of **DAI-2Ph** at S_1 state

Excited State	Spin Multiplicity	Energy / eV	Wavelength / nm	f	Composition	Coefficient
1	Singlet-A	3.0022	412.98	0.5814	HOMO -> LUMO	0.69704
2	Singlet-A	4.2584	291.15	0.0994	HOMO-1 -> LUMO	0.69188
3	Singlet-A	4.6608	266.02	0.0047	HOMO-3 -> LUMO+2	-0.12006
					HOMO-3 -> LUMO+5	0.10396
					HOMO-2 -> LUMO	0.62063
					HOMO-1 -> LUMO+4	0.15728
					HOMO -> LUMO+2	0.1611

HOMO -> LUMO+5		0.15408

Table S28. Optimized geometry of **DAI-2Ph** at FF MECI

Element	Coordinates (Angstroms)		
	x	y	z
B	0.1233	0.6796	1.0223
F	0.2135	-0.4367	1.871
F	0.465	1.8581	1.7298
N	0.862	0.5046	-0.3046
N	-1.393	0.9453	0.4844
C	-1.4206	2.205	-0.2068
C	-0.5773	2.1869	-1.3435
C	0.4972	1.3133	-1.3663
H	-0.6764	2.9235	-2.115
C	2.1702	-0.0735	-0.3138
C	2.3277	-1.4417	-0.0963
C	3.5997	-2.0097	-0.1083
C	4.7192	-1.2172	-0.347
C	4.5608	0.1479	-0.5609
C	3.3012	0.7172	-0.5361
C	-2.3146	0.0028	0.1712
C	-2.148	-1.3545	0.5688
C	-3.0984	-2.2961	0.2194
C	-4.2328	-1.933	-0.515
C	-4.4186	-0.6049	-0.8841
C	-3.494	0.3541	-0.5458
H	-1.7159	3.0756	0.3402
H	1.148	1.2964	-2.2171
H	1.4616	-2.0447	0.0824
H	3.7128	-3.0631	0.0622
H	5.6987	-1.6551	-0.3599
H	5.4204	0.7675	-0.7314
H	3.1848	1.7759	-0.6669
H	-1.2921	-1.6345	1.1391
H	-2.9606	-3.3162	0.5192
H	-4.9642	-2.672	-0.7766
H	-5.2998	-0.3191	-1.4244
H	-3.6681	1.3776	-0.8034

DKI-4Ph

Table S29. Optimized geometry of **DKI-4Ph** at S_0 state

Atomic Number	Coordinates (Angstroms)		
	x	y	z
6	-1.214818	0.764378	-0.02089
6	-2.447437	1.592314	0.101501
6	-3.317399	1.4325	1.178094
6	-2.704644	2.584965	-0.840824
6	-3.825383	3.39414	-0.7193
6	-4.427064	2.252831	1.306152
6	-4.687485	3.231218	0.355487
1	-2.030696	2.714221	-1.679249
1	-4.023017	4.154044	-1.465676
1	-3.123708	0.667498	1.918625
1	-5.093006	2.125017	2.150894
1	-5.56008	3.865712	0.453726
6	0.004598	1.437373	-0.095246
6	1.226083	0.766958	-0.092426
6	2.464522	1.5937	-0.125517
7	1.275086	-0.560878	-0.078065
1	0.003054	2.514776	-0.107933
7	-1.263709	-0.561327	-0.028036
6	2.63782	2.626428	0.792543
6	3.427326	1.390564	-1.112568
6	4.544343	2.207943	-1.17666
6	3.76579	3.432751	0.737181
6	4.719941	3.226529	-0.248784
1	3.298003	0.594174	-1.834011
1	5.282357	2.046882	-1.953036
1	1.892129	2.789431	1.561412
1	3.897161	4.224376	1.464973
1	5.598373	3.858857	-0.295974
6	-2.511643	-1.274518	-0.068604
6	-3.3412	-1.162724	-1.176771
6	-2.858227	-2.115896	0.980284
6	-4.052206	-2.820939	0.929971
6	-4.53492	-1.86669	-1.219886
6	-4.895421	-2.694546	-0.165369
1	-2.183571	-2.222947	1.818772
1	-4.320412	-3.476353	1.749859
1	-3.043884	-0.531261	-2.0042
1	-5.179622	-1.775375	-2.085673
1	-5.826082	-3.247867	-0.202241
6	2.503447	-1.276734	0.124042
5	0.003006	-1.440484	-0.238307
6	3.242513	-1.08514	1.284619
6	2.921279	-2.20557	-0.821256
6	4.093146	-2.918406	-0.612969
6	4.415871	-1.796202	1.483832
6	4.846967	-2.712493	0.534235
1	2.317491	-2.369626	-1.70388
1	4.41576	-3.641256	-1.352688
1	2.893861	-0.383481	2.031723
1	4.988883	-1.640446	2.389983
1	5.761353	-3.271275	0.693057
9	0.032804	-2.464853	0.701952
9	-0.03656	-1.975774	-1.533003

Table S30. Calculated low frequencies for the optimized structure of **DKI-4Ph** at S_0 state

Low Frequencies:					
-2.3062	-0.0005	-0.0003	0.0005	0.6921	2.3004
13.0848	21.5414	45.7098			

Table S31. Calculated electronic transitions for the optimized structure of **DKI-4Ph** at S_0 state

Excited State	Spin Multiplicity	Energy / eV	Wavelength / nm	f	Composition	Coefficient
1	Singlet-A	3.6734	337.52	0.6122	HOMO -> LUMO	0.68736
2	Singlet-A	4.3841	282.81	0.2496	HOMO-1 -> LUMO	0.67933
3	Singlet-A	4.7612	260.4	0.1057	HOMO-4 -> LUMO	0.1755
					HOMO-2 -> LUMO	0.62808
					HOMO-1 -> LUMO+1	0.175
4	Singlet-A	5.0398	246.01	0.0018	HOMO-5 -> LUMO	0.11571
					HOMO-4 -> LUMO+6	0.16666
					HOMO-3 -> LUMO	0.45887
					HOMO-2 -> LUMO+8	-0.10512
					HOMO-1 -> LUMO+5	0.16346
					HOMO-1 -> LUMO+9	-0.14085
					HOMO -> LUMO+1	-0.27249
					HOMO -> LUMO+6	-0.10839
					HOMO -> LUMO+8	0.1445
5	Singlet-A	5.1008	243.07	0.0159	HOMO-7 -> LUMO	0.13021
					HOMO-7 -> LUMO+3	-0.14002
					HOMO-6 -> LUMO+1	0.2497
					HOMO-5 -> LUMO	0.45936
					HOMO-5 -> LUMO+3	0.11225
					HOMO-2 -> LUMO+2	0.14134
					HOMO-1 -> LUMO+3	-0.15689
					HOMO -> LUMO+1	0.16159
6	Singlet-A	5.1009	243.06	0.001	HOMO-6 -> LUMO	0.10984
					HOMO-4 -> LUMO	0.50132
					HOMO-4 -> LUMO+5	-0.10591
					HOMO-3 -> LUMO+6	0.18453
					HOMO-2 -> LUMO+9	0.13336
					HOMO-1 -> LUMO+6	-0.10346
					HOMO-1 -> LUMO+8	0.18433
					HOMO -> LUMO+5	0.17219
					HOMO -> LUMO+9	-0.13489
7	Singlet-A	5.1103	242.61	0.007	HOMO-8 -> LUMO+3	0.10509
					HOMO-7 -> LUMO+2	0.11076
					HOMO-6 -> LUMO	0.49332
					HOMO-5 -> LUMO+1	0.2537
					HOMO-4 -> LUMO	-0.11994
					HOMO-2 -> LUMO+3	-0.18581
					HOMO-1 -> LUMO+2	0.15241
8	Singlet-A	5.1974	238.55	0.0008	HOMO-5 -> LUMO	-0.12935
					HOMO-3 -> LUMO	0.30959
					HOMO-2 -> LUMO+1	0.11057

					HOMO -> LUMO+1	0.58127
9	Singlet-A	5.4406	227.89	0.0438	HOMO-8 -> LUMO+1	-0.1297
					HOMO-7 -> LUMO	0.45101
					HOMO-5 -> LUMO	-0.15873
					HOMO-4 -> LUMO+6	-0.11674
					HOMO-3 -> LUMO	0.2291
					HOMO-1 -> LUMO+5	-0.11156
					HOMO-1 -> LUMO+9	0.14042
					HOMO -> LUMO+1	-0.15777
					HOMO -> LUMO+6	0.17473
					HOMO -> LUMO+8	-0.14197
10	Singlet-A	5.4944	225.65	0.0043	HOMO-8 -> LUMO	0.26005
					HOMO-4 -> LUMO	0.37879
					HOMO-3 -> LUMO+6	-0.1309
					HOMO-2 -> LUMO	-0.18203
					HOMO-1 -> LUMO+1	0.1468
					HOMO-1 -> LUMO+8	-0.17587
					HOMO -> LUMO+5	-0.25769
					HOMO -> LUMO+9	0.13923
11	Singlet-A	5.5347	224.01	0.0368	HOMO-7 -> LUMO	-0.18333
					HOMO-3 -> LUMO	0.13753
					HOMO-1 -> LUMO+3	0.14
					HOMO -> LUMO+2	0.59333
					HOMO -> LUMO+8	-0.10688
12	Singlet-A	5.6304	220.2	0.0094	HOMO-8 -> LUMO	-0.16877
					HOMO-1 -> LUMO+2	0.19762
					HOMO-1 -> LUMO+6	-0.10813
					HOMO -> LUMO+3	0.54241
					HOMO -> LUMO+5	0.13973
					HOMO -> LUMO+9	0.17168
13	Singlet-A	5.638	219.91	0.04	HOMO-7 -> LUMO	0.31708
					HOMO-5 -> LUMO	-0.19899
					HOMO-3 -> LUMO	-0.30233
					HOMO-1 -> LUMO+5	0.16209
					HOMO-1 -> LUMO+9	-0.12293
					HOMO -> LUMO+2	0.2423
					HOMO -> LUMO+6	-0.14988
					HOMO -> LUMO+8	0.18498
14	Singlet-A	5.6833	218.15	0.0989	HOMO-8 -> LUMO	0.4957
					HOMO-7 -> LUMO+1	-0.14599
					HOMO-6 -> LUMO	0.18847
					HOMO-6 -> LUMO+3	-0.1038
					HOMO-2 -> LUMO	0.15111
					HOMO-1 -> LUMO+1	-0.18758
					HOMO -> LUMO+3	0.18266
					HOMO -> LUMO+5	0.14676
15	Singlet-A	5.7629	215.14	0.0449	HOMO-3 -> LUMO+5	-0.11047
					HOMO-1 -> LUMO+3	-0.10056
					HOMO-1 -> LUMO+9	-0.12462
					HOMO-1 ->	0.10744

					LUMO+15	
					HOMO -> LUMO+2	0.15602
					HOMO -> LUMO+6	0.51668
					HOMO -> LUMO+8	0.1933
16	Singlet-A	5.8508	211.91	0.0639	HOMO-6 -> LUMO	0.11349
					HOMO-2 -> LUMO+3	0.12002
					HOMO-1 -> LUMO+6	0.14417
					HOMO-1 -> LUMO+8	0.12851
					HOMO -> LUMO+3	0.35445
					HOMO -> LUMO+5	-0.28823
					HOMO -> LUMO+7	0.26449
					HOMO -> LUMO+9	-0.27335
17	Singlet-A	5.9205	209.41	0.0003	HOMO-2 -> LUMO+2	0.10411
					HOMO-1 -> LUMO+3	-0.16043
					HOMO -> LUMO+4	0.58132
					HOMO -> LUMO+6	-0.12334
					HOMO -> LUMO+12	0.16221
18	Singlet-A	5.954	208.24	0.0194	HOMO-8 -> LUMO	-0.23591
					HOMO-7 -> LUMO+2	-0.10563
					HOMO-6 -> LUMO	0.37743
					HOMO-4 -> LUMO+3	0.1015
					HOMO-2 -> LUMO+3	0.21022
					HOMO-1 -> LUMO+1	-0.11442
					HOMO-1 -> LUMO+2	-0.27912
					HOMO-1 -> LUMO+4	0.12312
					HOMO-1 -> LUMO+8	-0.10078
					HOMO -> LUMO+9	0.14737
19	Singlet-A	5.9709	207.65	0.0554	HOMO-7 -> LUMO	0.21131
					HOMO-7 -> LUMO+3	0.12338
					HOMO-6 -> LUMO+1	-0.12786
					HOMO-5 -> LUMO	0.38789
					HOMO-2 -> LUMO+2	-0.19876
					HOMO-2 -> LUMO+4	0.12799
					HOMO-1 -> LUMO+3	0.25764
					HOMO -> LUMO+4	0.21373
20	Singlet-A	5.9778	207.41	0.0008	HOMO-8 -> LUMO	0.16765
					HOMO-2 -> LUMO+3	0.12902
					HOMO-2 -> LUMO+5	0.13711
					HOMO-1 -> LUMO+1	0.50193
					HOMO-1 -> LUMO+2	-0.13735
					HOMO -> LUMO+5	0.1811
					HOMO -> LUMO+7	-0.11125

Table S32. Optimized geometry of **DKI-4Ph** at FF MECI

Element	Coordinates (Angstroms)		
	x	y	z
N	0	0	0
B	1.4978	0	0
C	-0.6653	0	-1.2581
C	-0.7287	-0.3109	1.1867
N	1.7309	-1.3513	-1.0857

F	2.1238	1.0662	-0.6526
F	2.1005	-0.2708	1.2347
C	-0.0435	-0.4287	-2.387
C	-2.0278	0.5907	-1.3311
C	-1.6479	-1.3609	1.214
C	-0.5179	0.4336	2.3495
C	1.3366	-0.884	-2.3818
C	1.6185	-2.6594	-0.7531
H	-0.5229	-0.2707	-3.3305
C	-3.027	0.003	-2.1062
C	-2.3127	1.7839	-0.6584
C	-2.3535	-1.6527	2.3778
H	-1.8149	-1.9424	0.3281
C	-1.2098	0.1283	3.5151
H	0.1886	1.2386	2.3334
C	2.3746	-0.4391	-3.2866
C	1.784	-3.076	0.5936
C	1.3814	-3.6439	-1.7504
C	-4.2803	0.5959	-2.2164
H	-2.8315	-0.9245	-2.6099
C	-3.5628	2.3735	-0.772
H	-1.5516	2.2431	-0.06
C	-2.1353	-0.9125	3.5346
H	-3.0644	-2.4573	2.3784
H	-1.0339	0.7078	4.4013
C	2.0811	0.3839	-4.3902
C	3.7028	-0.866	-3.1177
C	1.6797	-4.415	0.9156
H	1.982	-2.3464	1.3469
C	1.2782	-4.9685	-1.405
H	1.3031	-3.344	-2.7737
C	-4.5512	1.7785	-1.5533
H	-5.0393	0.1268	-2.8131
H	-3.7667	3.2921	-0.2561
H	-2.6764	-1.1391	4.4332
C	3.0682	0.7514	-5.2801
H	1.085	0.7514	-4.5321
C	4.6934	-0.4793	-4.0102
H	3.9615	-1.4935	-2.2882
C	1.4219	-5.3638	-0.0754
H	1.7974	-4.7236	1.935
H	1.1001	-5.7036	-2.1646
H	-5.519	2.2347	-1.636
C	4.3806	0.3263	-5.0989
H	2.8215	1.3839	-6.1111
H	5.7034	-0.8075	-3.8559
H	1.3463	-6.4014	0.1842
H	5.1449	0.6226	-5.7909

Table S33. Optimized geometry of **DKI-4Ph** at PC MECI

Element	Coordinates (Angstroms)		
	x	y	z
N	1.2598	-0.5005	-0.1663
B	-0.0072	-1.3902	-0.294
C	1.1854	0.8955	-0.1591
C	2.4787	-1.1447	-0.0157

N	-1.2947	-0.5775	-0.1051
F	0.0688	-2.4195	0.6968
F	-0.0498	-2.0265	-1.5802
C	-0.088	1.474	-0.0799
C	2.3724	1.6675	-0.2152
C	3.6072	-0.4078	0.5591
C	2.688	-2.429	-0.5437
C	-1.2754	0.7568	-0.0301
C	-2.5153	-1.336	-0.2176
H	-0.1646	2.537	-0.0773
C	2.4301	2.9994	0.2924
C	3.6383	0.9715	-0.5505
C	4.8812	-1.1165	0.6358
H	3.3739	0.1152	1.4716
C	3.9371	-3.0086	-0.494
H	1.8793	-2.9448	-1.0099
C	-2.5407	1.5384	0.1108
C	-3.29	-1.2455	-1.3714
C	-2.8908	-2.1966	0.8068
C	3.6019	3.6815	0.4286
H	1.5234	3.4679	0.6195
C	4.8655	1.7873	-0.4253
H	3.6154	0.4477	-1.4955
C	5.0532	-2.3485	0.0935
H	5.6929	-0.6118	1.1232
H	4.0708	-3.984	-0.9199
C	-2.8684	2.5105	-0.8329
C	-3.3785	1.35	1.2131
C	-4.4557	-1.991	-1.4817
H	-2.9734	-0.6086	-2.173
C	-4.0585	-2.9436	0.6859
H	-2.2656	-2.292	1.6701
C	4.8389	3.0535	0.0418
H	3.6122	4.6786	0.8216
H	5.789	1.3406	-0.7413
H	6.0054	-2.8405	0.1252
C	-4.0217	3.2735	-0.6852
H	-2.2317	2.6633	-1.6831
C	-4.5224	2.1212	1.3611
H	-3.135	0.6096	1.9488
C	-4.8423	-2.8389	-0.4493
H	-5.0516	-1.9181	-2.3709
H	-4.345	-3.6071	1.4789
H	5.7514	3.6162	0.1099
C	-4.8469	3.0825	0.4079
H	-4.2676	4.0114	-1.4242
H	-5.1572	1.973	2.213
H	-5.7418	-3.4175	-0.5383
H	-5.7352	3.6734	0.5224

DKI-5Ph

Table S34. Optimized geometry of **DKI-5Ph** at S_0 state

Atomic Number	Coordinates (Angstroms)		
	x	y	z
5	0.010361	-2.068651	0.410747
9	-0.001836	-3.241861	-0.309039
9	0.0562	-2.316946	1.78159
7	-1.255313	-1.220982	0.077484
7	1.253221	-1.207579	0.026691
6	-1.226426	0.114355	0.04093
6	-0.009417	0.825733	0.052158
6	1.213385	0.12429	-0.006571
6	-2.510988	0.863902	0.007975
6	-3.405427	0.725398	1.071659
1	-3.161426	0.052627	1.892325
6	-4.594297	1.445896	1.085047
1	-5.281092	1.33778	1.9209
6	-4.905103	2.298616	0.02858
1	-5.837085	2.858695	0.036628
6	-4.020051	2.43265	-1.038601
1	-4.258583	3.095811	-1.86651
6	-2.823952	1.723982	-1.045439
1	-2.125697	1.836267	-1.873083
6	-0.019701	2.315676	0.077506
6	-0.497851	3.000198	1.198963
1	-0.853752	2.428668	2.055823
6	-0.528111	4.391116	1.228761
1	-0.908438	4.904166	2.109188
6	-0.067841	5.12296	0.136996
1	-0.087518	6.21005	0.159323
6	0.418443	4.453717	-0.983899
1	0.779483	5.016241	-1.842022
6	0.437055	3.063274	-1.012731
1	0.80986	2.543458	-1.894951
6	2.487678	0.882859	-0.124725
6	2.903743	1.710727	0.919038
1	2.289163	1.796464	1.813799
6	4.093153	2.422685	0.815331
1	4.412186	3.061696	1.63502
6	4.869081	2.321383	-0.336861
1	5.796689	2.882583	-0.420081
6	4.454872	1.499748	-1.382345
1	5.057082	1.416575	-2.28377
6	3.271428	0.777362	-1.274949
1	2.949137	0.129223	-2.088246
6	-2.472853	-1.941953	-0.134676
6	-2.929721	-2.819477	0.846818
1	-2.35009	-2.941633	1.758989
6	-4.116481	-3.517234	0.647345
1	-4.474336	-4.196063	1.41782
6	-4.844101	-3.348297	-0.528026
1	-5.77379	-3.891815	-0.677906
6	-4.369089	-2.490004	-1.516699
1	-4.92168	-2.365636	-2.444938
6	-3.179938	-1.795483	-1.326681
1	-2.794915	-1.133772	-2.09961

6	2.50545	-1.907056	0.039839
6	3.341121	-1.82134	1.150822
1	3.025119	-1.231624	2.008794
6	4.562273	-2.486558	1.147478
1	5.218055	-2.411845	2.011519
6	4.938863	-3.251704	0.046074
1	5.89396	-3.771431	0.045025
6	4.083436	-3.361404	-1.047439
1	4.365497	-3.971231	-1.902406
6	2.862635	-2.694109	-1.050943
1	2.178116	-2.774279	-1.891966

Table S35. Calculated low frequencies for the optimized structure of **DKI-5Ph** at S_0 state

Low Frequencies:					
-6.3525	-0.0003	0.0005	0.001	2.6754	10.0392
19.1109	24.582	28.5323			

Table S36. Calculated electronic transitions for the optimized structure of **DKI-5Ph** at S_0 state

Excited State	Spin Multiplicity	Energy / eV	Wavelength / nm	f	Composition	Coefficient
1	Singlet-A	3.7393	331.57	0.5157	HOMO -> LUMO	0.68869
2	Singlet-A	4.5851	270.41	0.0334	HOMO-1 -> LUMO	0.67602
3	Singlet-A	4.8408	256.12	0.1156	HOMO-2 -> LUMO	0.65817

References

[1] R. Yoshii, A. Hirose, K. Tanaka, Y. Chujo, *J. Am. Chem. Soc.* **2014**, *136*, 18131–18139.

[2] S. Ito, M. Yaegashi, K. Tanaka, Y. Chujo, *Chem. Eur. J.* **2021**, *27*, 9302–9312.

[3] M. J. Frisch, G. W. Trucks, H. B. Schlegel, G. E. Scuseria, M. A. Robb, J. R. Cheeseman, G. Scalmani, V. Barone, G. A. Petersson, H. Nakatsuji, X. Li, M. Caricato, A. V. Marenich, J. Bloino, B. G. Janesko, R. Gomperts, B. Mennucci, H. P. Hratchian, J. V. Ortiz, A. F. Izmaylov, J. L. Sonnenberg, D. Williams-Young, F. Ding, F. Lipparini, F. Egidi, J. Goings, B. Peng, A. Petrone, T. Henderson, D. Ranasinghe, V. G. Zakrzewski, J. Gao, N. Rega, G. Zheng, W. Liang, M. Hada, M. Ehara, K. Toyota, R. Fukuda, J. Hasegawa, M. Ishida, T. Nakajima, Y. Honda, O. Kitao, H. Nakai, T. Vreven, K. Throssell, J. A. Montgomery, Jr., J. E. Peralta, F. Ogliaro, M. J. Bearpark, J. J. Heyd, E. N. Brothers, K. N. Kudin, V. N. Staroverov, T. A. Keith, R. Kobayashi, J. Normand, K. Raghavachari, A. P. Rendell, J. C. Burant, S. S. Iyengar, J. Tomasi, M. Cossi, J. M. Millam, M. Klene, C. Adamo, R. Cammi, J. W. Ochterski, R. L. Martin, K. Morokuma, O. Farkas, J. B. Foresman, D. J. Fox, *Gaussian 16 Rev. C.01*, Wallingford, CT, 2016.

[4] J. Michl, E. W. Thulstrup, *Tetrahedron* **1976**, *32*, 205–209.

[5] H. Werner, P. J. Knowles, G. Knizia, F. R. Manby, M. Schütz, *Wiley Interdiscip. Rev. Comput. Mol. Sci.* **2012**, *2*, 242–253.

[6] H.-J. Werner, P. J. Knowles, F. R. Manby, J. A. Black, K. Doll, A. Heßelmann, D. Kats, A. Köhn, T. Korona, D. A. Kreplin, Q. Ma, T. F. Miller, A. Mitrushchenkov, K. A. Peterson, I. Polyak, G. Rauhut, M. Sibaev, *J. Chem. Phys.* **2020**, *152*, 144107.

[7] H.-J. Werner, P. J. Knowles, G. Knizia, F. R. Manby, M. Schütz, P. Celani, W. Györffy, D. Kats, T. Korona, R. Lindh, A. Mitrushenkov, G. Rauhut, K. R. Shamasundar, T. B. Adler, R. D. Amos, S. J. Bennie, A. Bernhardsson, A. Berning, D. L. Cooper, M. J. O. Deegan, A. J. Dobbyn, F. Eckert, E. Goll, C. Hampel, A. Hesselmann, G. Hetzer, T. Hrenar, G. Jansen, C. Köppl, S. J. R. Lee, Y. Liu, A. W. Lloyd, Q. Ma, R. A. Mata, A. J. May, S. J. McNicholas, W. Meyer, T. F. M. III, M. E. Mura, A. Nicklass, D. P. O'Neill, P. Palmieri, D. Peng, T. Petrenko, K. Pflüger, R. Pitzer, M. Reiher, T. Shiozaki, H. Stoll, A. J. Stone, R. Tarroni, T. Thorsteinsson, M. Wang, M. Welborn, *Molpro, 2021.2, a Package of Ab Initio Programs*, Stuttgart, DE, 2021.

[8] K. Momma, F. Izumi, *J. Appl. Crystallogr.* **2011**, *44*, 1272–1276.